HEAT LEAKAGE

THROUGH FLOORS, WALLS, AND CEILINGS OF

APPLE STORAGES

Marketing Research Report No. 315

Agricultural Marketing Service—Marketing Research Division
UNITED STATES DEPARTMENT OF AGRICULTURE

PREFACE

This report covers work done under a long-range research project at the Wenatchee, Wash., field office of the Transportation and Facilities Branch, Marketing Research Division, Agricultural Marketing Service, to improve the operation and design of cold storage houses for apples and other tree fruits. It is in two parts, one dealing with the heat flow through the floors of storage houses and the merits of insulating the floors, and the other dealing with the same two factors for walls and ceilings.

W. V. Hukill, of the Agricultural Research Service, U.S. Department of Agriculture, advised in the preparation of this report. Also, the permission of Professor C. O. Mackey, of Cornell University, and of the American Society of Heating and Air Conditioning Engineers to reproduce portions of a report by Professors Mackey and L. T. Wright, Jr., is gratefully acknowledged.

The following organizations cooperated by making their storage houses available for test purposes: Auvill Fruit Co., Inc., Orondo, Wash.; Bardin Bros., Monitor, Wash.; Blue Ribbon Growers, Yakima, Wash.; Cashmere Fruit Growers Union, Cashmere, Wash.; Cashmere Pioneer Growers, Cashmere, Wash.; Cooperative Growers of Okanogan, Okanogan, Wash.; Entiat-Wenoka Growers, Entiat, Wash.; Hanson Fruit and Cold Storage Co., Yakima, Wash.; Lloyd Garretson Co., Yakima, Wash.; Methow-Pateros Growers, Pateros, Wash.; Ninth Street Skookum Growers, Wenatchee, Wash.; Oroville Independent Growers, Oroville, Wash.; Small Bros., Entiat, Wash.; Ted Waterhouse, Orondo, Wash.; and A. Z. Wells Orchards, Azwell, Wash.

Washington, D.C. October, 1959

For sale by the Superintendent of Documents, U.S. Government Printing Office, Washington 25, D.C. Price 40 cents.

CONTENTS

SUMMARY

Part I—Floors

Present methods of insulating floors of apple storages are too costly and cannot be justified economically where the ground water level remains at least 12 feet below floor level.

Studies show that the critical ground water level—at which insulation is justified—is somewhere between 5 and 10 feet below floor level. Allowing a safety margin of 2 feet, therefore, when the normal water level is less than 12 feet, floor insulation is recommended.

The heat flow rate from all storage floors is high when the storage is first refrigerated, running from 20 to 25 Btu per hour per square foot. After the first 2 or 3 days of operation, insulated floors permit heat to flow at the rate of 2 to 4 Btu/hr/sq ft. For uninsulated floors, the rate declines more slowly from the high initial rate.

Where ground water level is below the critical level, however, the heat flow from uninsulated floors continues to decline as the season progresses, and approaches that through insulated floors. Storages without insulated floors should always be refrigerated for a week or 10 days before large volumes of fruit are received.

Breaker strips of insulation, separating the edge of the floor from the outside walls, are of value with uninsulated floors and are recommended. A strip of insulation extending down the wall to the footing is even more effective. Use of a horizontal ribbon of perimeter insulation, extending from the wall 3 to 4 feet under the floor, can be justified if the subfloor beneath the ribbon can be eliminated.

Pumice-concrete and pumice-fill insulation are not always effective, and should be protected from moisture infiltration by a vapor barrier at the lower face of this material.

Conclusions on insulation reached in these studies do not apply to storage houses where temperatures are held below 25 degrees F.

Part II—Walls and Ceilings

In designing cold-storage houses for apples, the effect of hourly variations in outside temperatures usually is not considered in calculating the heat flow through the walls and ceilings. Generally, average daily temperatures are used and an allowance is made for solar-heat loads on roofs. In this allowance, temperatures several degrees higher than the outside air are used. This practice is satisfactory if the more common mass-type insulation is used, because of its ability to absorb and store some heat. However, if lightweight reflective-type insulation, which can store very little heat, is used, variations in outside temperatures become an important consideration in determining refrigeration loads and the design of apple storages.

Because of these problems, research was undertaken to measure the performance of various types of insulation under periodic heat flows and to correlate the observed and predicted heat flow variations; to obtain outside air temperatures in relation to surface temperatures of various types of walls and roofs; to determine the proper structural design for use with reflective insulation; to determine the influence of joists and studs on the heat flow when insulations of various types are used; and to estimate the influence of daily variations in heat flow on the refrigeration load of a cold storage.

In this research, the performance of walls and ceilings of seven apple storage houses was studied. These houses were selected so that different types of insulation, methods of construction, structural materials, and surfaces could be considered. Three of the storages were insulated with reflective-type insulation, three were insulated with mass-type insulation, and one had both types of insulation in different parts of the building. The effect of aluminum paint on the heat flow rate through an insulated roof also was studied.

Results of these studies indicate that, depending on the insulation and exposure of the insulated surface to solar radiation, there are daily variations in heat flow rates. Because of these variations, it was found that the actual refrigeration load may be greater than the load for which the storage was designed. At midday during the receiving period, this may be less than 10 percent greater than the design load, but it could be as much as 25 or 35 percent. The latter condition would be found in a storage designed to handle products already cooled or frozen.

It was found that the variation in heat flow affects the temperatures maintained inside the

storage rooms. At 1 test location, fluctuations from the proper storage temperature ranged from 8° to 9° F. This range was observed when the refrigeration load was heavy and reserve refrigeration capacity was not available to cope with the load. At other locations, fluctuations of 0.5° to 2.5° were observed. Observations at 1 location may be considered as a standard for comparison, because the insulation used was 4 inches of cork, which has been accepted as a standard for the type of storage under study. Here the daily temperature variation was noted to be 1.0° to 1.5°. This variation may be used as a standard for evaluating storages with reflective insulation, to see whether or not room temperature variations are excessive.

For apple storages starting operation in mid-September, insulation should be such that a heat flow rate of 3 Btu per hour per square foot is not exceeded, and the daily average load calculation should be based on two-thirds of this value. For storages insulated with material having less heat storage than 4 inches of corkboard, the thermal resistance should be increased so that the maximum heat transmission rate at midday, under conditions for which the building was designed, does not exceed 3 Btu/hr/sq ft. A method of determining the resistance required to meet this condition is presented.

In certain cases, it may be more economical to combine mass with the insulator, so as to improve its heat storage or load-stabilizing characteristics, than to add extra insulation.

The average amount of heat transmitted per day was decreased about 5 percent when aluminum paint instead of black paint was used on a builtup roof.

HEAT LEAKAGE Through Floors, Walls and Ceilings of APPLE STORAGES[1]

By G. F. SAINSBURY, *agricultural engineer,*[2]
Transportation and Facilities Branch
Marketing Research Division

Part I — Floors

BACKGROUND OF STUDY

Many apple storage houses in the Pacific Northwest are constructed without insulation in the ground floors. Lower initial cost and apparently satisfactory performance have encouraged this practice.

Previous reports [*4*] [*13*][3] showed that stacking directly on ground floors results in higher commodity temperatures in the layers of product in contact with the floor. This effect is more pronounced on uninsulated floors, but is measurable in all instances, regardless of the insulation used. Floor racks or pallets have been recommended to avoid this undesirable condition.

Part I of this report is a further investigation of the performance of and requirements for floor insulation in mild-temperature storages. Observations and conclusions from this study should not be applied to storages maintaining temperatures below 25° F. In low-temperature storages, freezing and heaving of the ground below the floor is a serious problem and cannot be neglected. In mild-temperature storages, freezing of the ground does not occur, and consideration of the overall problem is much simpler.

OBJECTIVES

The purpose of Part I of this report is to present data obtained on the following phases of heat leakage into storage houses through the floors:

1. The heat leakage rates experienced during the initial cooling and first month's operation of an intermittently operated storage.
2. The heat leakage rates experienced through different types of floors during the midseason operation of the storage.
3. The effect of edge breaker strips of insulation and perimeter insulation on otherwise uninsulated floors.
4. The thermal conductivity of floors insulated with pumice and the thermal conductivity observed for the ground in certain test locations.
5. Methods of analyzing the performance of various types of floors placed on soils having different characteristics.
6. An analysis of the economic justification of floor insulation.

METHODS OF RESEARCH

At some of the test locations, copper-constantan thermocouples were buried in the ground at depths of 2, 4, and 5 feet beneath the floor, just beneath the concrete floor, and at the bottom of the insulation where insulation was used. Measurements were taken intermittently at these points to determine temperature changes and temperature differences as the season progressed. In the test to measure heat leakage during the starting up of the plant, floor and ground temperatures were recorded continuously.

Heat flow rates were recorded continuously, using a Gier and Dunkle heat flow meter. This instrument consists of a large number of thermocouple junctions connected in series to respond to the temperature difference across a thin bakelite slab. Since the temperature difference varies directly with the heat flow, the potential developed by the heat flow meter can

[1] The work which is the basis of this report was done with the cooperation of the Washington State Agricultural Experiment Station.
[2] Resigned from the Agricultural Marketing Service.
[3] Italic numbers in parenthesis refer to items in Literature Cited, p. 49.

be measured and converted into heat flow when the calibration constant of the meter is known. The meter was placed in a plywood frame cut so that the top of the meter was exposed to the room air. The meter itself was slightly warped and was positioned with the convex side to the floor. When the plywood frame was loaded with 20 to 30 pounds of weight on each end, the heat flow meter was flattened and brought into good contact with the floor.

Intermittent readings from buried thermocouples were obtained with a semiprecision hand-balanced potentiometer. Continuous readings of both thermocouples and the heat flow meter were made with a strip-chart, multipoint, electronically balanced recording potentiometer.

Where temperatures were continuously recorded at several positions beneath the floor, they were usually plotted on a chart and averaged graphically for the desired period. Where only surface temperature and air temperature were continuously recorded, average values were generally obtained by totaling the values from the strip chart and taking the arithmetic average. A similar procedure was used for heat flow meter readings. Care was required in this procedure to see that during the period of analysis there were no long-term warming or cooling trends in the room temperature. Since the heat flow measurement really indicated the amount of heat leaving the floor surface and passing into the air, there was some fluctuation with changing air temperature. During a long-term change in air temperature, a considerable quantity of heat may be absorbed or liberated by the concrete wearing floor located on top of the insulation. This action obscures the true heat flow coming through from the ground. Some of the data available give an indication of the extent of this effect.

In addition to the experimental observations, the predicted performance of various floor arrangements was calculated graphically by the analytical method proposed by E. Schmidt [*16*] as described by Eckert [*2*]. A description of this method is available also in the chapter on Heat Transfer of the ASHAE Guide [*1*].

RESULTS

Location 1

The floor of the storage (fig. 1) at location 1 consists of 9 inches of a pumice-concrete mixture laid directly on compacted soil underlaid by river gravel, with a 4-inch concrete wearing floor above the pumice-concrete mixture. At the time of construction, thermocouples were placed at the top of the concrete floor, at the top and bottom of the pumice-concrete layer, and at points 2 feet below the finished floor surface and approximately 4 feet below the surface. Three sets of thermocouples so arranged were placed: One set approximately 18 inches from a wall between the cold storage and a segregating room that is always somewhat warmer than outside; one set approximately 18 inches from an outside wall; and one set approximately 18 inches from a partition wall that separates the test cold room from another cold room. This last location was approximately 70 feet from the nearest outside wall.

Figure 2 shows the temperatures observed during one season. The position 2 feet below the floor has been omitted from the figure. The depths of the bottom positions vary slightly; that at the segregating room is 4 feet below the floor level, that at the outside wall is 4½ feet below floor level, and that at the interior partition wall is 5 feet below floor level. The temperature designated as the top of the pumice-concrete at the last location is actually the top of the concrete floor, because the thermocouple located at the top of the pumice-concrete was destroyed during construction. At the other two locations, the difference between temperatures at the top of the concrete and the top of the pumice-concrete was slight.

The temperatures at the bottom of the pumice-concrete and at the depth of 4 to 5 feet were very similar for all locations for the first 2 months. After this, the locations near the segregating room and near the outside wall were influenced by outside temperature variations. The outside wall location showed the effects of low winter temperatures most clearly; the segregating room wall position indicated some of this effect, but, more markedly, the effect of warmer temperature in the spring. The location that is distant from the side walls showed a continued downward trend throughout the spring season and less warmup at 4 to 5 feet of depth during the period the plant was shut down.

A continuous recording later was made of temperatures and heat flow from the locations near the segregating room wall and near the partition wall during the first 3 weeks of the season's operation. Figure 3 presents the temperature record obtained. During the first 2 weeks, the temperature of the top of the concrete at the segregating room wall locations was practically identical with that shown for the partition wall position. During the last week, it was slightly higher. The curves show little temperature change initially at the 4- and 5-foot depths. These temperatures also indicate that, in the position distant from the outside walls, the ground had not warmed up as much as the ground near the edges.

Figure 4 presents the average daily heat flow rates observed during this 3-week period. Since only one heat flow meter was available, it was moved from one position to the other, remaining

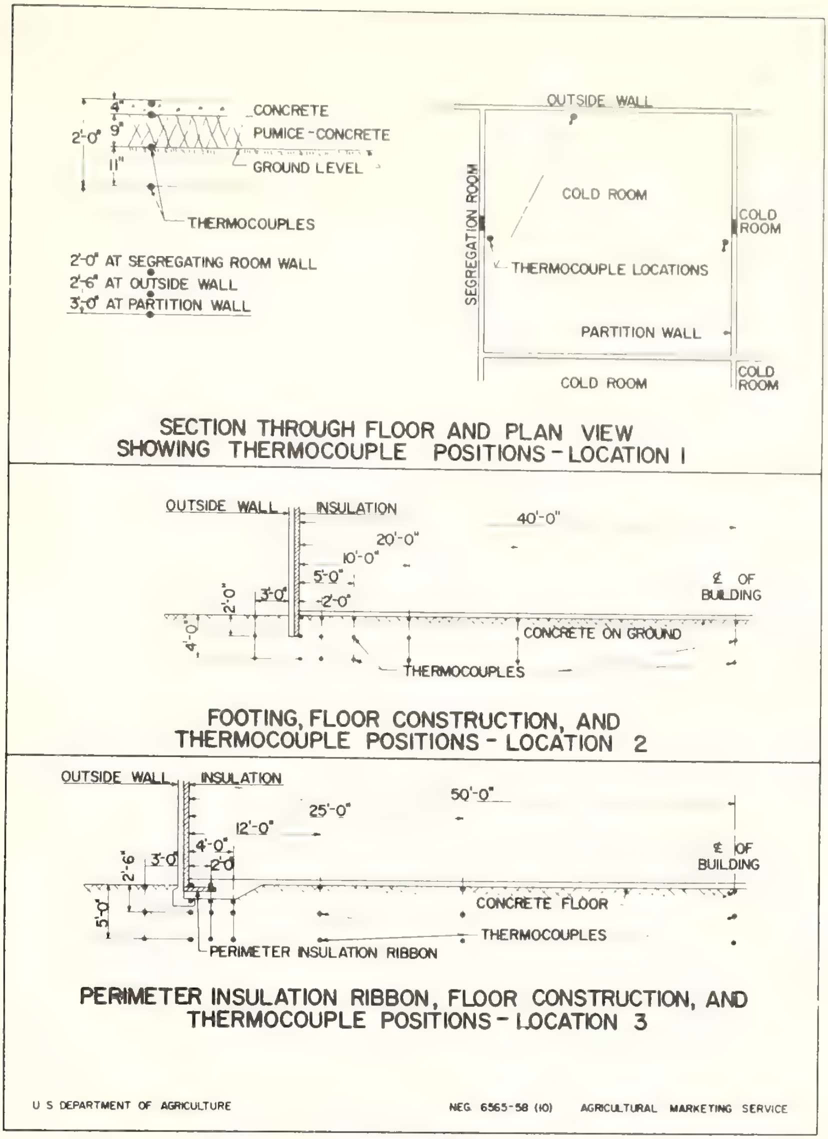

FIGURE 1

in a given position for at least 24 hours. A substantial fluctuation of air temperature during each day was caused by defrosting operations and by warm fruit coming into the room during the day. This fluctuating temperature produced considerable variation of instantaneous values of heat flow; but the flow rate assumed a cyclical pattern over a 24-hour period. In addition, on August 27, 28, and 29, a consistent upward trend in room temperature resulted in lower than normal heat flow from the floor. On the 30th and 31st, the trend was reversed, and greater heat flow rates resulted.

From the first through the fourth day of the test, there were periods when the heat flow meter potential exceeded the full scale of the recorder. Heat flow rates during this time were determined by plotting the temperature difference between the heat flow meter and the air for about a week. During the periods of less than full-scale instrument deflection, the heat flow rate and temperature difference were calculated and a film coefficient was determined for each location. This film coefficient was then applied to the observed surface-to-air temperature difference for the periods of more than full-scale deflection to obtain heat flow during these periods. The film coefficient determined for the position near the partition wall was 1.35 Btu/hr/sq ft/°F. Td. For the segregating room wall position, an average value of 1.61 was obtained.

Smoothed curves have been drawn in figure 4 between the actual values of average daily heat flow. After the first 3 or 4 days, the heat flow

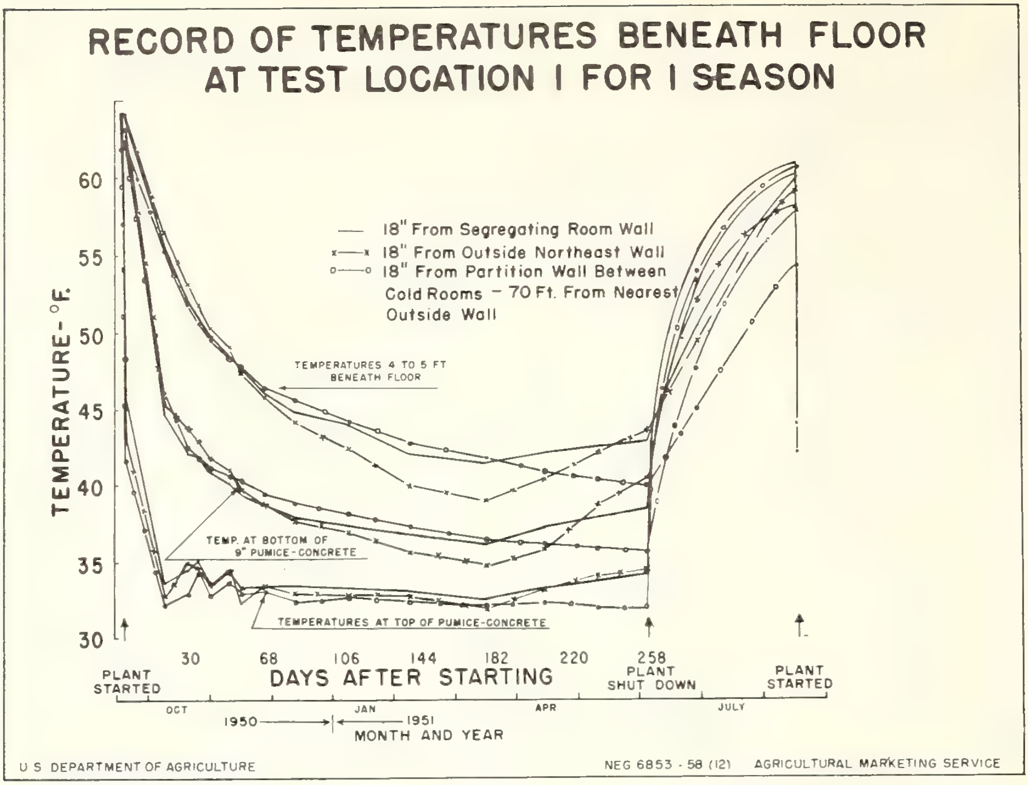

FIGURE 2

at the partition wall position tended to be about 1 Btu/hr/sq ft less than that observed near the segregating room wall position. The lower initial temperature of the soil beneath this position accounts for this difference.

At first, very high heat flow values were observed, but such values persisted for a comparatively short time. In 7 or 8 days, the average heat flow rate was down to about 6 Btu/hr/sq ft. From this point on, the heat flow rate declined less rapidly and was between 4 and 5 Btu/hr/sq ft after 18 and 19 days.

Several periods of heat flow observation have been used to determine a conductivity of the pumice-concrete. From this value and the observed temperature differences, the heat flow has been calculated and charted for the season at the locations near the partition between storage rooms and the location near the segregating room wall. The calculation includes allowance for heat released by the pumice-concrete as well as heat conducted through the pumice; but after the first month, the amount of heat released by the pumice-concrete was negligible. Figure 5 shows the declining values of floor heat leakage encountered as the season progressed. This record is for the first season this plant was operated, starting in 1950, and in this case the ground at the position near the partition between cold rooms was as warm initially as the ground near the segregating room wall. The record of heat flow under starting conditions was made in 1956 and is somewhat influenced by lower ground temperature at the partition wall location.

The conductivity of pumice-concrete used in calculating the heat flow at the segregating room wall was 3.12 Btu/hr/sq ft/inch thickness/°F. Td. determined in April 1951. Later values determined for this location were somewhat higher; but the low value was used in preparing figure 5. Occasional leakage of water through the roof above the test location was indicated. At these times, water accumulated on the floor and gradually passed through the concrete and into the pumice-concrete. This occurrence has likely impaired the insulating value of the material to some extent.

The conductivity of pumice-concrete used in calculating the heat flow at the partition wall between the cold rooms was 3.17 Btu/hr/sq ft/inch thickness/°F. Td. This value was the average of tests in February and September 1956.

The conductivity observed in various tests was substantially greater than the value of 2.42 given in the ASHAE Guide for pumice-concrete aggregates and much greater than the conductivity observed at this station for pumice block walls. The use of a dense aggregate in this instance, or the lack of a vapor barrier between

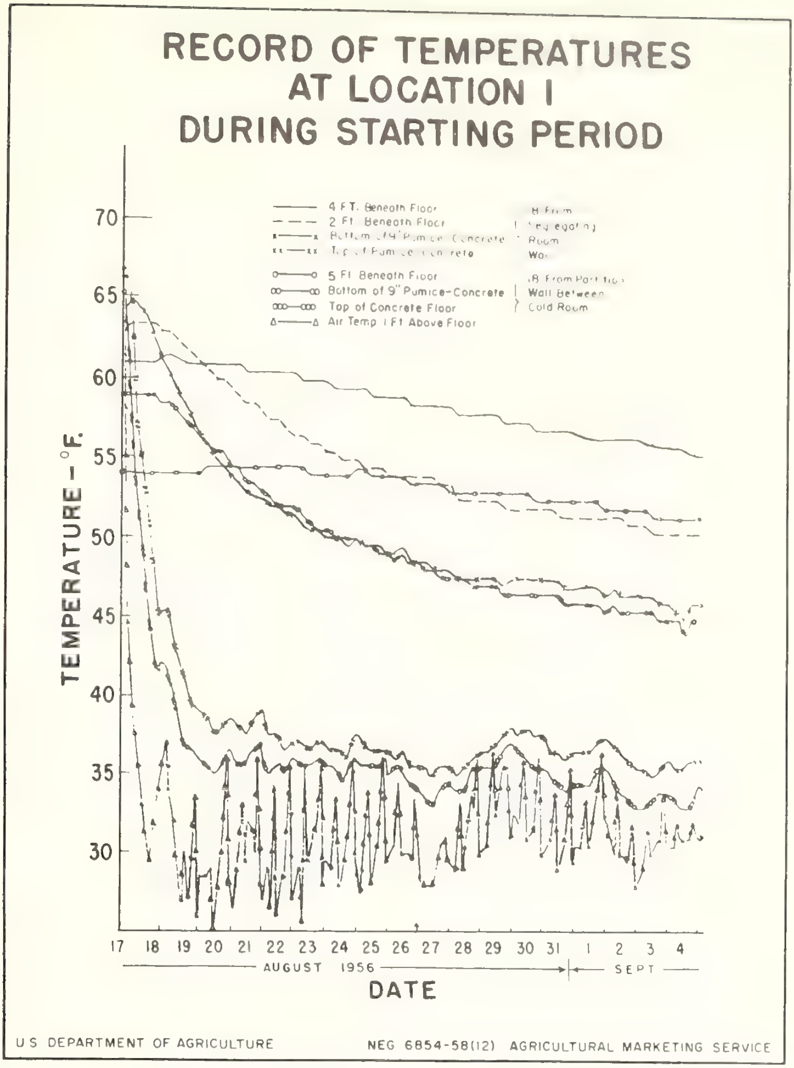

FIGURE 3

the ground and the pumice-concrete, may account for this difference. Without a vapor barrier, moisture is drawn toward the storage room from the ground and a higher moisture content may be present in the pumice-concrete floor insulation than in a pumice block wall.

Location 2

At location 2, intermittent temperature observations were made during the season. Heat flow from the floor at different locations in the storage was recorded during a 10-day period. The floor at this location was 5-inch concrete laid directly on the ground, which was principally sand and heavy river gravel. The drainage at this location was good, and at the time the thermocouples were placed in the ground, no trace of ground water was noted. Two-foot-deep footings around the building were insulated with 2-inch fiberglass asphalt-enclosed board. Thermocouples were placed directly beneath the concrete, and at 2 feet and 4 feet down, at the following positions with respect to the building: 3 feet outside the building, at the inside edge of the midpoint of the east wall of the building, 2 feet in from the edge, 5 feet in from the edge, 10 feet in from the edge, 20 feet in, and at the center of the 80-foot-wide building.

An initial temperature observation was made on September 18, 1953. The storage was placed in operation October 1, and additional observations were made on October 9, October 19, and November 12. The plant was shut down shortly after November 12, operating over a much shorter season than is normal for most storages in the vicinity.

Figure 6 presents part of the temperature record obtained. A steady decline of tempera-

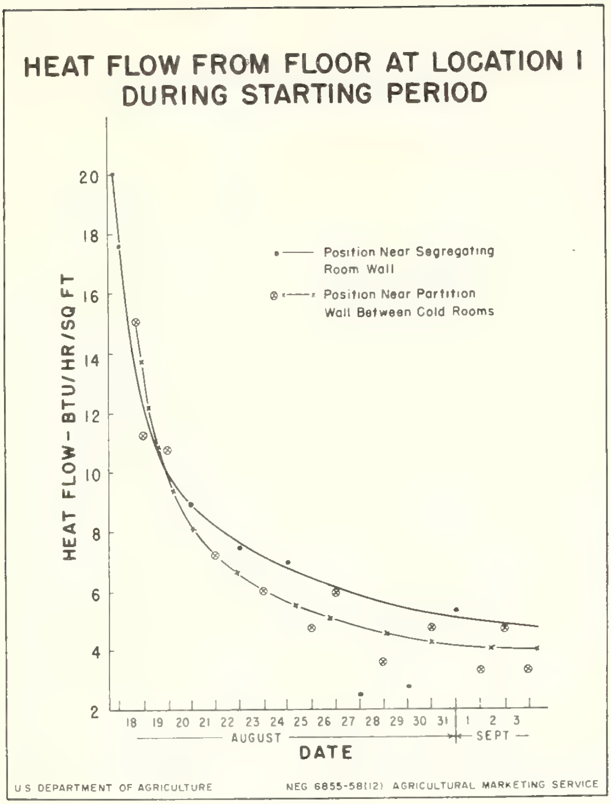

FIGURE 4

tures during the period of observation is apparent. The edge position shows generally warmer temperatures at the comparable depths than other positions, but the other positions are not progressively cooler as one goes from the edge toward the center. This indicates that, for the period of observation, the effect of conduction around the edge does not extend very far into the storage.

Observed heat flow records at this location are summarized in table 1. From these data and temperature observations, conductivity of the ground was determined and the heat flow for the various periods of observation was calculated. Figure 7 shows the variation of heat flow as the season progressed for the position 2 feet in from the wall and for the position at the center of the room. These calculations include the heat conducted through the earth and also the heat released from the section of ground through which temperature differences were measured.

Location 3

At location 3, temperatures under the floor and heat flow from the floor were measured in much the same manner as at location 2. The floor at this location is 5-inch concrete poured on 10 to 12 inches of gravel with a rather heavy silt soil beneath. Drainage through this soil is rather poor, and water was encountered in the center location at the 5-foot depth. Thermocouples were placed directly beneath the concrete floor, 30 inches beneath the concrete, and 5 feet beneath it at each location. These locations were as follows: 3 feet outside the midpoint of the north wall of the building; at the edge of the north wall midpoint; and at points 2, 4, 12, 25, and 50 feet in from the edge of the building, the last point being at the center of the 100-foot-square building. A form of perimeter insulation was used on this building, but it differed from that used at location 2. A 3-foot-wide ribbon of 4-inch-thick fiberglass asphalt-enclosed board was installed as shown in figure 1. In the thermocouple positions covered by the ribbon, 2 additional thermocouples were installed to measure the temperature at the top and middle of the insulation.

This storage was placed in operation October 1, 1953, and was refrigerated until mid-February 1954. Part of the intermittent temperature record is presented in figure 8. The heat flow observations are summarized in table 1. These heat flow measurements and the temperature measurements have been used to calculate the heat flow at various times during the season for the position at the center of the building. Figure 7 shows the change in heat flow rate as the season progressed.

The pattern of heat flow from the center of the floor at this location differed considerably from the pattern observed at location 2. Initially, the heat flow was much higher at location 2, but the rate dropped off much faster. Soils of the type at location 2 normally have a greater conductivity but a lower moisture content than those at location 3. At location 2, more heat flowed into the storage at first; but the heat stored in each foot of the soil was less, and a greater layer of cooled ground was available sooner to act as insulation for the floor.

Location 4

At location 4 is the storage described by Hukill and Wooten [4]. Thermocouples were buried in two sections of the basement floor. One section was insulated with 6 inches of wet pumice placed on top of the earth without a vapor barrier between the ground and the pumice. The other section was insulated with 5 inches of dry pumice protected from moisture by a vapor seal. In both sections, a 4-inch concrete wearing floor was poured above the pumice. A complete discussion of the insulating characteristics observed during the first 2 seasons of operation in 1943 and 1944 is available in the report [4]. The authors concluded that the conductivity of wet, unprotected pumice was 1.9 times as great as that of the dry, protected pumice.

TABLE 1.—*Floor heat leakage and conductance observed at locations 1–5*

Location	Date of test	Construction details	Heat flow observed	Conductivity of—		Surface-to-air film conductance
				Insulation	Ground	
			Btu/hr/sq ft	Btu/hr/sq ft	/in/°F. Td.	Btu/hr/sq ft/°F. Td.
#1—At segregating room wall	Apr. 27–30, 1951	9″ pumice concrete on ground with 4″ concrete finish floor.	1.51	3.14	11.8	
	Feb. 24–27, 1956		2.17	4.88	11.9	
	Sept. 4–5, 1956		[1] 4.4	3.78	11.6	1.65
—At partition wall	Feb. 18–20, 1956		1.57	3.44	13.4	
	Sept. 1–4, 1956		[2] 3.71	2.88	14.8	1.35
#1A—In center of room	Feb. 20, 1956	12″ pumice fill-5″ concrete finish floor.	1.40			1.39
	Sept. 10, 1956		[3] 4.58			1.53
#2—1 ft. from wall	Oct. 9–13, 1953	5″ concrete finish floor on ground, 2″ insulation down footings.	6.16		17.0	
—5 ft. from wall	Oct. 13–16, 1953		5.68			
—At center room	Oct. 16–21, 1953		4.24		13.5	
#3—1½ ft. from W. wall	Nov. 18–20, 1953	5″ concrete finish floor on ground-4″ thick Fiberglas AE. board ribbon 3 ft. wide all around outside of bldg.	1.94			
—5 ft. from W. wall	Nov. 17–18, 1953		3.08			
—Center of bldg.	Nov. 16–17, 1953		3.63		10.3	
—Center of bldg. covered by fruit	Nov. 20–23, 1953		.32			
#4—Center of room	Feb. 29–Mar. 2, 1956	6″ unprotected pumice on ground.	.99	1.64	6.31	1.24
—Center of room	Mar. 2–5, 1956	5″ protected (dry) pumice on ground.	1.02	1.09	8.0	1.44
#5—Center of room	Mar. 22–23, 1956	3″ corkboard-waterproof membrane and concrete subfloor-53°F. water in ground at floor level.	1.79	.272		1.28

[1] 18 days after starting.
[2] 15, 16, and 17 days after starting.
[3] 10 days after starting.

Since the thermocouples were still in place and operative, a test was made in 1956 to determine whether this difference still existed after 13 seasons of operation. The results, given in table 1, indicate that the conductivity of the wet pumice is still 1.5 times greater than that of the dry, protected pumice. However, the ground conductivity determined for each location shows a greater conductivity beneath the dry pumice. Possibly the presence of a vapor barrier in this area tends to accumulate moisture in the ground. In some respects this action tends to minimize the advantages of dry pumice, because at midseason, when these observations were made, the insulating effect of the ground is an important factor in the overall insulating effect. During the first month or two of operation, however, until a considerable depth of ground can be cooled and its resistance added to that of the floor insulating material, the dry insulation would show a much reduced heat flow into the room as compared to the wet pumice.

Location 5

At location 5, the ground water level was as high as the basement floor level. The temperature difference across the floor insulation was determined by measuring the temperature of a stream of water entering a well just below floor level. The observed conductivity for the insulation compared very well with published "K" values for corkboard.

When this particular storage was constructed, the owner was aware of the proximity of ground water to the basement floor level and insulated the floor and protected the insulation. The observed temperature difference, 19.7° F., through the insulation at location 5, is much greater than the 4.7° F. difference observed through the insulation at location 4 at the same time of the year. This difference is a clear indication of the need for insulation where the ground water level is close to the floor level.

Other Locations

In addition to the above tests, floor heat leakage has been measured in other storage rooms and the results are given in tables 2 and 3. In these storages, thermocouples for determining temperatures at various depths in the ground were not available and an evaluation of ground conductivity is not possible.

A number of the floors were tested in February and March. At this time, all had been in operation for 5 months and some had operated for 6 to 6½ months. Most of the uninsulated or

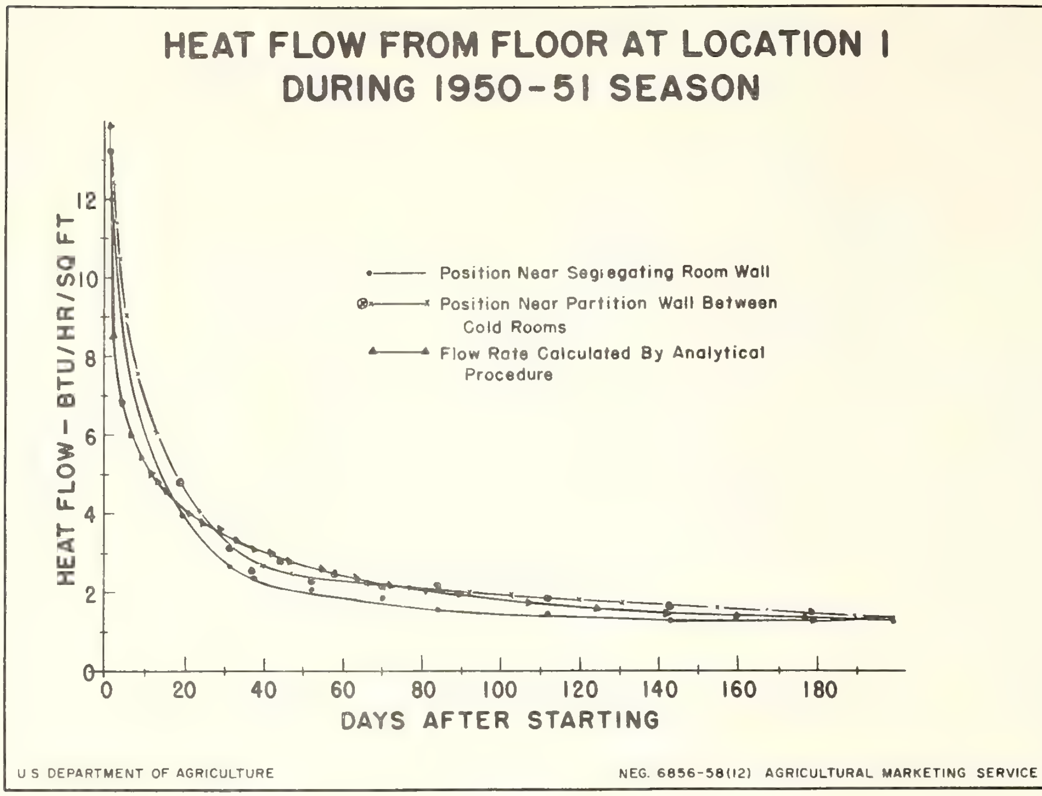

FIGURE 5

semi-insulated floors tested had a heat leakage rate of from 1.0 to 1.68 Btu/hr/sq ft in the uncovered area of the floor. The floors at locations 6, 7, and 10, which are insulated in various ways, had leakage rates substantially less than 1 Btu/hr/sq ft. The floors at locations 1A and at 14 did not show such a favorable heat flow rate, although they are insulated with 12 inches and 10 inches of pumice and this is similar to the insulation at location 10. The reason for this is not clear, but it is possible that moisture content of the pumice, conductivity of the ground beneath, and water level in the ground are factors entering into this difference.

Film coefficients for the conductance from surface to air have been obtained in a number of cases, and these serve as a check on the heat flow measurements. Film coefficients for the tests at locations 6 and 10 are the highest and lowest values obtained. Both these locations experienced low rates of heat leakage. Therefore, the temperature difference from surface to air is small and a very slight error in the measurements would make a considerable difference in the calculated film coefficient. Most of the film coefficients are in the range considered normal.

DISCUSSION

Heat Flow Through Covered Sections of Floor

Measurements were made at locations 3, 11, and 12 where the heat flow meter was covered by a stack of boxes containing fruit that was already cooled. In all such cases, a very low rate of heat flow was observed. Usually the heat flow was about 10 percent of that observed from the uncovered floor in the same vicinity.

Perimeter Insulation of Floors

Dwellings constructed with concrete slab floors laid on the ground have often experienced serious heat losses around the edges during the winter. The ASHAE Guide contains a discussion of this subject, together with data on suggested forms of perimeter insulation. Some observations concerning the relation between heat leakage from floors and the distance from the outside walls of the storages were obtained during this study.

At location 15, the concrete floor extended unbroken to the outside building-wall footings and provided an excellent heat conduction path. Measurements of heat flow rates at various distances from the wall are given in table 3.

Table 2.—*Floor heat leakage and surface film conductance observed at locations 6–13*

Location	Date of test	Construction details	Heat flow observed	Temperature difference, surface to air	Film coefficient	Remarks
			Btu/hr/sq ft	*Degrees F.*	*Btu/hr/sq ft/°F. Td.*	
#6—Center of room...	Feb. 28–29, 1956	3″ corkboard, 1″ air space, wood finish floor, concrete subfloor.	0.62	0.75	0.83	
#7—Center of room...	Jan. 14–20, 1954	6″ shavings, wood finish floor, concrete subfloor.	.64	....	....	
—2 ft. from sidewall......	Jan. 14–20, 1954	....	.58	....	....	
#8—Center of room..	Mar. 5–8, 1956	Concrete on ground, basement room.	1.20	1.2	1.03	
—Center of room..	Mar. 8–9, 1956	Concrete on ground at grade level.	1.65	1.1	1.5	
#9—Center of room..	Mar. 9–10, 1956	Concrete on 18″ gravel fill.	1.68	....	....	
#10—Center of room..	Mar. 14–15, 1956	12″ protected pumice fill on dry ground, concrete finish floor.	.46	.23	2.0	
#11—Center of room..	Nov. 13–20, 1951	Concrete on 12″ gravel fill.	.35			Heat flow meter under stack of fruit.
#12—Center of room..	Dec. 18–24, 1953	Concrete on ground.	.15	....	....	
—Center of room..	Dec. 18–24, 1953		.28			
—Center of room..	Dec. 18–24, 1953		1.68	....	....	Heat flow meter on uncovered section of floor.
—Center of room..	Dec. 18–24, 1953		3.03	....	....	Heat flow meter between box rows.
#13—15 ft. from W. wall......	Oct. 14–15, 1952..	Concrete on ground.	6.15	....	....	Storage had been in operation for about 3 weeks.

At location 14, an edge breaker strip of 4-inch pumice-concrete in the floor places additional thermal resistance in the heat conduction path from the outside. Measurements of heat flow rates from the floor at various distances from the outside are given in table 3.

Figure 9 compares the observation at locations 14 and 15. The two locations should not be compared directly because location 14 had been refrigerated for 8 months and location 15 had been cooled for only a month and was operating in the warmest part of the season when the observations were made. However, by adding about 50 percent to the observed values at location 14, the heat flow rate at points 3 feet and farther away from the edge will be

Table 3.—*Relation between floor heat leakage and distances from outside wall for storages with and without edge breaker strips*

Location	Date of test	Construction details	Heat leakage observed	Remarks
			Btu/hr/sq ft	
#14— 6 in. from S. wall...........	June 15–16, 1954	10″ protected pumice fill, 4″ concrete floor above, 4″ pumice concrete breaker strip at edge of finish floor.	3.51	Storage had been in operation since previous October.
— 2 ft. from S. wall...........	June 20–21, 1954		2.06	
— 4 ft. from S. wall...........	June 18–19, 1954		1.46	
— 6 ft. from S. wall...........	June 17–18, 1954		1.53	
—10 ft. from S. wall...........	June 16–17, 1954		1.22	
—15 ft. from S. wall...........	June 21–22, 1954		1.26	
#15—At W. wall.................	Aug. 8–10, 1951	8″ pumice fill between concrete subfloor and concrete finish floor no breaker strip at edge.	12.8	Storage had been operating about 4 weeks when these observations were made.
— 6 in. from W. wall..........	Aug. 10–13, 1951		7.27	
—22 in. from W. wall..........	Aug. 18–20, 1951		3.76	
—35 in. from W. wall..........	Aug. 16–18, 1951		2.19	
— 5 ft. 6 in. from W. wall......	Aug. 13–15, 1951		1.91	

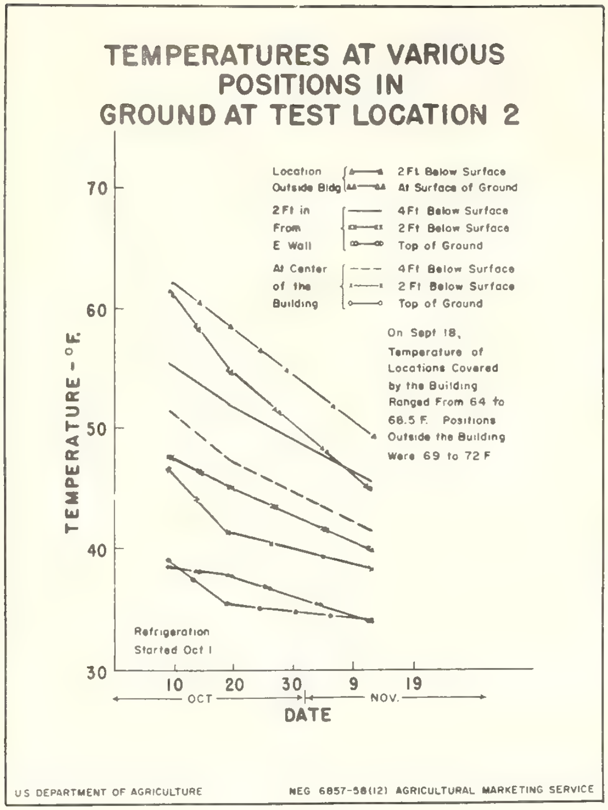

Figure 6

comparable at the two locations. After applying this factor, the heat flow rate at the 2-foot position at location 15 is about 20 percent greater, and at the 6-inch position is about 40 percent greater than the rate at location 14. This is a rather rough comparison, but it does indicate that an undesirably high rate of heat flow around the perimeter of the storage will be encountered if a breaker strip is not installed. The relation that this heat flow will have to the total load from the floor will vary with the size of the room and the shape of the room; that is, whether it is square, or long and narrow.

Some of the work done at locations 2 and 3 was intended as a comparison of two methods of providing perimeter insulation. At location 2, the insulation extended down the inside of the footing; at location 3, the insulation extended back under the floor for 3 feet. The latter method appears more effective but costs more to install. Here again, direct comparison of the results of the observations are difficult. The soil conditions at the two locations were greatly different. At location 3, the fruit was stacked directly on the floor; at location 2, fruit was on pallets and air could pass between the fruit and the floor and carry away the heat from the ground more readily. However, these conclusions can be drawn: At location 2, the heat flow rate near the edge was about 1½ times the rate at the center, whereas at location 14, where

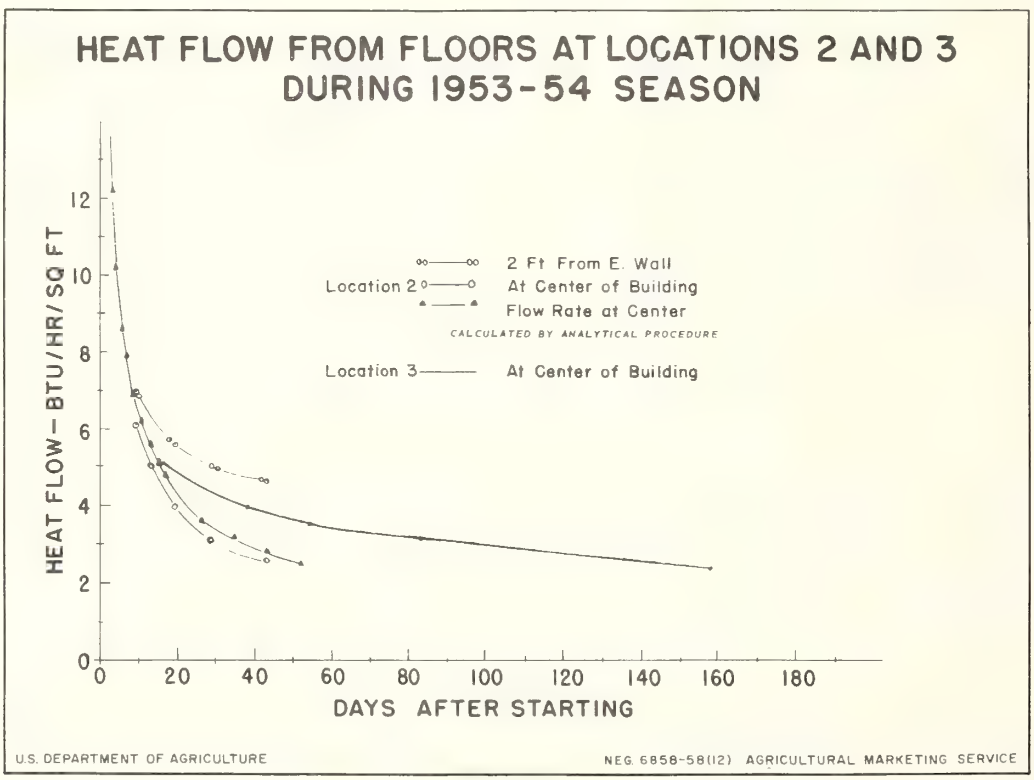

Figure 7

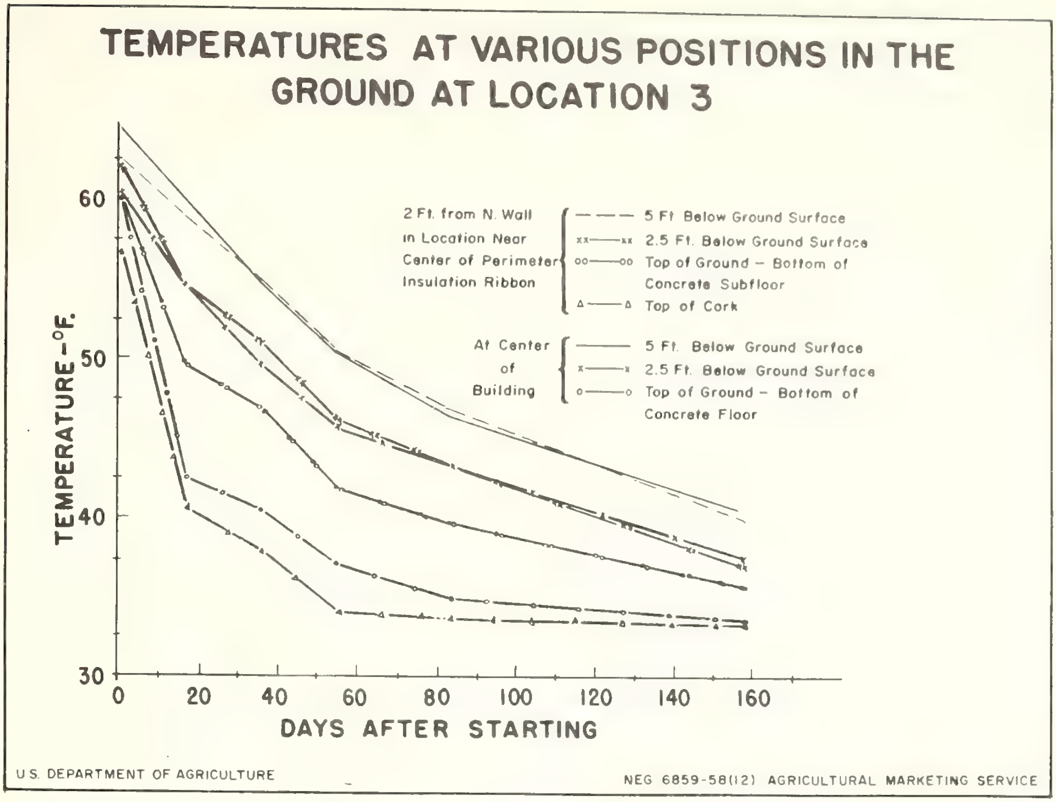

FIGURE 8

only a breaker strip was provided without insulation of the footing, the heat flow near the edge was 2 to 3 times greater than at positions substantially removed from the edge. Therefore, it seems that footing insulation has some merit. At location 3, the heat flow measured at the center of the section above the insulating ribbon was less than at the center of the room, and we can conclude that it was an effective edge insulation. One observation regarding this installation was that the measured heat flow from the floor above the insulating ribbon was 1.94 Btu/hr/sq ft. The calculated heat flow through the insulation of the ribbon, based on observed temperature difference across the insulation and the conductivity of the insulation used, was less than 40 percent of this amount. Conduction through the concrete from the subfloor beneath the insulating ribbon into the floor at the inner end of the ribbon probably accounts for this discrepancy.

The determination of a proper width for a perimeter ribbon insulation beneath a floor is a very complex problem; but the curves on figure 9 indicate that beyond 4 feet, the edge effects of conduction from the outside are not serious. Probably a 4-foot-wide ribbon is adequate. A board form insulator that is impervious to moisture would allow the installation of a ribbon without a connection between the main slab and the ribbon subfloor and possibly achieve somewhat better performance than was observed in this case.

Ward and Sewell [*18*] have published some information that can be used to estimate the additional heat load due to edge effect with floors insulated in various ways. They used a ratio that involves ground temperature, storage room temperature, and temperature of the boundary between ground and bottom of insulation. This temperature ratio is plotted against a ratio between conductivity of insulation and width of room. The distance from the edge at which a given temperature ratio will prevail can be obtained from the plotted data. The temperature of bottom of insulation can be determined for a given ground temperature, and the heat flow into the room calculated.

A calculation of this type was made to determine the edge effects in a room 100 feet square where the floor is 5 inches of concrete. The edge effect increased the heat flow from the floor during the loading period 24 percent, if the plant operated to receive fruit in September, and 19 percent, if the plant started operation in October. The total heat load encountered in a season running from October through May would be increased by 15 percent by the edge effect. If a 6-inch breaker strip of insulation between the floor and the footing is used, the

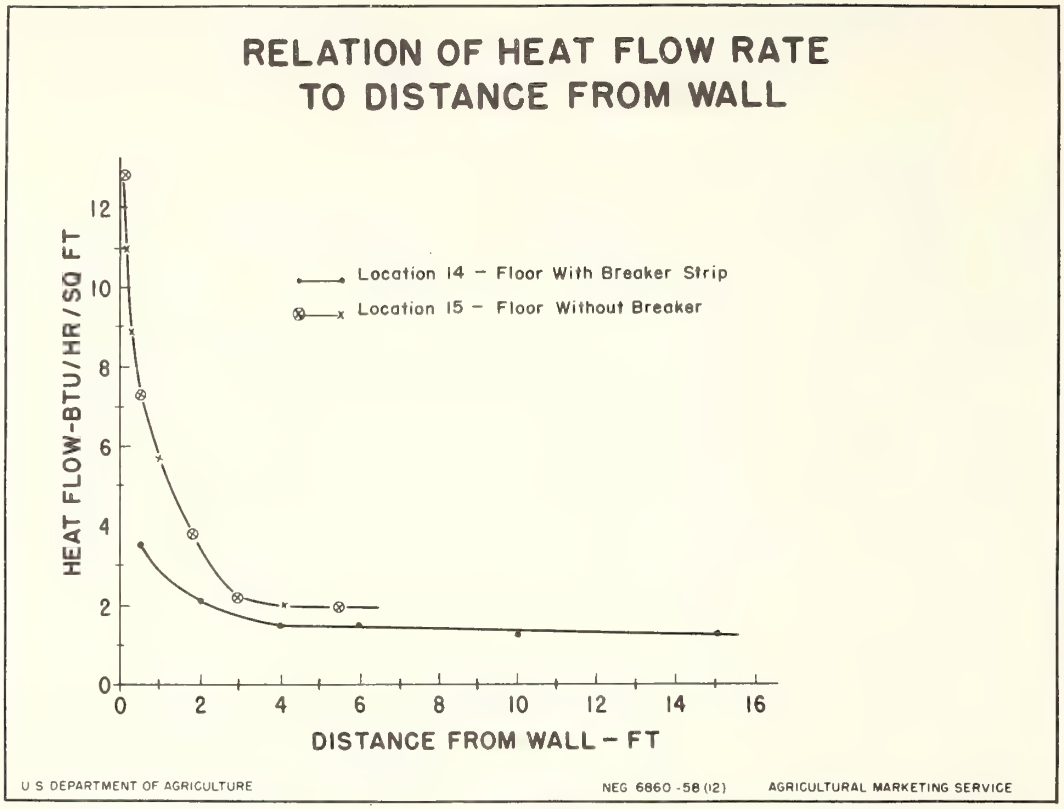

FIGURE 9

September design load is increased only 10 percent by the edge effect; the October design load is increased 7.5 percent and the overall season load is increased only 5 percent.

A similar calculation for a floor insulated with 2-inch sheet cork indicated that edge effects were negligible as far as overall heat load and design heat leakage are concerned with a plant that is operated intermittently and must be pulled down to temperature each year in the late summer.

Analytical Determination of Heat Flow Rates

The experience gained in obtaining the various results presented here has called attention to many of the shortcomings of field observation of heat flow from floors. Obtaining a reasonably comprehensive body of data is laborious; fluctuations in storage temperatures can influence the observations greatly. Temperature beneath floors can be obtained only in those cases where thermocouples can be placed at time of building construction. Moisture changes in the soil beneath the floor are of great importance and are usually undetermined as the season progresses.

To supplement the data in this report, graphic analyses of temperature changes beneath floors have been made by the methods described by Eckert [2]. Details of the analysis used to compare the analytical and observed results at location 2 are given in the appendix. On figure 7, the heat flow rates calculated by the analytical method are shown on the same chart with the observed heat flow, and generally good agreement is apparent.

In figure 5, heat flow determined by the analytical method for location 1 is shown. A calculation has not been made for location 3, because of the uncertainties regarding water level in the ground beneath the floor, and also because the temperature in this room was not immediately reduced to the normal operation level. Instead, the temperature was first set at 38° to 40° F., and then the control point was reset several times during the following 8 weeks until the air temperature was finally brought to 32° F. This change in room air temperature setting complicated the analysis to the point that it did not seem worthwhile.

Since the method of analysis gave reasonable agreement with observed heat flow rates in the two instances where a check could be made, it appeared that the method could be useful in extending this study of floor heat leakage. With this method, the effect of selected variables could be evaluated far better than is possible in field testing.

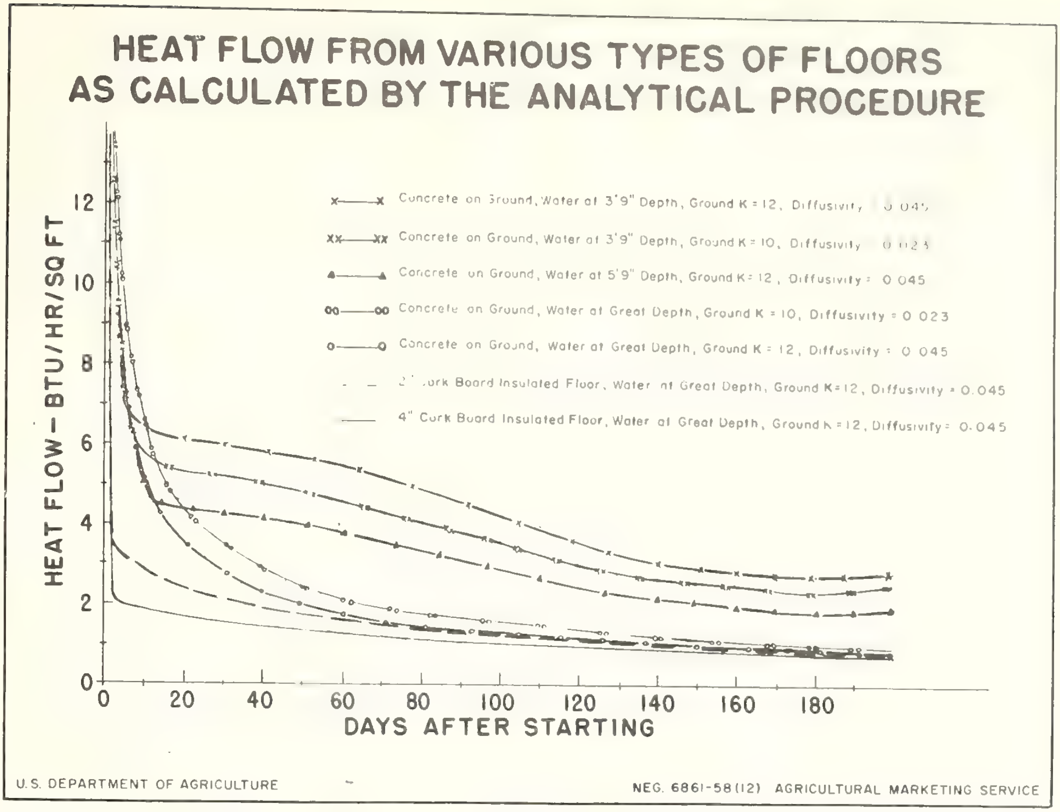

FIGURE 10

Figure 10 shows the season heat flow rates as calculated by this method of analysis for various combinations of floor insulation, water level in the soil, and soil characteristics. Two soil characteristics have been considered, one having a conductivity of 12 Btu/hr/sq ft/inch thickness/°F. Td. and a diffusivity of 0.0455 sq ft/hr, and the other having a conductivity of 10 and a diffusivity of 0.023. The first condition represents a heavy gravel soil with a dry density of 140 pounds per cubic foot and about 1 percent moisture content; the second represents a silt or clay soil with a dry density of 110 pounds per cubic foot and 13 percent moisture.

Heat flow rates were calculated for floors without insulation and placed over dry ground, and over ground with water at depths of 11 feet, 9 inches, of 5 feet, 9 inches, and of 3 feet, 9 inches. Heat flow curves for floors with 2-inch and 4-inch cork insulation also are shown.

All curves were calculated from data obtained in the manner detailed in appendix A. In all cases where the water level was 11 feet, 9 inches or lower, the initial surface temperature and ground temperature for the first 4 feet was taken as 65° F. and the ground temperature declined from this value to a steady value of 52° F. ± ½° at a depth that is dependent upon the diffusivity of the soil. For diffusivity of 0.0455 this depth is 43 feet, and for the soil with diffusivity of 0.023 it is approximately 30 feet. The 1° fluctuation that takes place at these depths lags behind the seasonal temperature variation by approximately 220 days. Formulas used in calculating ground temperature range and lag time for various depths are given in appendix A. The 52° value has been selected, since it is the average annual temperature in this region.

Where water in the soil has been assumed at various depths, the analysis has been simplified by assuming that the soil characteristics are constant as the water level is approached, and that the water level is constant at the assumed level. It is unlikely that either assumption is strictly correct. Where heat flow has been calculated with water in the ground, the average water temperature has been taken as 52° F. The October 1 water temperature was taken as 60° and the water temperature was assumed to fluctuate with an annual cycle that is about 60 days behind outside conditions. On this basis, ground water temperatures are near their maximum at the start. These water temperatures are similar to conditions observed in this area.

In the analyses made for the uninsulated floor with water at the depths of 3 feet, 9 inches and 5 feet, 9 inches, the initial ground temperature has been assumed to decline on a straight line from 65° F. at the surface to 60° F. at the water level. This is slightly different from the initial ground temperature profile used on the other analyses.

In all cases, the curves have been drawn for a reduction in room air temperature from 65° to 32° F. at a rate of 3° per hour, and steady maintenance of 32° F. air temperature from 11 hours onward. The curves are drawn for locations sufficiently distant from the edge to be free of edge effects. Admittedly these assumptions tend to simplify the case and it may be argued that the various factors will depart somewhat from the assumptions; but analyses based on these assumptions show a number of very important characteristics for floors in intermittently operated coolers.

The curves in figure 10 show that for the first day of operation the heat flow from all floors is extremely high because heat is coming directly from the concrete slab. After the first day, the load decreases more rapidly with the cork-insulated floors than with the uninsulated floors. After the fourth day, the cork-insulated floors reach a heat flow rate of 2 Btu/hr/sq ft and 3.2 Btu/hr/sq ft, respectively. The decline in heat flow rate is relatively slow thereafter. By the end of the fourth day, most of the heat stored in the concrete wearing floor and insulation had been removed and the heat came from the ground beneath the insulation.

Heat flow rates for the uninsulated floors decline more gradually. Most floors reach the 6 Btu/hr/sq ft rate in 7 or 8 days and some reach the 4 Btu/hr/sq ft rate in 15 to 25 days. Approximately 50 to 70 days is required to reach the 2 Btu/hr/sq ft rate. The uninsulated floors where water exists at the levels of 3 feet, 9 inches and 5 feet, 9 inches exhibit a unique characteristic. Their pulldown curves are similar to the curves for dry ground until they reach a certain point; thereafter, the curve flattens out and tends to drop only as the ground water temperature drops. When the ground water temperature increases in the late spring, the heat flow rate starts to rise. The heat flow rates for the uninsulated floor with water level at the depth of 11 feet, 9 inches compare so closely with those calculated for dry ground that the curve has not been included in figure 10.

The calculation made for heat flow where an uninsulated floor is located on a silt or clay soil is of interest. Where water is present at the level of 3 feet, 9 inches, the heat flow is not as great as with the heavy gravel soil; but where the water table is so far down as to be no factor in the analysis, the heat flow from the floor on the silt or clay soil is greater than from a floor on gravelly soil.

The shape of the heat flow curve for an uninsulated floor is dependent on both the thermal conductivity and the diffusivity of the soil upon which the building is located. Examination of the analysis used in appendix A shows that the time interval used in the construction figures is a function of the diffusivity, and a lower value for this quantity gives larger time units. In figure 10, the curves for the two different soil conditions where water level in the ground is too deep to be a factor are compared. For the most part, the curve for the example with lower diffusivity, the silt or clay soil, is similar to the other except that the time interval to get to a given heat flow value is about 40 percent greater.

The relationship of conductivity and diffusivity for various soils is important in this discussion. Figures 11 and 12 give some information on these quantities for various soils. The data on conductivity have been taken from Kersten's [*8*] work and replotted as a function of moisture for different dry densities of soil. The diffusivity values have been calculated for the various densities, moisture contents, and corresponding conductivities, using a dry soil specific heat of 0.2 and a specific heat of water of 1.0. The data are shown on two charts, one for sandy or gravelly soils, the other for clay and silt soils.

Economic Analysis of Floor Insulation

The average heat flow from each of the various types of floors has been determined graphically for a 7-month period and is given in table 4. An adjusted value of heat flow that takes account of the increase due to edge effects on a building 100 feet square is given for uninsulated floors on ground where the water level is 11 feet, 9 inches deep or lower. When the water levels are at 5 feet, 9 inches and 3 feet, 9 inches, the edge effect is not significant.

The table also indicates the load encountered with each type of floor 7 days after starting. It is assumed that the storage would be cooled for a week before loading is started. The heat flow rate at 7 days determines the load for which refrigeration capacity would be provided. The average season load determines the seasonal operation cost.

To compare the economy of various floor treatments, the operating and refrigerating equipment investment costs and the investment charges for the various floor insulation treatments are evaluated.

The economic evaluation has been based on the following factors:

1. Refrigeration equipment costs $600/T.R. capacity.
2. Total annual fixed charges on refrigeration equipment—15 percent.
3. Total annual fixed charges on insulation and subfloors—9.5 percent.
4. Average power required per T.R. capacity = 1 kw.

TABLE 4.—*Heat flow calculated from various types of floors by analytical procedure*

Description of floor construction	Average annual heat flow rate	Average annual heat flow rate adjusted for edge effect	Heat flow rate 7 days after start	Refrigeration capacity required per 1,000 sq ft
	Btu/hr/sq ft	*Btu/hr/sq ft*	*Btu/hr/sq ft*	*Tons*
Ground K 12, diffusivity 0.0445				
4″ cork under 5″ concrete finished floor and above 4″ concrete subfloor	1.225	....	1.9	0.158
2″ cork under 5″ concrete finish floor and above 4″ concrete subfloor	1.5	....	3.0	.25
5″ concrete on ground, water level much lower than 11′–9″, no edge breaker	1.95	2.14	6.5	.54
Same as above with edge breaker	1.95	1.98	6.1	.502
5″ concrete on ground, water level at 11′–9″ depth, no edge breaker	2.15	2.31	6.5	.54
Same as above with edge breaker	2.15	2.15	6.1	.502
5″ concrete on ground, water level at 5′–9″ depth	3.24	3.24	6.5	.54
5″ concrete on ground, water level at 3′–9″ depth	4.55	4.55	7.1	.59
Ground K 10, diffusivity 0.023				
5″ concrete on ground, water level much lower than 11′–9″ with edge breaker	2.5	2.5	7.6	.633

5. Average energy cost, 1.5¢ kw hr.
6. Annual operating period, 210 days=5,040 hours.
7. Installed cost of insulation in floors at 20¢/ft b.m.
8. Installed cost of subfloor beneath board insulation at 45¢/sq. ft.

On this basis, the cost of insulating a floor with 4 inches of cork board and providing a subfloor is $1.25 per square foot. The cost of 2 inches of cork board placed on a subfloor is $0.85 per square foot. The cost of a 6-inch-wide cork breaker strip, 5 inches deep, around the edge of a 100′ × 100′ room is $0.02 per square

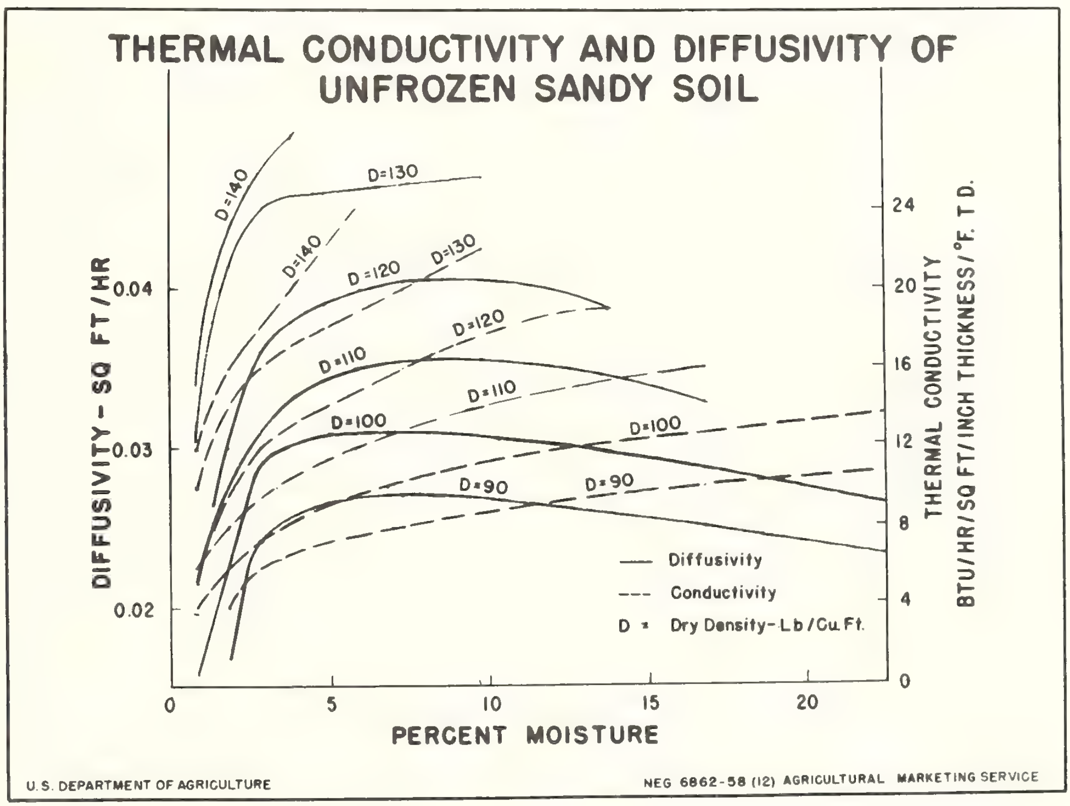

FIGURE 11

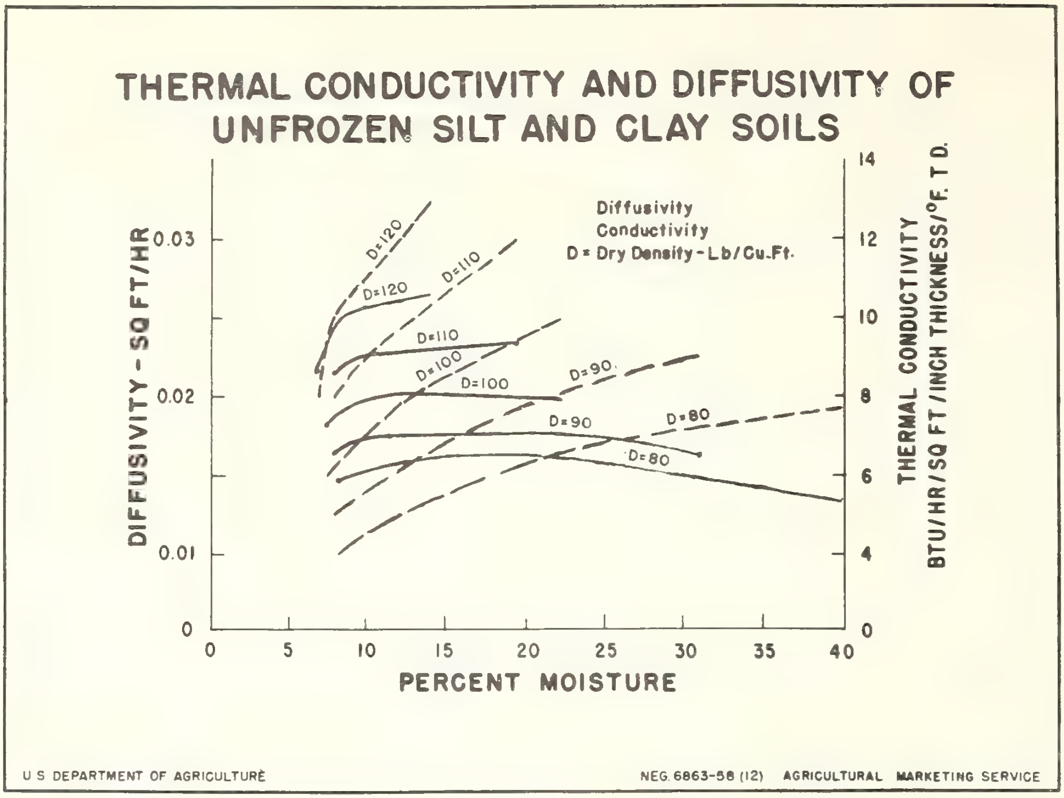

FIGURE 12

foot of floor area. This last figure will vary with room size and shape.

Storages with uninsulated floors should be operated for about a week to 10 days before loading starts, whereas a storage with insulated floors can start receiving after about 3 days. Therefore, the analysis includes an extra charge in the annual operating cost column for a week's operation for storages without floor insulation. This has been calculated on the basis of a 100- × 100-foot palletized storage room and is approximately \$5.00/1000 square feet of floor. This figure varies for different sizes and shapes of storages, but for the purposes of this analysis the figure given represents a reasonable value.

Table 5 shows the annual investment charges on the refrigeration capacity required per 1000 square feet of floor, the annual operating cost, and the investment charges for any insulation that may be involved. Total annual costs show that where ground water level is at least 11 to 12 feet below the floor, satisfactory performance may be expected at a lower cost than if insulation is used. In these cases, a breaker strip will pay for itself.

Although the total annual cost of operating an uninsulated floor, where the water level is about 4 feet below floor level, is less than the cost for the 2-inch or 4-inch cork insulated floors, another factor must be considered in this instance. Here the average season heat leakage rate is 4.55 Btu/hr/sq ft, and for the first month and a half it is between 6 and 7 Btu/hr/sq ft. These values are above normally tolerated levels of heat inflow to fruit storages. Maintenance of a satisfactory humidity in a storage where such a large heat leakage rate occurs is difficult if not impossible. Insulation would be required for this floor to maintain acceptable conditions in the storage regardless of the economic considerations. Probably the floor with water at the 5-foot, 9-inch depth would require insulation for the same reason.

RECOMMENDATIONS

The experimental and analytical results of this study may be combined to answer some questions regarding ground floor construction for intermittently operated coolers. Where ground water is close to the floor level, the experimental results at location 5 and the analytical calculations show the necessity for insulation.

The use of breaker strips for uninsulated floors located where the ground water level is

TABLE 5.—*Fixed and operating costs per 1000 square feet of floor area for various types of floors calculated from heat flow rates shown in table 4*

Description of floor construction	Annual investment charges on equipment	Annual operating cost for equipment	Annual investment charges on insulation	Total
	Dollars	*Dollars*	*Dollars*	*Dollars*
Ground K 12, diffusivity 0.0445				
4″ cork under 5″ concrete finish floor and above 4″ concrete subfloor	14.23	7.72	118.70	140.65
2″ cork under 5″ concrete finish floor and above 4″ concrete subfloor	22.50	9.45	80.70	112.65
5″ concrete on ground, water level much lower than 11′-9″, no breaker	48.60	18.50	......	67.10
Same as above with edge breaker	45.20	17.50	1.90	64.60
5″ concrete on ground, water level at 11′-9″ depth, no edge breaker	48.60	19.56	......	68.16
Same as above with edge breaker	45.20	18.56	1.90	65.66
5″ concrete on ground, water level at 5′-9″ depth	48.60	25.42	......	74.02
5″ concrete on ground, water level at 3′-9″	53.10	33.70	......	86.80
Ground K 10, diffusivity 0.023				
5″ concrete on ground, water level much lower than 11′-9″, with edge breaker	57.00	20.70	1.90	79.60

lower than the critical depth can be recommended on the basis of the analytical results. The experimental results indicate an even stronger case for the breaker strip. The observations regarding the use of perimeter insulation down the footing do not provide sufficient information to make an economic analysis; however, the economic analysis for a breaker strip shows that with an annual investment charge of $4.40 per 1000 square feet, the installation of an edge strip is a break-even proposition. On this basis, 2.3 times as much material could be installed as was contemplated in the breaker strip. Instead of using a 6-inch-wide breaker, a 3-inch breaker and footing insulation 2 feet deep could be provided and would stay within the allowable cost. Experimental data indicate that the footing insulation does reduce the edge heat flow more than a breaker in the slab; therefore, footing insulation can be justified. The width of a breaker strip should be about 6 inches, because the benefit is gained by placing additional ground in the path through which heat must pass before coming up through the floor. When the insulating material is applied as a footing insulation, 3-inch thickness should be adequate for this service and it is possible that insulating the footings for a 3-foot depth with 2-inch material would represent a more advantageous distribution of material than that suggested above.

On the basis of insulating material costs, a 3-foot-wide, 2-inch-thick perimeter ribbon could also be justified; but the problem of a base for the material must be considered. If a moisture-impervious insulation is laid on well compacted soil without a subfloor, the use of a ribbon is justified. When the cost of a subfloor for the ribbon is added, the ribbon treatment becomes less attractive.

Table 5 may be used to evaluate the allowable cost of a contemplated floor insulation for an intermittently operated cooler. Assume that the proposed insulation is known to approximate the performance of 4 inches of corkboard. From table 5, the sum of the annual investment charges on equipment, plus the annual equipment operating charge for the floor with 4 inches of cork insulation, is $21.95 per 1,000 square feet. Assume that the floor is located on gravelly soil with ground water at a noncritical level and is similar to the third item in table 5. The sum of the various charges against this treatment are $67.10 per 1,000 square feet. If the difference between the charges ($67.10 — $21.95 = $45.15) is divided by 0.095, the total of annual investment charges on insulation, an investment of $476 per 1,000 square feet is the maximum that can be justified. The amount that could be justified for insulation equal to 2-inch corkboard is $370 per 1,000 square feet when calculated in the same manner.

These figures point up one of the problems of justifying floor insulation. The cost of the subfloor is a very substantial portion of the cost and contributes nothing to the insulating qualities of the floor. Some study of conventional floor insulating methods in this type of structure should be made in order to devise a suitable construction eliminating the subfloor and using a moisture-impervious insulator directly on the ground.

The results obtained with semi-insulators such as pumice fill or pumice-concrete in these tests were quite variable. Some pumice fills tested have shown markedly lower heat flow rates than uninsulated floors while others have not shown very great advantages. The performance of the pumice-concrete floor was not much better than the average uninsulated floor. Those instances where semi-insulators have performed to best advantage have been installations where a vapor barrier was used to protect the insulation from the influx of moisture from the ground.

CONCLUSIONS

This study shows that where the ground water level is at a considerable depth beneath a floor, present insulation methods are too costly to be justified. The critical water level appears to be somewhere between 5 and 10 feet below floor level, and this is lower than the level at which insulation can be justified on a strictly economic basis. Insulation for floors where water level is critical is suggested on the basis that heat flow into the building through any surfaces should not exceed 3 to 4 Btu/hr/sq ft for any extended period, if suitable humidities are to be maintained for the storage of products susceptible to dehydration.

With all types of floors, the initial heat flow rate from the floor is very large, approximately 20 to 25 Btu/hr/sq ft. With insulated floors, a normal heat flow rate is established within 3 days, and thereafter the flow rate decreases very gradually. The heat flow rate from uninsulated floors drops more slowly and the character of the soil influences this decrease in rate. Storages with uninsulated floors should be refrigerated for a week or 10 days before receiving a large volume of warm produce.

As the season progresses, the heat flow rates from insulated floors and from uninsulated floors where the water table is 10 feet or more below the surface approach the same values. This indicates an increasing depth of soil being used as an insulator, and the thermal resistance in the insulated floors is assuming less importance in the total resistance in the heat flow path. Where ground water level is near the surface, the depth of ground available to act as an insulator is small and heat flow rates remain high for uninsulated floors.

Breaker strips in uninsulated floor slabs are definitely justified and evidence indicates that perimeter footing insulation can be justified. Horizontal ribbon-type perimeter insulation can also be justified if construction without a subfloor under the ribbon can be arranged.

Variable results have been obtained with semi-insulators such as pumice fill or pumice concrete. To obtain thermal resistance better than the ground, the semi-insulator should be protected from moisture by a vapor barrier at the lower face of the material.

An analytical method is presented for the investigation of performance of different floors under pull down and continued refrigeration during a normal apple storage season. An evaluation of the additional leakage experienced around the perimeter of uninsulated floor has been made.

Part II—Walls and Ceilings

BACKGROUND OF STUDY

In cold storage house design, the effect of daily temperature variations is not directly considered in calculating the gain in transmission heat through the walls and ceiling. The transmission loads are normally calculated on the basis of average daily temperature. Some allowance for the effect of solar loads on roofs is made by using an outside temperature several degrees higher than the ambient temperature for which the building was designed (the "design temperature"). This practice has been satisfactory with storages using the more common mass-type insulation, because the heat travels rather slowly through the insulation, which absorbs a certain amount of heat during the peak load period and releases it later. The ability of this type of insulation to store heat provides a load stabilizer for the refrigeration system.

A previous report discussed the performance of reflective insulation in fruit storage warehouses and made comparisons with conventional insulations on the basis of average daily heat flow rates [*15*]. Additional work has shown that for reflective-type insulation, daily variations of the outside air temperature and of the temperature of the outside surface of the building are important in calculating refrigeration loads and should be considered in making such calculations. In most reflective-insulated structures, the insulation mass is negligible and the only heat storage available is in the structural materials supporting or protecting the reflective materials. Reflective insulation finds its most ready application in light frame structures; consequently, very little heat storage is available and the effects of variation of heat flow are noticeable.

A study was made of the heat flow through reflective-insulated structures and through conventionally insulated structures to determine the importance of this effect, and observations are presented here.

OBJECTIVES

This study was designed: (1) To learn the performance of various types of insulation under periodic heat flow and to correlate the observed and predicted heat flow variations; (2) to obtain data in the central Washington region regarding daily variations in air temperature and surface temperatures of various types of walls and roofs; (3) to determine the proper design for use with reflective types of insulation so that maximum loads encountered under conditions for which the building was designed would not exceed those encountered with the more common mass types of insulation; (4) to secure data on the effect of joists and studs in buildings with insulation of various types; and (5) to make some estimate of the conditions under which daily variations in heat flow are significant in calculating the refrigeration load of a cold storage house.

PREVIOUS INVESTIGATIONS

Little information is available on this subject that specifically pertains to cold storage work, but the American Society of Heating and Air Conditioning Engineers (formerly known as the American Society of Heating and Ventilating Engineers) has given considerable attention to variation of heat flow into air-conditioned structures. As a result of research sponsored by that society, analytical methods are available that can be applied to cold storage structures. The reports published in the ASHAE Transactions by Mackey and Wright [*10, 11,* and *12*], the work by Johnson [*7*], and the report by Stewart [*17*] have been most helpful in connection with the present study. The basic formulas presented by those authors are given in appendix B.

PROCEDURE

Experimental Methods

Data presented in this report were obtained from tests conducted at 7 apple storages over a period of several years. Three storages (locations 1, 2, and 4) used reflective-type insulation; three (locations 5, 6, and 7) used various types of mass-type insulation; and one storage (location 3) had reflective insulation in one section and mass insulation in another section. The construction of ceilings and walls tested is described in the section giving the results of the tests at each location.

In each location, researchers made continuous recordings of inside and outside surface temperatures and heat flow from the inside surface to the room air for several days. In most cases, outside air temperature at a shielded position and outside temperature of a thermocouple enclosed in a 4-inch black ball were recorded. In some instances, intermediate temperatures at points within the insulation were recorded. Where ceiling insulations were installed beneath an attic, the air temperature in the attic was measured.

Temperatures were measured with copper-constantan thermocouples of 24-gage wire connected to a multipoint recording potentiometer through 18-gage wire. Most tests included temperature recordings at each location every 16 minutes, although some tests recorded data for each location at 32-minute intervals.

Heat flow was measured with a Gier and Dunkle heat flow meter arranged to produce a potential of 1 mv (millivolt) when subjected to a heat flow of 5.6 Btu/hr/sq ft at calibration conditions. Under the conditions of most of these tests, the heat flow to produce 1 mv is about 10 percent greater than the 5.6 rate.

The same potentiometer used to record temperatures also recorded emf (electromotive force) from the heat flow meter. In some tests, a connection within the instrument was used to indicate zero potential of the instrument, and another connection from the heat flow meter indicated the potential developed by that instrument. Most tests were conducted with the leads of the heat flow meter connected to record the emf from the meter first as an upscale deflection on the potentiometer and then as a downscale deflection. In this way the sensitivity of the heat flow meter was doubled, and any question about the accuracy of the zero potential connection was eliminated. Later, all of the various connections used in making the heat flow tests were calibrated by imposing measured potentials ranging from 50 mcv (microvolts) to 800 mcv on the recorder and checking the recorded potential against the impressed emf. Some small corrections in the observations were made as a result of this calibration, but in general these were significant only at low heat flow values.

When roof surface temperatures were measured, about 6 inches of the thermocouple wire was inserted beneath a lap in the roofing material so that conduction from the thermocouple junction to the surrounding air would be minimized. This detail is particularly important when high surface temperatures are encountered.

Analytical Methods

The individual temperature records obtained with the recording potentiometer were transcribed from the strip charts to graphs on rectangular coordinates having time and temperature scales of proportion selected to simplify the interpretation of the records obtained. Average temperature values for selected periods were obtained by measuring—planimetering—the areas under the temperature curves for the period and dividing the area by the length of period to obtain average height. This value was converted to temperature by applying the scale used in plotting the temperature curve. In some instances, heat flow values were obtained from similarly plotted and measured data; in other cases, the values for heat flow meter deflection were totaled on an adding machine and average values determined. To determine maximum heat flow values, a plot of heat flow was made in all cases, and the peak values were read from the chart.

Average heat transmittance values from the records obtained in the various structures have been determined by analysis of even multiples of 24-hour periods for as many days as the record covers. In this way, the effect of the difference in the amount of heat stored in the structure at the start and at the end of the test run is minimized. On the other hand, peak heat flow rates were studied by comparing the average and maximum values for individual days selected from the record. An effort was made to select days when the various surfaces returned to approximately the same temperature at which they started the 24-hour period, to minimize the effects of heat storage; but this was not always possible. Where the structure showed an appreciable lag in heat transmission, records were analyzed, taking this lag into account (that is, if the inside surface temperature is 6 hours behind the outside, and the average outside temperature is computed from 4 a.m. one day to 4 a.m. the next, the average inside temperature and heat flow are computed from 10 a.m. to 10 a.m.).

Overall heat transmittance values for mass-type insulators have been calculated from formulas and basic values set forth in the ASHAE Guide [*1*] and compared with test values. For reflective insulations, the values for the thermal resistance of reflective spaces have been calculated from the data given in Housing Research Paper No. 32, entitled "The Thermal Insulating Value of Airspaces" [*3*].

The author has calculated thermal resistance for a pair of spaces in accordion-type insulation and presented the results in a previous report [*15*]. These values have been recalculated by the same method, using the basic data given in H.R.P. No. 32, and the overall values are somewhat revised. Table 6 gives the revised values of thermal resistance for a pair of spaces in the accordion-type insulation when used in various positions with respect to heat flow direction.

The method of predicting maximum heat flow for a given structure and a given outside daily temperature variation is essentially the same as set forth in the reports by Mackey and Wright [*10, 11*, and *12*] and by Stewart [*17*]. Basically, this method consists of finding an equivalent decrement factor, λ_e, for the various composite walls and ceilings used, and applying this decrement factor to the amplitude in outside sol-air temperature[4] variation to determine the amplitude in heat flow variation at the inside surface. This amplitude added to the average daily flow rate gives the maximum heat flow rate.

The equivalent decrement factors are calculated as shown in the appendix by methods given in the reports mentioned [*10, 11, 12,* and *17*]. When the equivalent decrement factors are obtained, it is apparent that, for insulated surfaces approaching zero heat storage capacity, the factors are close to the line given for steady heat flow in figure 1 in the Mackey and Wright report [*10*] (reproduced as figure 31 in appendix B).

The symbols used in the following formulas and discussion have meaning and dimensions as set forth at the beginning of appendix B.

In the factor 1.65 λ_e/U used by Stewart to determine equivalent temperature differential, the value U/1.65 for each K/L value follows the steady flow line on the Mackey and Wright chart. In this report, U/1.65 is referred to as the decrement factor λ_s, and it is the decrement factor read from the steady flow line on the chart for the K/L value for the insulation. The ratio λ_e/λ_s gives a comparison between the amplitude of heat flow variation actually encountered, and that encountered with a material having the same conductivity but with no heat

[4] For definition, see appendix B, p. 54.

Table 6.—*Calculated thermal resistance per pair of reflective spaces in accordion-type insulation for 10° temperature difference per space*

Position of insulation	Direction of heat flow	Resistance per pair of spaces = 1/c	C per pair of spaces Btu/hr/sq ft °F. temperature difference
			Btu
Vertical	Horizontal	5.15	0.194
Inclined 45°	Down	5.57	.179
Horizontal	Down	5.75	.174
Horizontal	Up	3.61	.277

storage, for a given amplitude in sol-air temperature variation.

Using this ratio, the formula 11–B in appendix B for maximum heat flow for a given insulation and outside conditions is written as follows:

$$q_{max} = U\left(t_{ea} - t_i + \frac{\lambda_e}{\lambda_s}\left[t_{em} - t_{ea}\right]\right) \qquad (1)$$

Maximum heat flow for an insulation having no heat storage capacity can be calculated from the same formula using $\lambda_e/\lambda_s = 1$, in which case the formula reduces to the form:

$$q_{max} = U(t_{em} - t_i) \qquad (2)$$

When analyzing the experimental data in this report, outside surface temperature was used instead of sol-air temperature, because surface temperatures are easy to record experimentally, whereas the sol-air temperature is still in the experimental stage and development of a suitable instrument has not come to the point where a standardized form has been accepted. Actually, there is some difference between sol-air temperatures and surface temperatures; but for the two conditions that are of interest in this report, the differences are not great for most of the surfaces tested.

The deviation that may occur between sol-air temperature and surface temperature for the average daily values and the maximum values are discussed in more detail in appendix B. For walls having exterior layers that are massive and are good conductors, the use of surface temperatures in place of sol-air temperatures involves a substantial error.

To use formulas 1 and 2, the average inside air temperature can be computed by the following formula:

$$t_i = t_{oa} - \frac{q_a}{1.65} \qquad (3)$$

The maximum heat flow rates in table 7 have been calculated using formulas 1 and 3.

Comparison of Calculated and Observed Heat Flow Rates

Table 7 presents a comparison of the calculated maximum heat flow rates and those actually observed at the various experimental locations. The difference between observed and calculated values is also indicated, along with the percentage of the calculated maximum that this difference represents. Table 7 also indicates the average temperature difference between inside and outside surfaces, the maximum outside surface temperature, and the average outside surface temperature. Also noted are the average and maximum outside air temperatures during the period of observation. The actual time lag between outside maximum temperature and inside maximum heat flow are tabulated and may be compared with the calculated values given in appendix B.

The comparisons between observed maximum heat flow rates and calculated maximums show several instances of grave discrepancy, some of which can be explained. At location 1, the discrepancy for the roof calculation arises chiefly from variation of inside air temperature during the day. The calculations are based on a constant inside air temperature, and a substantial deviation from this condition will affect adversely the accuracy of predicting maximum heat flow rates by the method proposed.

Another source of discrepancy may lie in the use of thermal transmittance value determined for the overall test period at each location, rather than the transmittance observed for the particular period set forth in table 7. Because transmittance values determined for the overall period are less likely to be distorted by heat storage effects and are felt to be generally more reliable, they have been used in this table.

The disagreement between calculated and observed values for maximum heat flow through the roof at location 4 arises probably from the heat storage capacity of the heavy joists in the roof structure. In calculating decrement factors for all of the various sections where studding or joists occupied space in the insulation, the factor was calculated for the position between such members and no allowance was made for the member. This procedure is probably in error with reflective-insulation treatments, and particularly in the case of the roof for location 4. This point will be dealt with in more detail when the tests at location 4 are discussed.

Daily Variations in Air Temperatures and Surface Temperatures

The temperatures given in table 7 show that the amplitude of variation between average air temperature and maximum air temperature on the days considered varies from 8° to 25°, and the most frequent values are around 15°. This is somewhat greater variation than would be encountered in most of the United States. The ASHAE Guide, in considering the problem of periodic heat flow as it pertains to air-conditioning applications, has set up basic data on a 20° variation between maximum and minimum, which is an amplitude of 10°. This is considered normal for the major part of the central United States, but the greater amplitude observed in this area is to be expected in semiarid regions.

The relation between average and maximum surface temperature observed is much more variable, because surface absorptivity, orientation to the sun's travel, and conductivity of the various sections vary and affect this relation. The figures are presented as being representative of what may be encountered under various conditions. The data presented in table 7 were selected from cloudless days when solar radiation was high.

Discussion of Tests at Individual Locations

Figure 13 shows sections through the various walls and ceilings tested. Locations 2, 3, and 5 are the same storages designated by these numbers in a previous report by the author [*15*].

Location 1

Location 1 is a 50,000-box storage used for cooling and holding unpacked apples harvested from a large orchard, before the fruit was moved to the packinghouse and main cold storage. Normally this storage operates about 4 months of the year. The construction was selected to minimize initial cost, and was very light compared to that of many conventional structures. Pumice-block walls were insulated by using prefabricated frame sections with accordion-type reflective insulation placed between the studs. Figure 14 shows one of the prefabricated wall sections before it was placed inside the building. The foil side of the insulation faces the pumice-block wall and the hardboard face is the inside room surface. All roof and wall sections were prefabricated outside the building and moved into position as construction proceeded. After fabrication, roof sections were lifted into place, nailed to the roof trusses, and then covered with corrugated aluminum roofing. This roof structure was of the lighest construction tested. It represents as light a structure as will be encountered in fruit storage.

Table 8 and figures 15 and 16 present the details of the heat flow rates and temperatures obtained at this location. From this test, it appears that the wall is performing satisfactorily, but the ceiling does not have the anticipated thermal resistance. The maximum rate of heat flow through the walls occurs 7 or 8 hours

Table 7.—*Temperature difference, average and maximum surface and outside air temperatures; average and maximum observed and calculated heat flow rates for various locations tested*

Location and surface	Date	Average temperature difference $T_{sa} - T_i$	Average outside surface temperature T_{sa}	Maximum outside surface temperature T_{sm}	Average outside air temperature T_a	Maximum outside air temperature T_m	λ_e/λ_s	Observed transmission U' [1]	Heat flow—Btu/hr/sq ft: Average q_a	Heat flow: Maximum observed q_{max}	Heat flow: Maximum calculated q_{max}	Heat flow: Difference between maximum calculated and observed		Observed time lag	Observed diurnal variation in room temperature
		°F.	°F.	°F.	°F.	°F.		Btu/hr/sq ft/°F.td.	Btu	Btu	Btu.	Btu	Pct.	Hrs.	°F.
Location 1:															
Roof	Oct. 10–11, 1952	24.8	64.3	102.	61.4	86.5	1.0	0.0943	2.28	5.08	5.89	+0.81	+13.8	1	8 to 9.
Wall	Oct. 7–8, 1952	31.7	68.6	107.	61.9	86.0	.358	.0408	1.25	1.91	1.86	−.05	−2.7	7	
Location 2:															
Ceiling under attic	June 3–4, 1953	31.6	62.4	74.5	63.0	78.0	1.0	.0242	.81	1.19	1.07	−.12	−11.2	1	0.5 holding, 2 receiving.
Ceiling under sloping roof	June 7–8, 1953	28.6	60.5	83.0	55.8	68.0	1.0	.0415	1.20	2.06	2.12	+.06	+2.8	0	
	June 5–6, 1953	36.4	69.1	96.	61.6	75.	1.0	.0415	1.49	2.50	2.63	+.13	+4.9	0	
Wall	June 11–12, 1953	41.6	73.6	93.0	69.1	78.0	1.0	.0344	1.39	2.12	2.10	−.02	−1.0	1	
Location 3:															
Aluminum—painted roof	Sept. 26–27, 1953	22.5	54.4	90.0	52.5	66.0	.645	.0458	1.14	2.34	2.08	−.26	−12.5	6	1 to 1½.
	Oct. 2–3, 1953	19.9	51.6	88.5	51.4	63.5	.645	.0458	.88	2.13	2.00	−.13	−6.5	6	
Black roof	Oct. 5–6, 1953	26.5	58.5	116.0	54.8	73.5	.645	.0512	1.25	2.70	3.25	+.55	+16.9	6	
	Oct. 7–8, 1953	28.2	60.8	101.0	59.2	74.0	.645	.0512	1.25	2.62	2.77	+.15	+5.4	6	
	Oct. 11–12, 1953	21.6	51.9	102.5	50.8	70.0	.645	.0512	1.13	2.40	2.78	+.38	+13.7	6	
N. wall	Sept. 8–9, 1956	33.1	63.1	69.5	......	......	.659	.0290	.92	1.01	1.08	+.07	+6.5	3	½.
	Sept. 9–10, 1956	32.0	61.8	69.0	......	......	659	.0290	.90	1.06	1.07	+.01	+1.0	3	
Location 4:															
Roof	Apr. 21–22, 1955	19.6	51.0	78.0	47.6	55.5	.987	.0415	1.02	1.77	1.92	+.15	+7.8	2.5	1.
	May 7–8, 1955	42.2	72.6	120.0	58.7	75.0	.987	.0415	1.81	2.88	3.70	+.82	+22.2	2.5	
Wall	Apr. 30– May 1, 1955	34.0	65.8	98.0	54.1	67.0	.681	.0625	2.2	3.59	3.49	−.10	−2.9	3	
Location 5:															
Ceiling under attic	May 19–20, 1951	42.2	75.7	95.0	64.7	75.0	[2]	.0100	.42	.42	.422	+.002	+.5	24	0.
Location 6:															
Roof	May 25–26, 1956	60.7	93.7	175.0	67.5	81.0	.591	.0243	1.56	2.91	2.65	−.26	−9.8	6	2.
Wall	May 16–17, 1956	45.4	79.1	112.0	72.5	91.0	.616	.0331	1.70	2.28	2.18	−.10	−4.6	7	
Location 7:															
Ceiling under attic	Aug. 12–13, 1952	31.9	81.5	108.5	83.2	98.0	.896	.080	2.56	4.27	4.49	+.22	+4.9	2	2 to 2½.
	Aug. 14–15, 1952	28.0	78.0	98.0	77.3	91.0	.896	.080	2.20	3.65	3.67	+.02	+.6	2	
	Aug. 16–17, 1952	20.4	71.7	97.0	68.8	84.5	.896	.080	1.63	3.37	3.45	+.08	+2.3	2	
	Aug. 17–18, 1952	24.9	74.8	100.5	73.0	88.5	.896	.080	1.98	3.50	3.83	+.33	+8.6	2	
Wall	Aug. 8–9, 1952	36.8	83.9	98.0	81.7	98.5	.234	.063	2.27	2.81	2.53	−.28	−11.1	12	

[1] U' values taken from tables 8 through 14 and adjusted to include inside film coefficient $h_o = 1.65$.

[2] Less than 0.01.

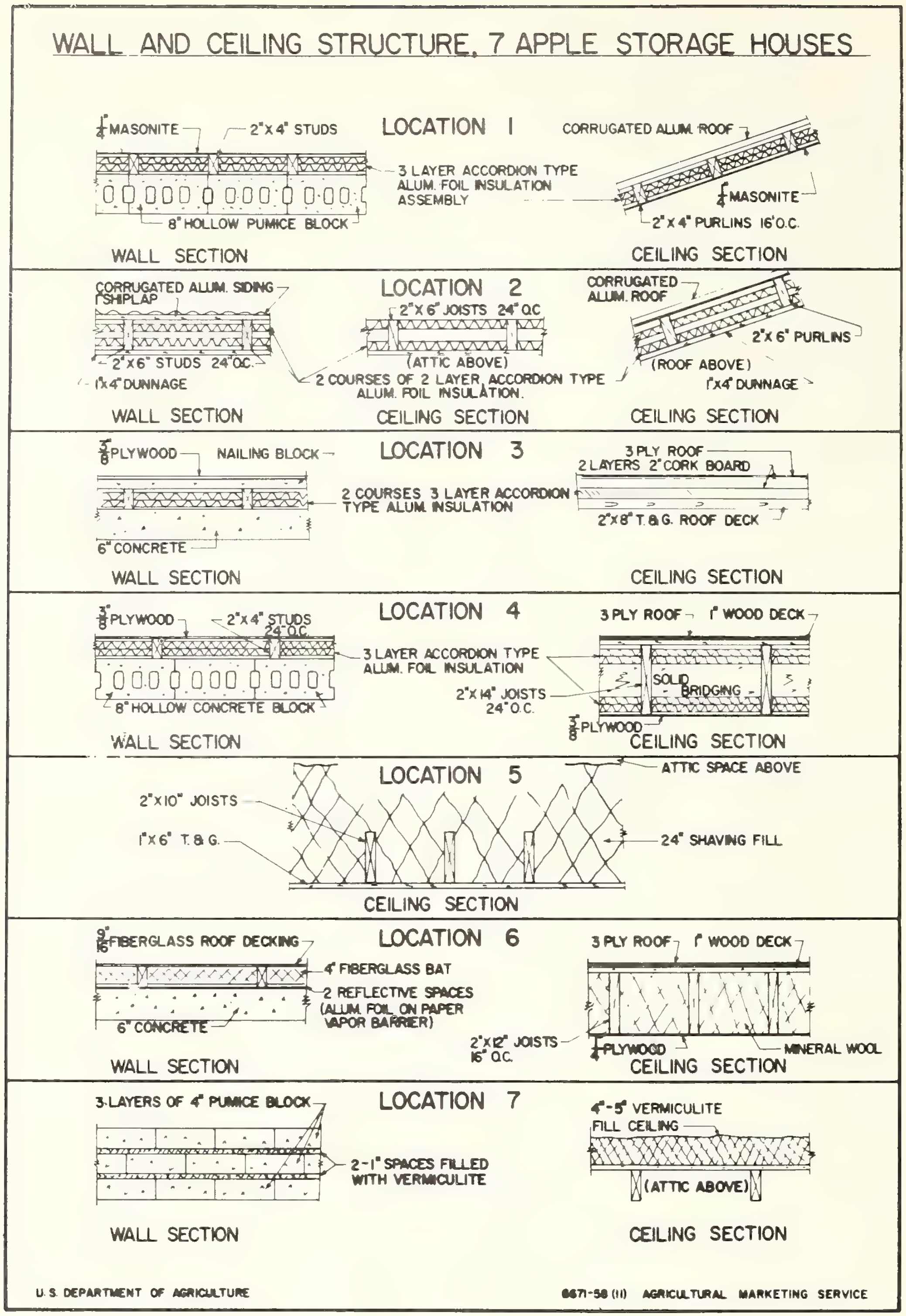

FIGURE 13

after the time of maximum outside surface temperature, whereas maximum heat flow from the roof section practically coincides with the time of maximum roof surface temperature. At the time of the test, desired storage temperature was difficult to obtain. Part of the difficulty was due to restrictions in the eliminators in the cooling units, reducing the air quantity circulated

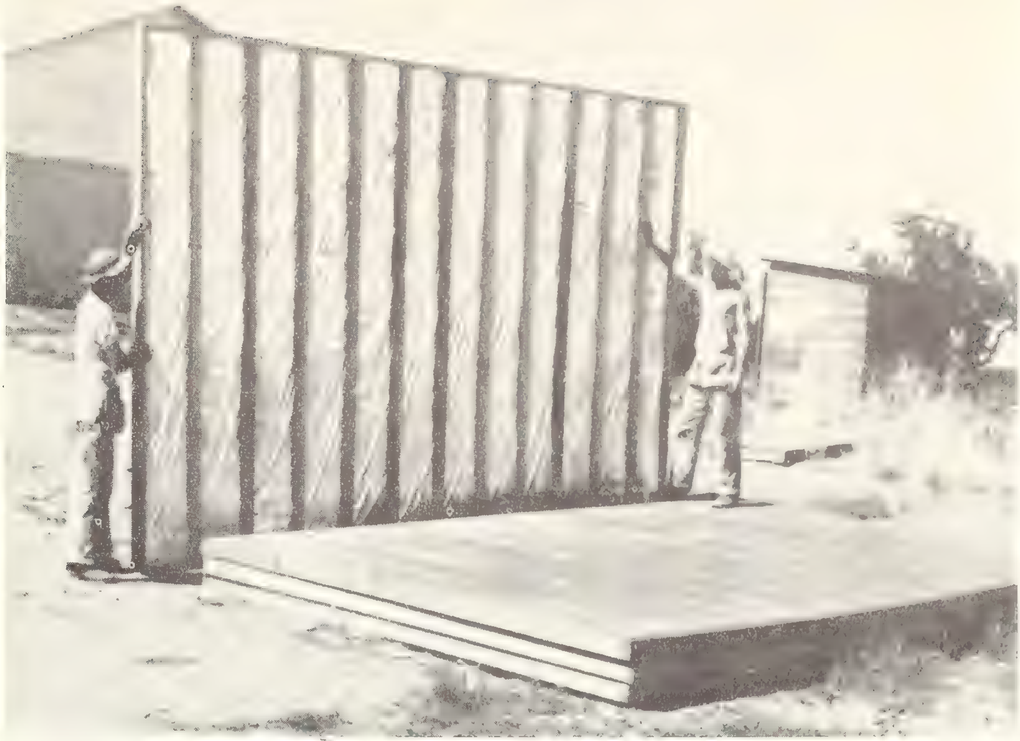

FIGURE 14.—*Prefabricated insulated wall section used at location 1.*

and consequently decreasing the refrigeration capacity. It was also found that floor heat leakage was much higher than was anticipated; however, the fact that the inside air temperature starts to rise at the same time the ceiling heat flow rate starts to increase, and reaches a maximum very shortly after the heat flow through the ceiling does so, indicates that heat flow through the ceiling is a very serious factor in the plant load. The original design calculations for the storage had anticipated that, with an average 40° temperature difference through the roof, the average heat flow would approximate 2 Btu/hr/sq ft. Since something more than this value was experienced with a difference of 22.6°, there was a decided deficiency in the insulation. When the maximum heat flow rate of more than 5 Btu/hr/sq ft is combined with the circumstance described, the fluctuation of inside temperature becomes understandable.

Several factors probably contributed to the poor performance of the ceiling insulation. First, the corrugated aluminum roofing was not sealed at the edges of the building, and allowed air to pass between the roofing and the upper face of the foil insulation. This probably destroyed much of the insulating value of this upper space by allowing for more heat transfer by convection than would be experienced with natural air currents. At the same time, it is doubtful that enough air could pass through this space to carry away a substantial portion of the heat being transmitted by the under side of the roofing.

TABLE 8.—*Average temperatures, heat flow, and transmittance through wall and roof at location 1*

Factor observed (averages)	Unit	Period No. 1 Oct. 6–10, 1952 east wall location	Period No. 2 Oct. 10–13, 1952 roof location
Outside air temperature	°F.	61.9	63.0
Outside black ball temperature	°F.	66.0	67.3
West roof deck temperature	°F.	63.4	66.0
East wall temperature	°F.	66.8	....
Inside surface temperature (heat flow meter temperature)	°F.	38.8	43.2
Inside air temperature 1 ft. from heat flow meter	°F.	35.3	....
Inside air temperature returning to cooling unit	°F.	34.8	38.1
Temperature difference outside to inside surface	°F.	28.0	22.8
Heat flow—Btu/hr/sq ft	Btu	1.17	2.30
Observed U′—Btu/hr/sq ft/ °F. Td	Btu	.0418	.101
Calculated U′—Btu/hr/sq ft/ °F. Td	Btu	.0404	.0575

Poor installation also was responsible for the increased transmittance. The insulating ma-

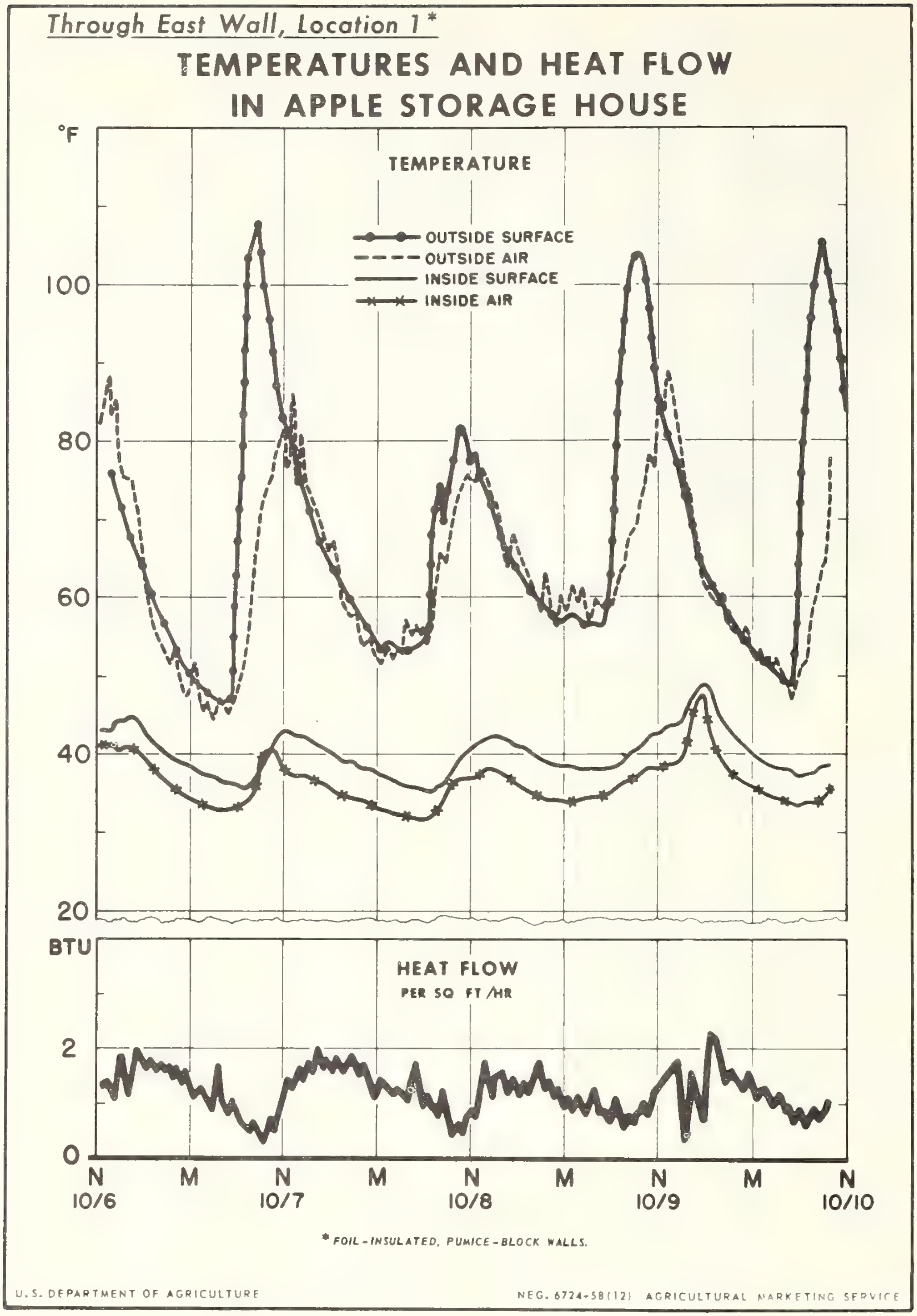

FIGURE 15

terial had been stapled to the purlins and the flanges of the assembly had not been held continuously against the purlins by a lath or some other kind of batten. This left places between staples where the material could bow and open up passages from the warm side to the cold side of the insulation. The existence of such openings and the configuration of the material between the horizontal purlins was such that a circulation was possible from the space between

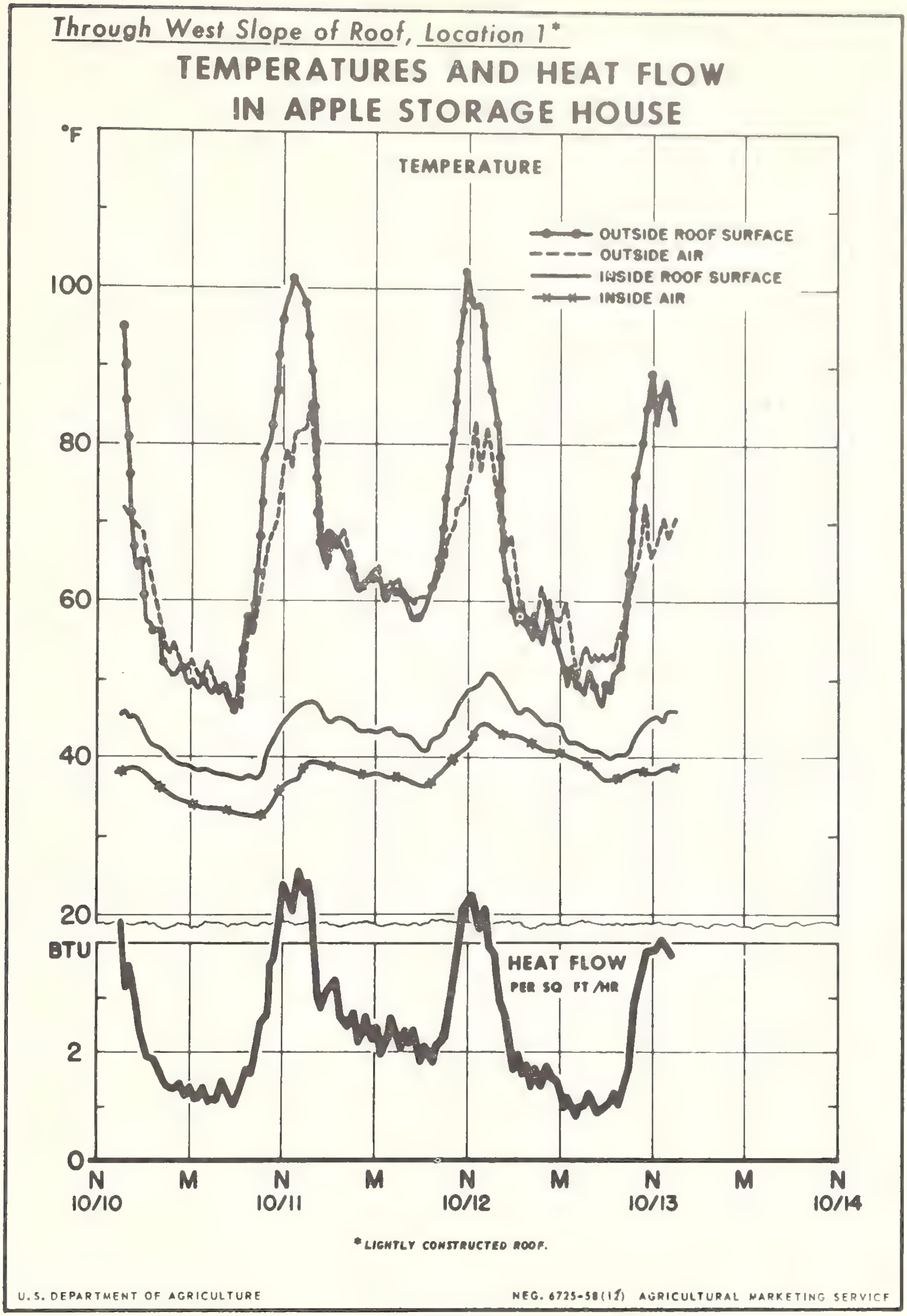

FIGURE 16

the roof cover and outer foil layer to the space between the inner foil layer and the Masonite sheathing on the inside of the building.

To check this possibility, one thermocouple was inserted into this last air space near the upper end of a division formed by a purlin, and another thermocouple was inserted in the same space in the lower end of a division formed by a purlin. At night when the heat flow rate was around 1 Btu/hr/sq ft, the two locations were at the same temperature. As the heat flow increased, the temperature at the upper end of the purlin space became higher than that at the lower end, and at the time of maximum flow was approximately 3½° higher than at the lower end.

Increased convection in the first reflective space and air passage from warm to cold side of the insulation appeared to be the major cause of deficiency in this roof insulation. Some improvement was obtained by cutting a trim strip on a band saw to match the contour of the corrugated roofing and closing the spaces left where the roofing rested on the building walls. Nothing could be done about battening the flanges of the insulation to the purlins, but this experience certainly points to the importance of such a procedure.

It is the writer's belief that an additional course of 3-layer accordion-type insulation should be applied to wood spacers fastened to the underside of the ceiling. As a result of these tests, it has been recommended that two courses of 3-layer insulation should be used directly under roofs for this kind of storage. Location 4 embodies such a construction and will be compared with location 1 when the tests at location 4 are discussed.

Location 2

Location 2 is a foil-insulated storage that has been described in a previous report [*15*]; but the data on this location were taken after two seasons of operation, whereas those previously reported were taken soon after construction of the storage house. Part of the purpose of this second test was to determine whether any measurable change had taken place in the conductance of the insulation during 2 years of operation.

Table 9 and figures 17 and 18 present the data obtained on temperatures and heat flow at location 2. At this location, the observed thermal transmittance values, observed U′, for walls and ceiling under the attic were much lower than the originally calculated thermal transmittance values, (calculated U′). These transmittance values also are lower than those observed at the time of the original test when the plant was new. Investigation of a possible explanation for this situation shows that the insulation is subjected to a certain amount of wind pressure at various times. On the ceiling under the attic, this action has billowed out the foil so that a space 1½ to 2 inches between each foil layer and its paper separator is common and the top layer is actually billowed upward above the tops of the ceiling joists. This action of providing more separation between the layers is particularly effective with ceiling insulation. When the U′ value is calculated on the basis of 2 inches of separation between layers in the insulation, a value reasonably close to that given by the test is obtained. To some extent, the same action has taken place in the sidewalls, and here also a lower U′ value is obtained when there is complete separation between the layers of foil and paper.

From the results obtained in these tests, it appears that the insulation value had not deteriorated during the period of use. The fact that certain mechanical changes had taken place to provide better separation of the various layers of material was entirely accidental, but should give some clues for possible improvement of this type of insulation.

The comparison between the performance of the portion of the ceiling under the sloping roof at location 2 for June 5–6, 1953 and the ceiling at location 1 as given in table 7 is interesting. Although the average temperature difference is somewhat greater at location 2, the average heat flow is only about two-thirds of that at location 1. The outside surface temperature at location 1 reached 102° and that at location 2 rose to 96°. The maximum temperature difference was actually 62.5 for location 1 and 63.3 for location 2; yet the maximum heat flow at location 2 was

TABLE 9.—*Average temperatures, heat flow, and transmittance through walls and ceiling at location 2*

Factor observed	Unit	Period No. 1 June 2–4, 1953 on ceiling under attic	Period No. 2 June 5–8, 1953 on ceiling under sloping roof	Period No. 3 June 8–11, 1953 on south wall	Period No. 4 June 11–12, 1953 on south wall
Outside air temperature	°F.	60.4	58.7	64.8	69.1
Outside black ball temperature	°F.	68.6	65.0	75.8	73.5
Outside roof temperature	°F.	67.4	62.7	......	......
Outside wall temperature	°F.	......	......	74.1	73.6
Under side roof temperature	°F.	66.2	......	......	......
Attic air temperature in vicinity of heat flow meter location	°F.	61.8	......	......	......
Temperature of top of foil in attic	°F.	59.5	......	......	......
Inside surface temperature	°F.	31.2	33.0	32.9	32.9
Inside air temperature returning to cooling coils	°F.	30.5	30.0	30.6	......
Temperature difference across insulation	°F.	28.3	29.7	41.2	40.7
Heat flow—Btu/hr/sq ft	Btu	.75	1.26	1.49	1.39
Observed U′—Btu/hr/sq ft/°F. Td	Btu	.0246	.0425	.0362	.0342
Calculated U′—Btu/hr/sq ft/°F. Td	Btu	.0282	.0418	.0396	.0396

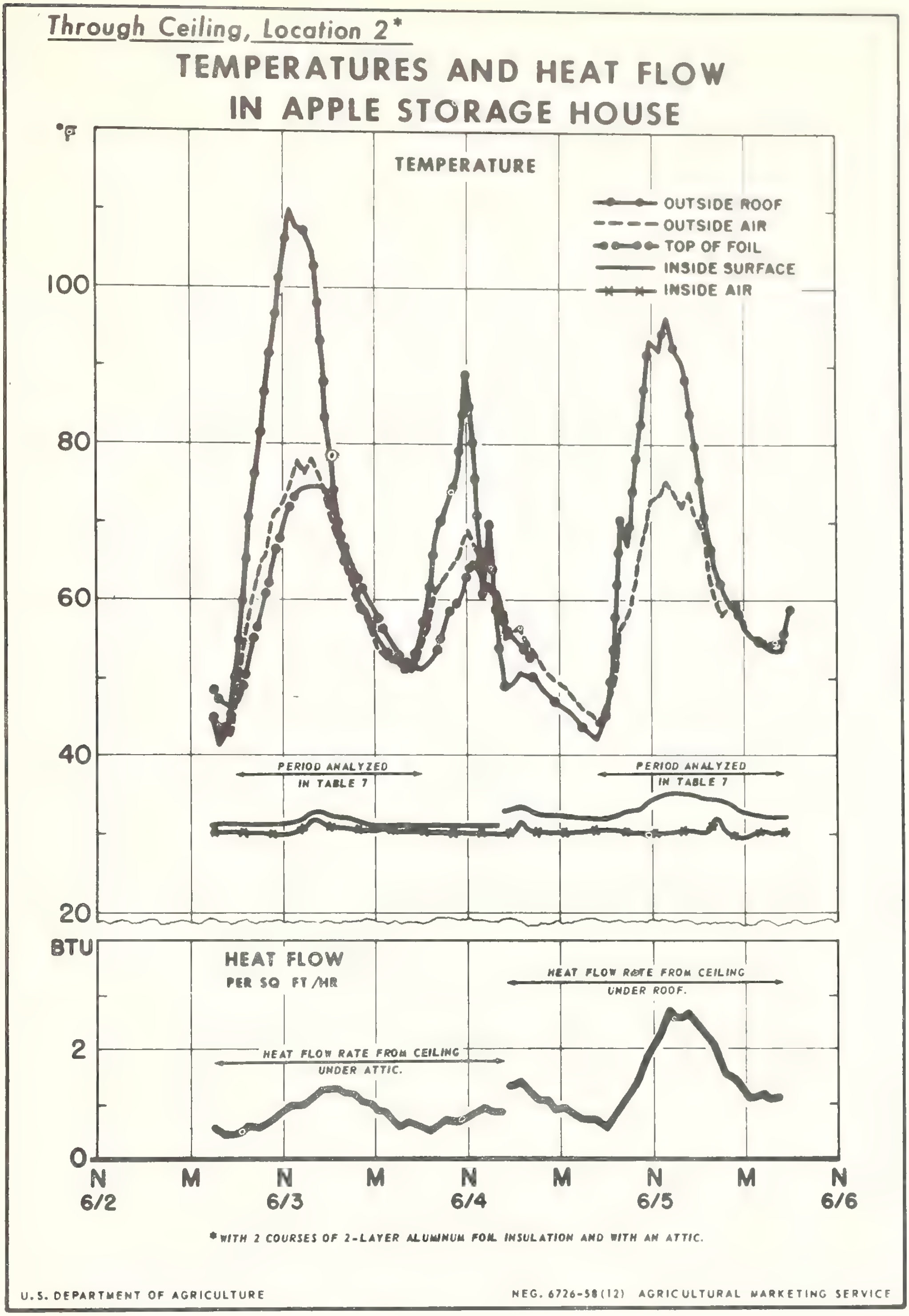

FIGURE 17

only half that experienced at location 1. At location 1, the arrangement of 3 sheets of aluminum and 2 paper separators in the structure provided 6 reflective spaces. At location 2, the arrangement of 4 sheets of aluminum and 2 paper separators and no interior sheathing also provided 6 reflective spaces plus a discontinuous space between the corrugated roofing and the roof deck. Such a difference between performance of the same make of material at the two

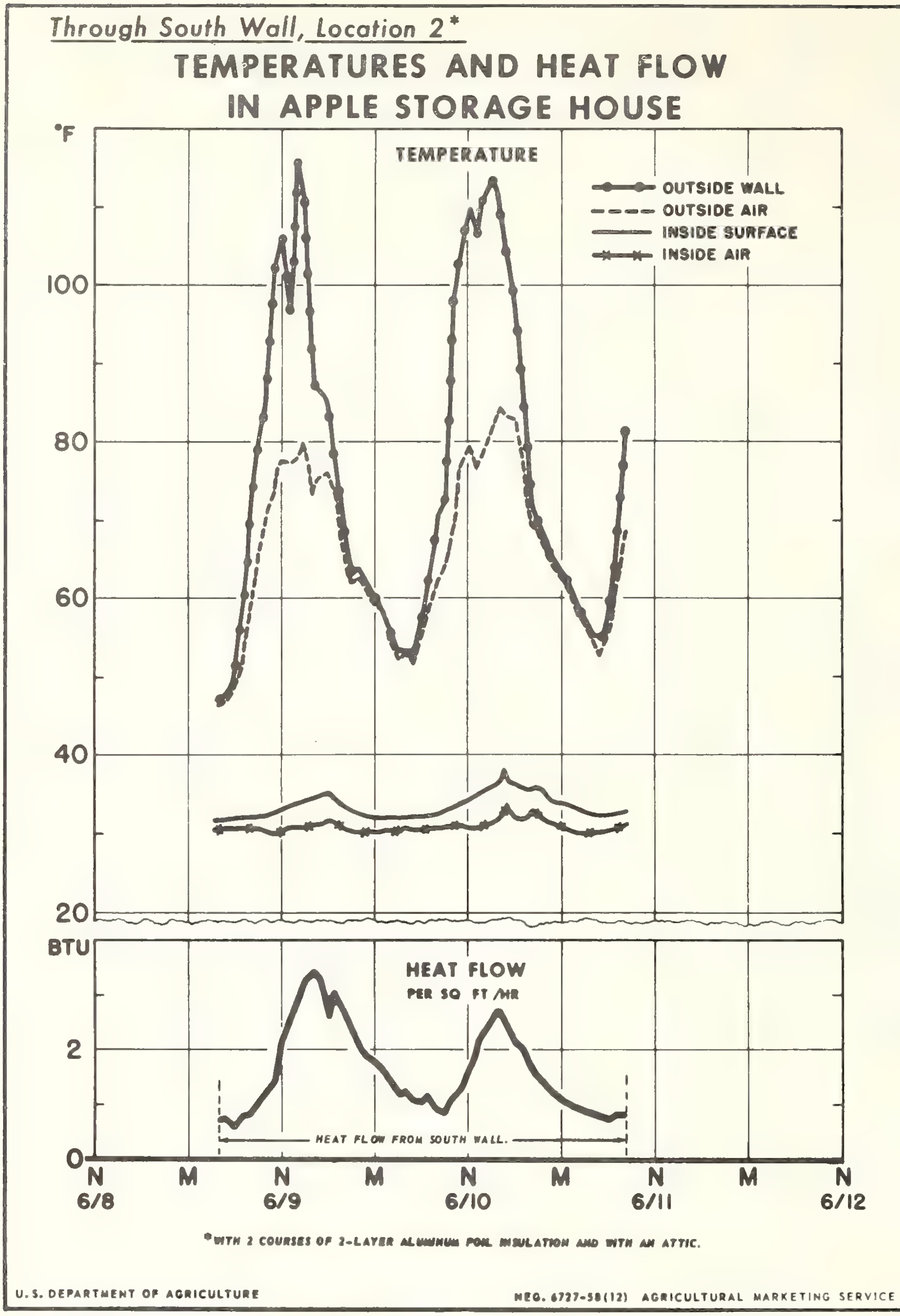

FIGURE 18

locations indicates that workmanship and attention to detail are important factors in the installation of this material, just as they are with any other commonly used insulating material.

The comparison of the performance of insulation under the sloping roof at location 2 for June 7, 1953 with the roof insulation at location 3 for Sept. 26, 1953 gives some index of the ability of the insulation at location 2 to cope with periodic loads. These 2 days were rather similar as far as average and maximum outside air temperatures are concerned. The maximum roof temperature at location 2 is 83° and at location 3 is 90°. The average surface temperature and average temperature difference through the insulation at location 2 is the greater. The maximum temperature difference at location 3 is 58.1° compared to 51.1° at location 2. The average heat flow at location 2 is slightly more than at location 3, but the maximum observed is less. The calculated maximum for the two roofs for these days would be rather close together. It appears that the two roof sections would experience comparable maximum values at operating conditions that are normal for this type of storage. On this basis, it is reasonable to expect that a reflective-insulated roof similar to the one tested would be adequate for operation as an apple storage, where operation during the hot months of August and early September are not required.

Location 3

At location 3 is a very large palletized storage. The roof insulation tested is 4-inch-thick sheet cork laid in two layers above a 2 × 8 tongue-and-groove wood deck. The roofing is applied above the cork. Thermocouples had been placed at the bottom, middle, and top of the cork when the storage was built, and some tests at these locations have been described in previous reports [*14*]. The data submitted here are additional data, more recently obtained, to compare roof insulation performance when the roof is black and when it has a coat of aluminum paint. During the first 8 days of the test run, the roof had a coat of aluminum paint. Then for the last 7 days of the run, a 10-foot-square section of the roof where the thermocouple and heat flow meter were located was painted black.

At location 3, a room had been added, with walls insulated with two courses of accordion-type aluminum foil, each course having three sheets of aluminum. The outside wall is of 6-inch concrete, and the inside of the room is finished with 3/8-inch plywood. The studding that carries the foil in this wall is not sufficinetly deep to provide spaces between foil courses and between foil and inside wall. These additional spaces should have been provided to secure maximum thermal resistance from the material installed.

The results of the tests on the roof at location 3 are given in table 10. Figure 19 shows a typical portion of the record obtained when the roof had a coat of aluminum paint and a part of the record when the roof was painted black. During the period when the roof was painted black, several failures of the recorder chart feed mechanism occurred, so that the data are not continuous for the full period. Therefore, the data have been recorded for three shorter periods, each of which comprises units of one or more 24-hour periods. The U′ values obtained from each period are then averaged, with each period weighted in the proportion that it bears to the total time.

This test was conducted primarily to compare the effect of the two types of paint on the roof. Unfortunately, the weather was appreciably warmer during the latter part of the test when the roof was painted black, and at first glance there seems to be more difference in performance than is actually revealed by closer examination of the data.

A determination of the observed U′ value for the roof shows a lower value during the first period than during any of the succeeding periods when the roof was painted black. This difference is about 6 percent and may represent experimental error. No thermocouples were

Table 10.—*Temperatures, heat flow, and transmittance through ceiling at location 3*

Factor observed (averages)	Unit	Roof with aluminum paint Sept. 25–Oct. 3	Roof painted black			Weighted average for 3 periods on blackpainted roof
			Oct. 5–6	Oct. 7–8	Oct. 9–11	
Outside air temperature	°F.	51.7	54.8	59.2	56.5	....
Outside black ball temperature	°F.	54.0	57.8	60.9	58.5	....
Top of cork temperature	°F.	52.1	58.5	60.8	57.5	....
Middle of cork temperature	°F.	44.6	48.7	50.6	48.2	....
Bottom of cork temperature	°F.	35.9	37.3	38.6	37.4	....
Inside ceiling temperature	°F.	32.2	32.8	33.4	32.7	....
Temperature difference across section	°F.	19.9	25.7	27.4	24.8	....
Heat flow—Btu/hr/sq ft	Btu	.92	1.275	1.295	1.232	....
Observed U′—Btu/hr/sq ft/°F.Td	Btu	.0462	.0496	.0473	.0497	0.0491
Calculated U′—Btu/hr/sq ft/°F.Td	Btu	.0584	.0584	.0584	.0584	.0584
Temperature difference between outside air and inside ceiling surface	°F.	19.5	22.0	25.8	23.8	....
Apparent "U" based on outside temperature—Btu/hr/sq ft/°F.Td.	Btu	.0472	.058	.0502	.0517	.0529
Ratio Td. across section / Td. outside air to inside surface	Pct.	102	117	106	104	108

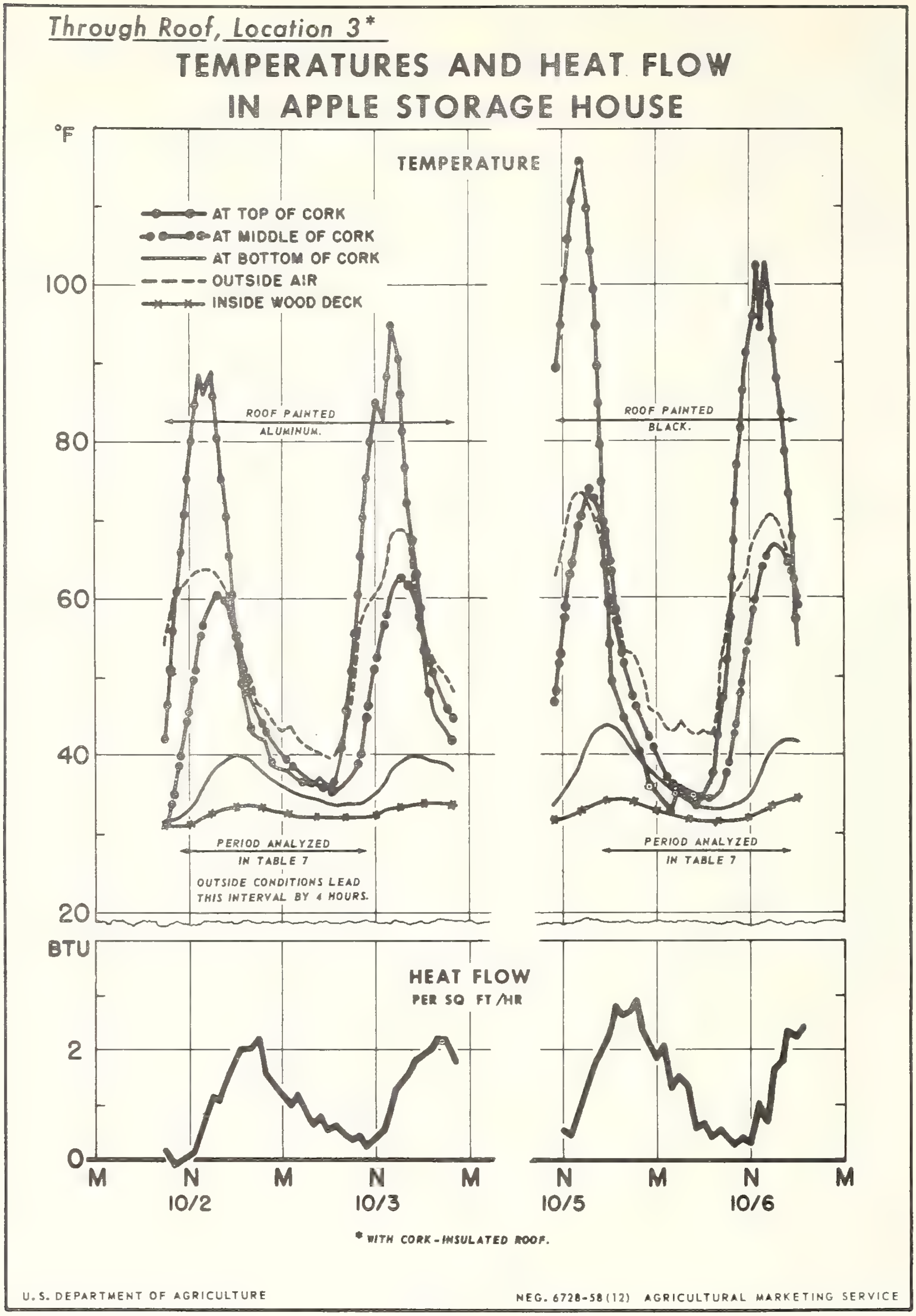

FIGURE 19

changed during the entire test, the heat flow meter was not moved and the only change was to paint the section of the roof where the test apparatus was located. Although the second series of tests were conducted with a mean temperature slightly higher than the first test, and the maximum surface temperatures encountered were considerably higher, it does not seem likely that increased conductivity of the insulation associated with operation at higher temperatures would account for this much difference.

An apparent heat transmittance value was determined, based on temperature difference between outside air temperature and inside surface temperature. When these U values are adjusted for the 6 percent difference that exists in the true values determined from surface temperatures, a difference of about 5 percent exists in favor of the aluminum roof. A similar result is obtained if the ratio of difference between outside and inside surface temperatures and difference between outside air and inside surface temperature is compared. From this we may conclude that an aluminum-painted roof, located in an area where it does not become rapidly discolored due to soot and other impurities settling out of the air, will decrease the average daily heat transmission load by about 5 percent. Indications are that for periods of high solar intensity the decrease may be greater than this (note the record for October 5, 1956). It should also be noted that maximum roof surface temperatures are decreased by the aluminum paint and this may contribute to longer life of the roof.

Since 4-inch sheet cork is considered a standard insulation for cooler storage, observance of maximum heat flow at this location serves to define an acceptable variation in heat flow for installations of this type. The average outside air temperatures encountered throughout the tests are somewhat lower than the normal outside design temperature of 65° for apple storages. In table 7, examine the data for the period October 7 through 8 when the outside air temperature averaged 59.2°. The average heat flow measured was 1.25 Btu/hr/sq ft and the maximum was 2.62. If the average heat flow were adjusted for an average 65° outside air temperature, the average heat flow would be 1.5 to 1.6 Btu/hr/sq ft. Normal calculated design would make an allowance for solar radiation by using 75° roof temperature and 32° room temperature, or a temperature difference of 43°. Using the observed U′ values, this would yield a design load of $43 \times 0.0491 = 2.11$ Btu/hr/sq ft, which is average daily load.

From this comparison, it appears that normal design procedures, using an arbitrary allowance for solar radiation, produce an average expected heat flow that is intermediate between the average and maximum flow encountered. Actual maximum heat flow is probably about 50 percent greater than average design heat flow. The actual maximum heat flow as shown in table 7 is slightly more than 100 percent greater than the observed average. The fluctuation in heat flow through this type of roof is greater than one would expect for satisfactory operation; but little trouble has been experienced because the factors used tend toward overestimating the average heat transmission load.

Table 11 presents the data of the test on the wall at location 3. Figure 20 shows the record obtained. In this test, the heat flow meter was located behind the plywood facing that is the interior surface of the room. This location resulted in a steady operation of the heat flow meter, comparatively undisturbed by the rapid variations in room air temperature which often operate to produce substantial variations in the amount of heat passing through meters mounted directly on the interior surface of the room. This location was on a wall facing northeast, subject to sun effect for only a short while in the morning. The diurnal variations of exterior wall surface temperature were rather slight and the variation in heat flow rate was small.

At this location, an error was made in the selection of stud size to carry the inner layer of prefabricated foil, the stud depth being the same as the foil assembly depth, 2½ inches. If 2- by 4-inch inner studs had been used, placed on edge, the wall thickness would have been 7¼ inches, allowing space for the two foil assemblies plus a ¾-inch space between outer wall and first assembly, a ¾-inch space between assemblies, and a ¾-inch space between the second foil assembly and the inner wall. As the building was constructed, only the space between the outer wall and the first foil assembly exists. Addition of the spaces between assemblies and between the inner wall and the second foil assembly would add to the thermal resistance of the wall.

TABLE 11.—*Temperatures, heat flow, and transmittance through wall at location 3*

Factor observed (averages)	Unit	Period Sept. 5–10
Outside wall temperature	°F.	60.7
Temperature between foil assemblies	°F.	40.0
Inside stud face temperature	°F.	35.3
Temperature of foil side of plywood	°F.	32.3
Temperature of room side of plywood	°F.	31.6
Inside air temperature	°F.	30.3
Temperature difference from outer wall surface to inner wall surface	°F.	29.1
Heat flow—Btu/hr/sq ft	Btu	.86
Observed U′—Btu/hr/sq/ft/°F Td.	Btu	.0295
Calculated U′—Btu/hr/sq ft/F. Td.	Btu	.0355

Location 4

The building at location 4 is a medium-sized storage using prefabricated accordion-type reflective insulation in the walls and ceiling. The outside walls are 8-inch concrete block. Stud-

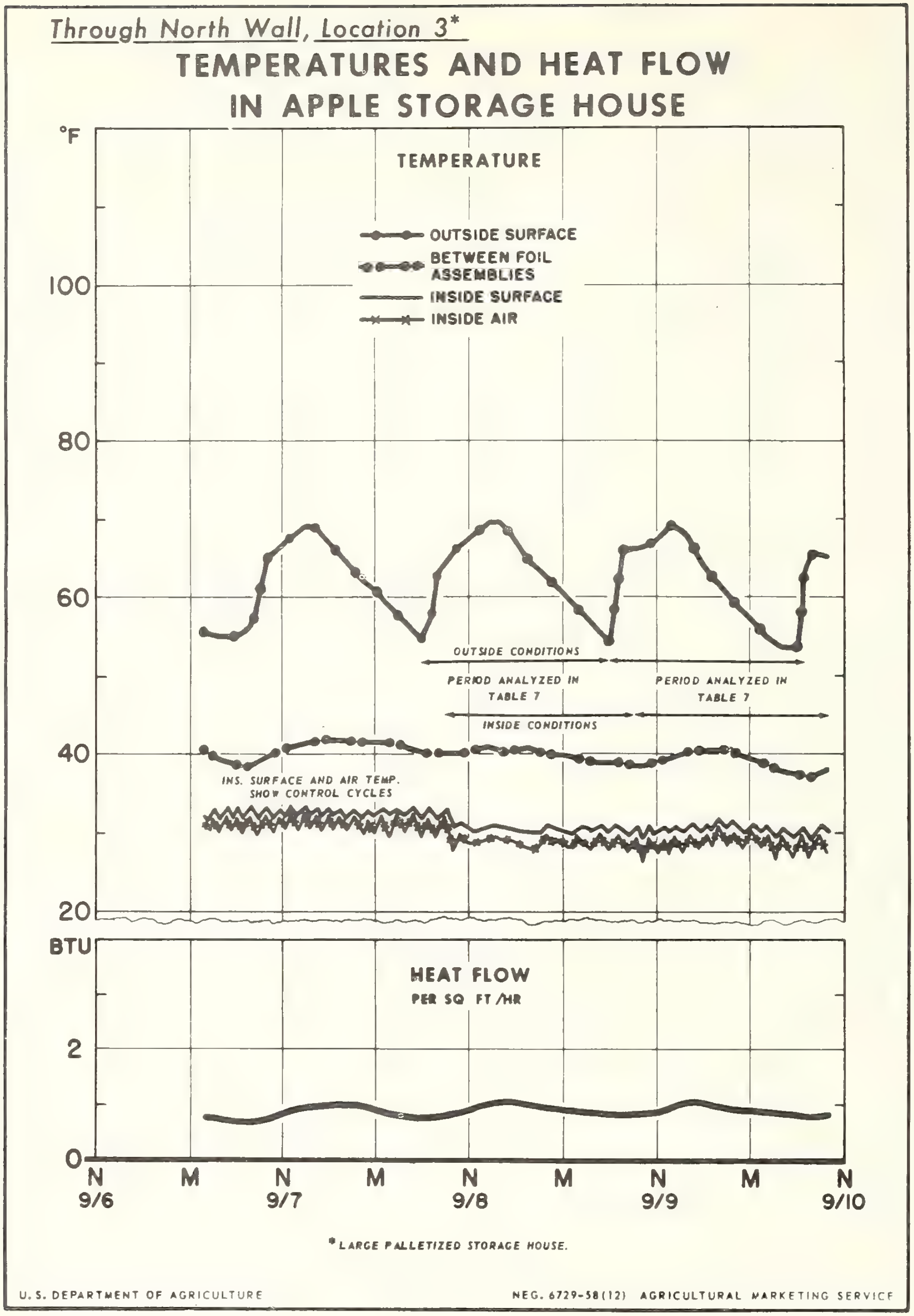

FIGURE 20

ding, placed 24 inches on centers, supports one course of the prefabricated foil assembly that has three sheets of aluminum. Studs are arranged so that a space is provided between the outside block wall and the first layer of aluminum and between the 3/8-inch interior plywood wall and the last layer of aluminum. Ceiling insulation is placed directly under the roof deck in spaces formed by 14-inch-deep roof joists. Two courses of the three-layer prefabricated foil are used, one course with the upper face about 1 inch below the plywood roof deck, and the other course spaced with the lower face about an inch above the plywood sheathing that forms the inside ceiling of the room. The roof deck is covered with a three-ply builtup roof and has a coat of aluminum paint.

The building at location 4 was tested because it represented modifications in selection and arrangement of accordion-type reflective insulation assemblies based on the experience at location 1, which had indicated the need for more insulation to resist high solar loads on roofs.

The results at this location are set forth in table 12, and selected portions of the test are shown in figures 21 and 22.

The difference in effect of the studding on the heat flow pattern through the wall and that observed for the ceiling deserves comment. On the wall, the transmittance determined by the test at midpoint between joists is reasonably close to the calculated value. Observed transmittance at the stud location is close to the calculated value through this section. The heat flow is high on the stud, intermediate at the quarter point, and low at the midpoint, and the transmittance values show this relationship also. On the ceiling, the heat flow for all positions is about the same for the first three test periods when the temperature differences are similar, and the transmittance values for all test periods are quite comparable and all are substantially higher than the calculated value.

In the ceiling, the placement of the foil assemblies leaves a space of about 6½ inches between assemblies, and solid 6-inch-high bridging is nailed between the joists at about 5-foot intervals. With this separation of foil assemblies, it is probable that the joist surfaces presented to this center space are warmer than the upper foil face surface at the top of the space and cooler than the lower foil face surface at the bottom of the space. Radiation between perpendicular surfaces in very long spaces having an extreme width-to-height ratio, such as were encountered in the wall spacing arrangement, is usually negligible. In this instance, the spaces are not especially long and the width-to-height ratio is such as would permit an appreciable amount of radiation from the joists. A rough calculation, based on the data given in the chapter on heat transfer of the ASHAE Guide, indicates that heat transferred to the lower foil face of this center space by the joists and bridging could be as great as the heat transferred from the upper foil face by radiation. Just how much the joist affects the amount of heat transferred across this space by convection has not been appraised.

Although the effect of the joists in the larger center spaces between foil assemblies in the ceiling construction increases the heat transmittance value obtained, it also operates to impart some mass to the insulation and cut down the maximum heat flow rate at peak outside temperatures during the middle of the day. Attention has already been called to the fact that the method predicting maximum flow rates did not check very well for this ceiling. Omission of the effect of the mass of the joists in calculating the decrement factor probably explains this situation. Some confirmation of this explanation is given by the fact that the calculated lag time determined in the decrement factor calculations is 0.8 hour, whereas peak heat flows actually lag behind peak outside temperatures by 2 to 3 hours.

The data in table 7 show that even on the relatively warm period of May 7–8, the maximum heat flow did not exceed the average by much more than 50 percent, and attained a value of less than 3 Btu/hr/sq ft. From this it appears that the combination of thermal resist-

Table 12.—*Temperatures, heat flow, and transmittance through wall and ceiling at location 4*

Factor observed (averages))	Unit	Heat flow meter on ceiling				Heat flow meter on wall		
		Centered between joists Apr. 19–22	Covering joist location Apr. 22–26	Quarter point between joists Apr. 26–29	Centered between joists May 6–8	Centered between studs Apr. 29–May 2	Covering stud location May 2–4	Quarter point between studs May 4–6–
Outside air temperature	°F.	47.1	45.5	45.5	56.9	52.7	51.6	53.3
Outside black ball temperature	°F.	50.9	49.6	51.2	62.7	56.5	55.5	60.2
Outside roof temperature	°F.	53.5	53.6	54.7	71.5	62.5	59.3	65.1
Outside wall temperature	°F.	....	....	....	....	64.7	61.2	67.1
Inside surface temperature at heat flow meter location	°F.	31.7	31.8	32.0	31.4	33.0	35.6	35.5
Inside air temperature	°F.	31.3	31.4	31.8	30.6	31.8	32.6	33.2
Temperature difference across section at heat flow meter location	°F.	21.8	21.8	22.7	40.1	31.7	25.6	31.6
Heat flow—Btu/hr/sq ft	Btu	.91	.87	.95	1.75	2.06	4.65	2.64
Observed U′—Btu/hr/sq ft/°F. Td.	Btu	.0416	.0398	.0418	.0436	.0648	.1817	.0835
CalculatedU′—Btu/hr/sq ft/°T. Td.	Btu	.024	.0616	....	.024	.0555	.179	....

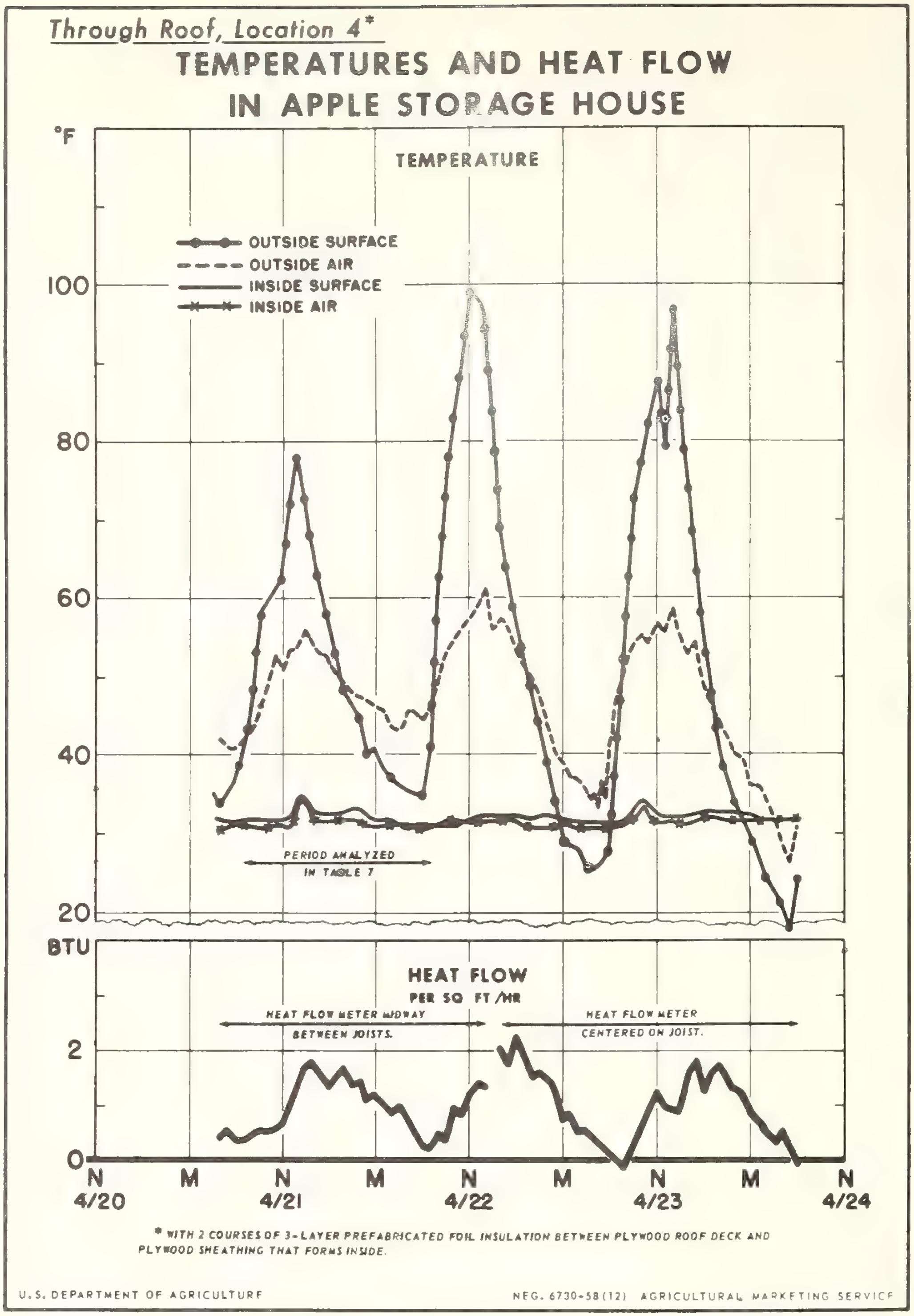

FIGURE 21

ance and mass that is present in this construction is adequate to limit the maximum flow rate to that obtained with roofs insulated with 4 inches of board form insulation.

The maximum flow observed for the wall raises the question whether the amount of insulation used with this type of exterior wall is entirely suitable for sun-exposed walls. The maximum heat flow for the observed period is well above 3 Btu/hr/sq ft and the observed

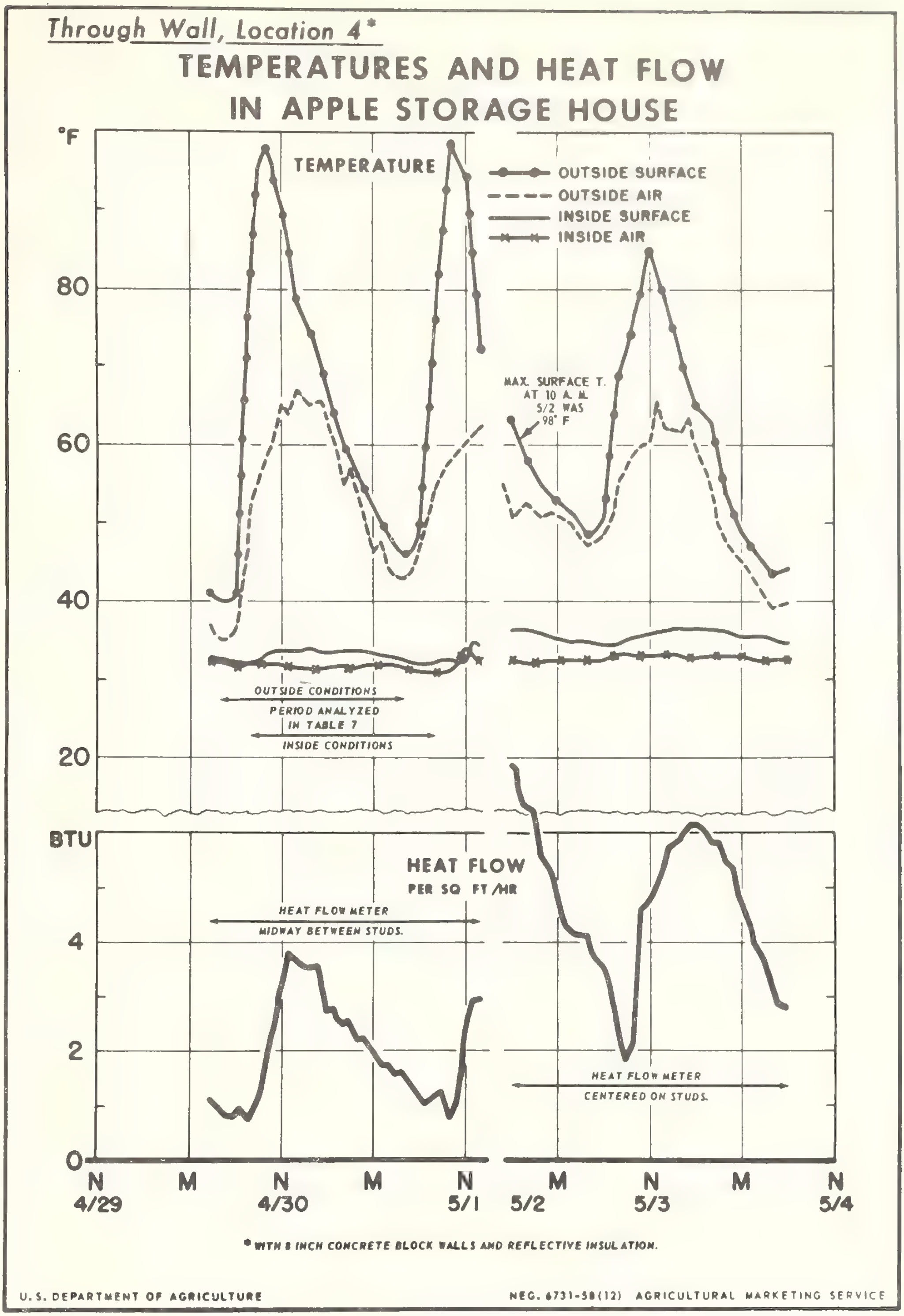

Figure 22

period was somewhat cooler than might be anticipated under normal design conditions. The comparison of a pumice-block wall with a concrete-block wall, each insulated with one assembly of three foil layers, is afforded by comparing the data for the walls at location 1 and location 4 in table 7.

The average temperature difference in each case is quite similar, but the pumice-block wall shows a lower U′ value, a lower average heat flow, and a lower maximum flow rate.

Location 5

The building at location 5 is a large, multifloor storage insulated with 24 inches of shavings above the ceiling of the upper room. An unventilated attic space about 6 feet high separates the roof structure from the top of the shavings. The roof deck is covered with composition roofing and has a coat of aluminum paint.

The data for location 5 used in this report have already been published [*14*]. Figure 23 illustrates the temperature variations at different levels in the insulation during the period analyzed in table 7. Data for this location have been included because this ceiling insulation provides complete dampening of diurnal variation in heat flow and this is demonstrated by inspection of the heat flow record, the steady temperature gradient through the lower third of the insulation, and the calculated maximum heat flow as determined by the calculation method proposed. The data show that complete dampening of diurnal heat flow variation is possible.

Location 6

At location 6 is a large, palletized storage with wall and ceiling insulation that is typical of many recently constructed large apple storages in the Pacific Northwest. The ceiling insulation is 11⅝ inches of mineral wool, blown into place between 2- by 12-inch roof joists that are placed on 16-inch centers. The fill is held in place by an interior sheathing of ¼-inch plywood nailed to the bottom of the joists. The tops of the joists are covered by a deck of 1- by 8-inch shiplap. Above this is a 3-ply roof coated with aluminum paint. The roof structure is carried by bowstring trusses so that the roof surface is not horizontal but slopes down increasingly as it approaches the side of the building.

The exterior walls at this location are 6-inch concrete. At the inside face of the concrete, a system of vertical and horizontal studding has been arranged to carry a layer of paper covered on both sides with aluminum foil. This membrane serves as a vapor seal and also provides two ¾-inch-wide reflective air spaces for insulation. Inside this is a 4-inch thickness of fiberglass insulation bat, faced on the inside with a layer of 9/16-inch fiberglass roof deck insulation.

The results of the tests on the wall and roof at location 6 are summarized in table 13. Part of the record obtained is illustrated in figure 24 for the ceiling and in figure 25 for the walls. Air currents passing over the heat flow meter were quite pronounced at all locations in this test, and individual readings were subject to considerable fluctuation. The average values have been determined from the sum of a large number of individual readings. Approximately 5,700 readings were involved in determining the wall heat flow and 1,500, 500, 2,200, and 2,100 readings in making the various roof heat flow determinations. During the period June 1–5, a break in the thermocouple lead wire to the couples measuring inside surface temperature and air temperature near the heat flow meter necessitated some estimating in calculating the final results. At the other ceiling locations, air near the heat flow meter was approximately 1° lower than the return air to the cooling unit, so the air temperature near the meter was estimated by deducting 1° from the average recorded return air temperature. Overall heat transmittance was calculated, including the inside film heat transfer coefficient. This value was then adjusted to

TABLE 13.—*Temperatures, heat flow, and transmittance through wall and ceiling at location 6*

Factor observed (averages)	Unit	Wall May 15–24	Ceiling				
			Between joists		On joist	At edge of joist	
			May 24-27	May 27-28	May 28–June 1	June 1–5	June 2 only
Outside air temperature	°F.	72.0	64.4	....	75.0	62.0	....
Outside black ball temperature	°F.	78.8	71.1	....	82.5	67.2	....
Outside wall temperature	°F.	78.3	....	....	....	....	....
Outside roof deck temperature	°F.	....	83.3	84.4	96.0	77.0	90.7
Inside surface temperature	°F.	34.4	33.5	32.8	34.7	....	....
Inside air temperature near heat flow meter	°F.	32.0	31.7	31.7	31.9	[1] 32.1	[1] 31.9
Return air temperature to cooling unit	°F.	32.3	32.6	32.3	32.9	33.1	32.9
Temperature difference across test section	°F.	43.9	49.8	51.6	61.3	[2] 44.9	[2] 58.8
Heat flow—Btu/hr/sq ft	Btu	1.49	1.23	1.26	3.46	1.95	2.62
Observed U′—Btu/hr/sq ft/°F. Td	Btu	.0338	.0247	.0244	.0565	.0450	.0462
Calculated U′—Btu/hr/sq ft/°F.Td	Btu	.0404	.0224	.0224	....	....	....
Inside surface film coefficient observed—Btu/hr/sq ft/°F. Td.	Btu	.62	.62	1.14	1.24	....	....

[1] Estimated from relation between air temperature near meter and air temperature at unit for previous periods.

[2] Includes temperature difference across interior film.

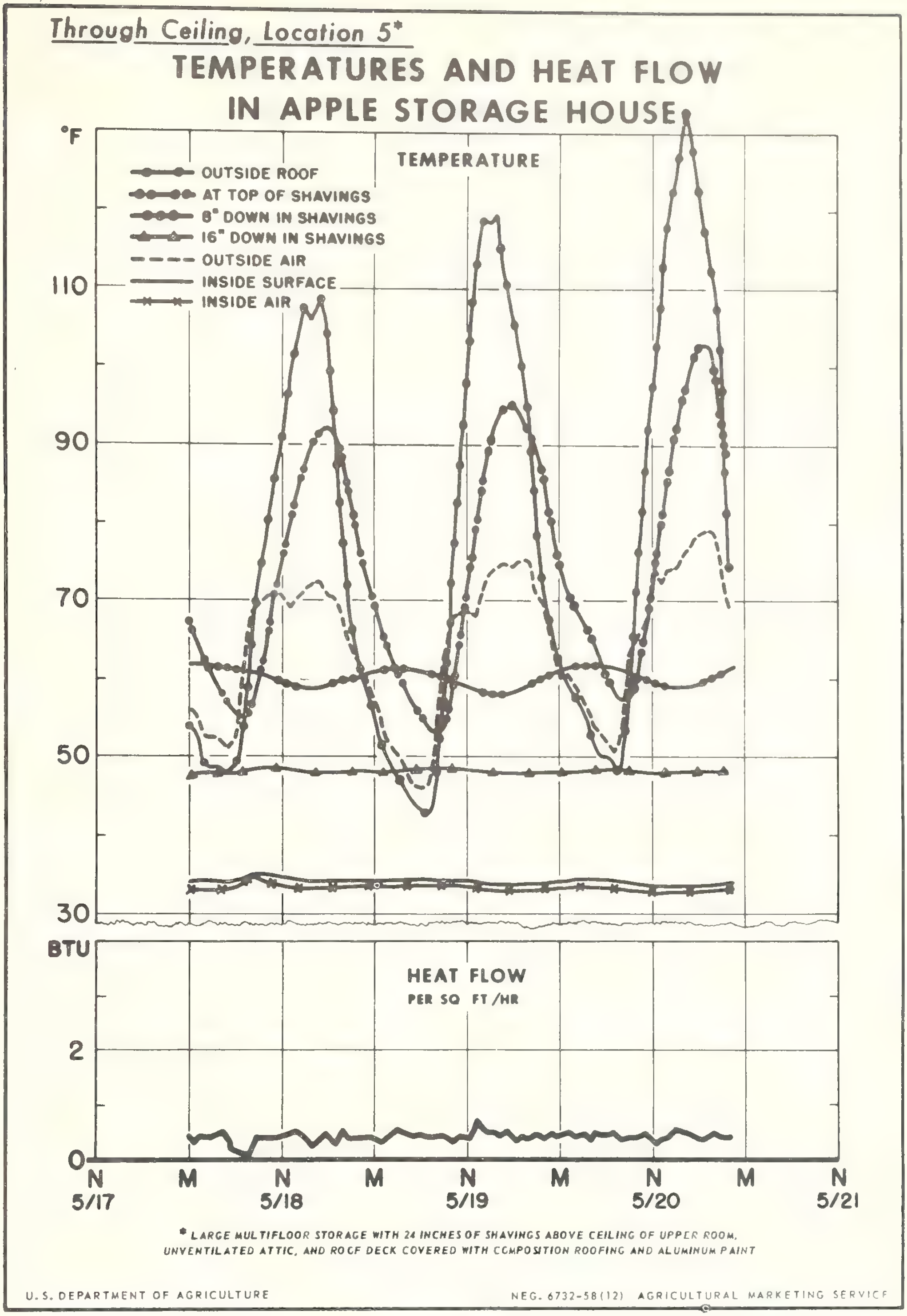

FIGURE 23

omit the film coefficient by subtracting the resistance for a film coefficient of 1.2 from the resistance corresponding to the overall transmittance first calculated.

In general, satisfactory transmittance values were obtained with this installation. The values obtained on the ceiling show some influence of the ceiling joists when the heat flow meter is

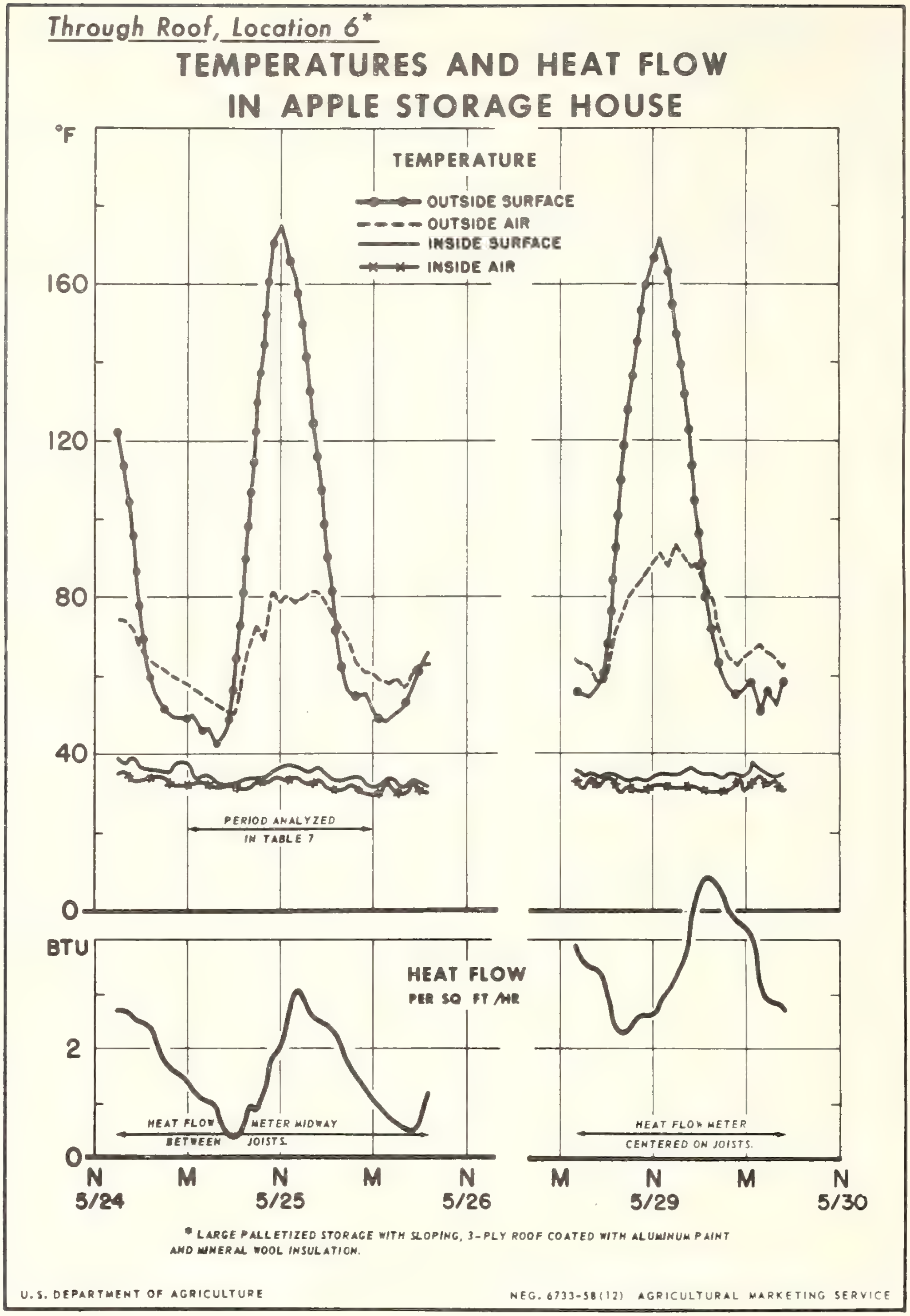

FIGURE 24

directly over a joist or placed at the edge of a joist, but little effect is shown at the center of the space between joists.

In one respect, the results with this roof were surprising. Since a shaving fill 24 inches deep will completely dampen out diurnal variations of heat flow, it was anticipated that this roof would even out the heat flow to a great extent, although probably not as much as the shaving fill installation. The tests were made under

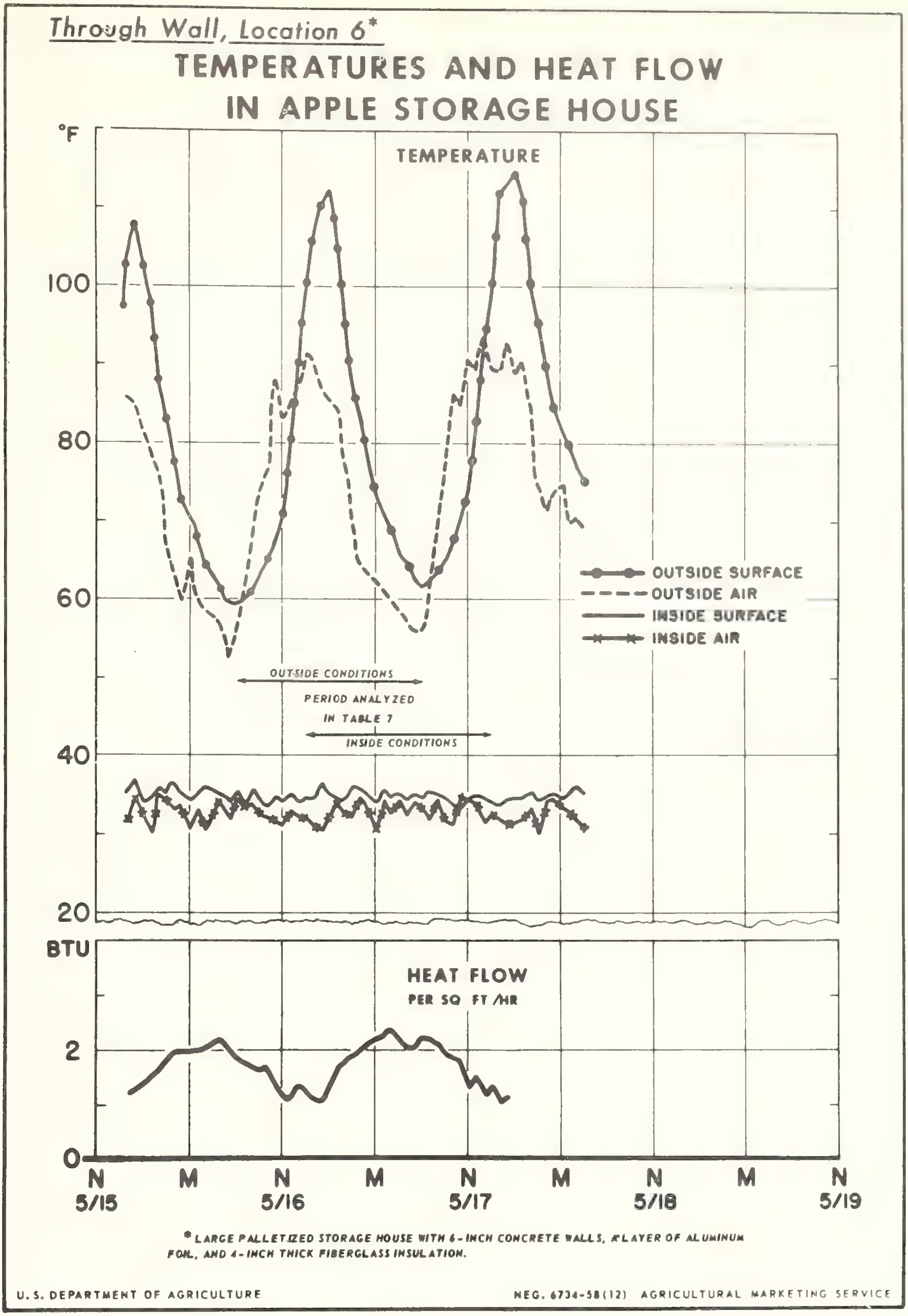

FIGURE 25

very warm weather conditions when an extremely high roof temperature of 175° maximum was encountered. A maximum flow 85 percent greater than average was encountered. The peak heat flow lagged behind the outside temperature by only about 6 hours. In the shaving-filled attics, the maximum temperatures of a point 8 inches down in the shavings lagged behind the top surface by 8 to 9 hours. A study of the characteristics of the material as used in calculating decrement factors in appendix B shows that the mineral wool fill used at location 6 has less weight and lower specific heat than shavings, and that the results obtained are justified when the characteristics of the material are fully considered.

Occasionally, fill type insulation is criticized for its susceptibility to moisture infiltration, and there are parts of the operating season when the roof deck surface may be considerably colder than the storage room. Since no vapor seal exists on the underside of the ceiling, some condensation in the insulation might be expected at that time.

To determine whether a permanent buildup of moisture had taken place in the insulation, holes were bored in the underside of the ceiling sheathing near the heat flow meter locations, and duplicate samples of insulating material were placed in tared weighing bottles having ground glass covers. The bottles were then covered and taken to the laboratory, where moisture determinations were made on the basis of 48 and 96 hours of drying at 100° C. The 6 samples averaged 0.15 percent moisture, expressed as a percentage of the original wet weight, and the maximum percentage observed was 0.29 percent. The lowest percentages were observed in the samples taken adjacent to a ceiling joist.

From this it was concluded that if there had been some moisture buildup in the insulation during the winter, the intense solar load encountered during the spring months and the action of the refrigeration apparatus in the room had dried the material quite thoroughly by the time these determinations were made.

Location 7

The building at location 7 is a 30,000-box storage of unusual construction, located at an orchard. The walls consist of three layers of 4-inch-thick pumice-concrete blocks having a density of approximately 67.5 pounds per cubic foot. Between each block layer is a 1-inch space that had been poured full of vermiculite as the walls were erected. The ceiling is insulated with a vermiculite fill 4 to 5 inches deep, supported by a 1-inch shiplap ceiling carried on ceiling joists that are within the storage. Thus the fill is continuous and there is no penetration of insulation by the ceiling joists, although some penetration by the structure that supports the roof joists exists at various points. The roof slopes, and is about 1 foot above the ceiling at the eaves and about 10 feet above at the peak. Good ventilation of the attic is provided by openings at the eaves, two end openings, and two louvered openings at the peak of the roof.

The observations of heat flow and temperatures obtained at location 7 are summarized in table 14. Figures 26 and 27 present typical parts of the record in graphic form. During the last part of the test, the analysis was broken into several 1-day intervals, because of plant shutdowns on the days omitted from the analysis.

The observed heat transmittance for the pumice-concrete block wall is considerably less than calculated. The data on pumice-concrete blocks is rather meager and that given in the ASHAE Guide specifically refers to pumice mined in California. Since the material obtained from various localities is quite variable, the difference between observed and calculated transmittance is probably justified. In 1942, W. V. Hukill made tests on a similar wall in this area by covering a 10-foot-square section of the wall with a false wall filled with shavings, and measured the temperature drop through the two layers of the composite pumice block and shaving wall thus formed. He concluded that the blocks had a thermal resistance equal to 6 inches of shavings and that the three-layer pumice block wall with two air spaces between layers had a U value of 0.065. Considering the close agreement of this test with the one reported here, and the fact that the two were conducted by different methods, a conductivity for solid pumice blocks of 0.083 Btu/hr/sq ft/ft thickness/° F. Td. has been used in appendix B in computing decrement factors for this wall.

When observations were made of the ceiling heat flow, the heat flow meter was not located directly under the point where temperatures were measured in the insulation. Fill thickness varied between 4 and 5 inches, and the meter was located in an area having a 5-inch depth of fill, whereas the temperatures in the fill were taken in an area having a 4-inch depth.

Inspection of the temperature curves for the different depths of the insulation shows that the heat storage capacity of this material is small, and that high maximum heat flow rates are encountered. Tests at this location were made in very warm weather characteristic of conditions encountered during the pear and peach harvesting season of the Pacific Northwest. At the time of the test, the storage was being used for short-time storage of peaches that were being packed and accumulated into truckloads for transportation to market in the western Oregon and Washington area. For this service, a storage temperature of 45° to 50° was adequate. Therefore, the average temperature difference through the various insulated sections was about the same as that encountered with many of the other storages tested under less severe outside conditions.

A comparison of roof deck temperatures, attic air temperatures, and the temperature of the top surface of the insulation indicates that ventilation through this attic is quite effective and is dissipating a substantial portion of the solar heat on the roof.

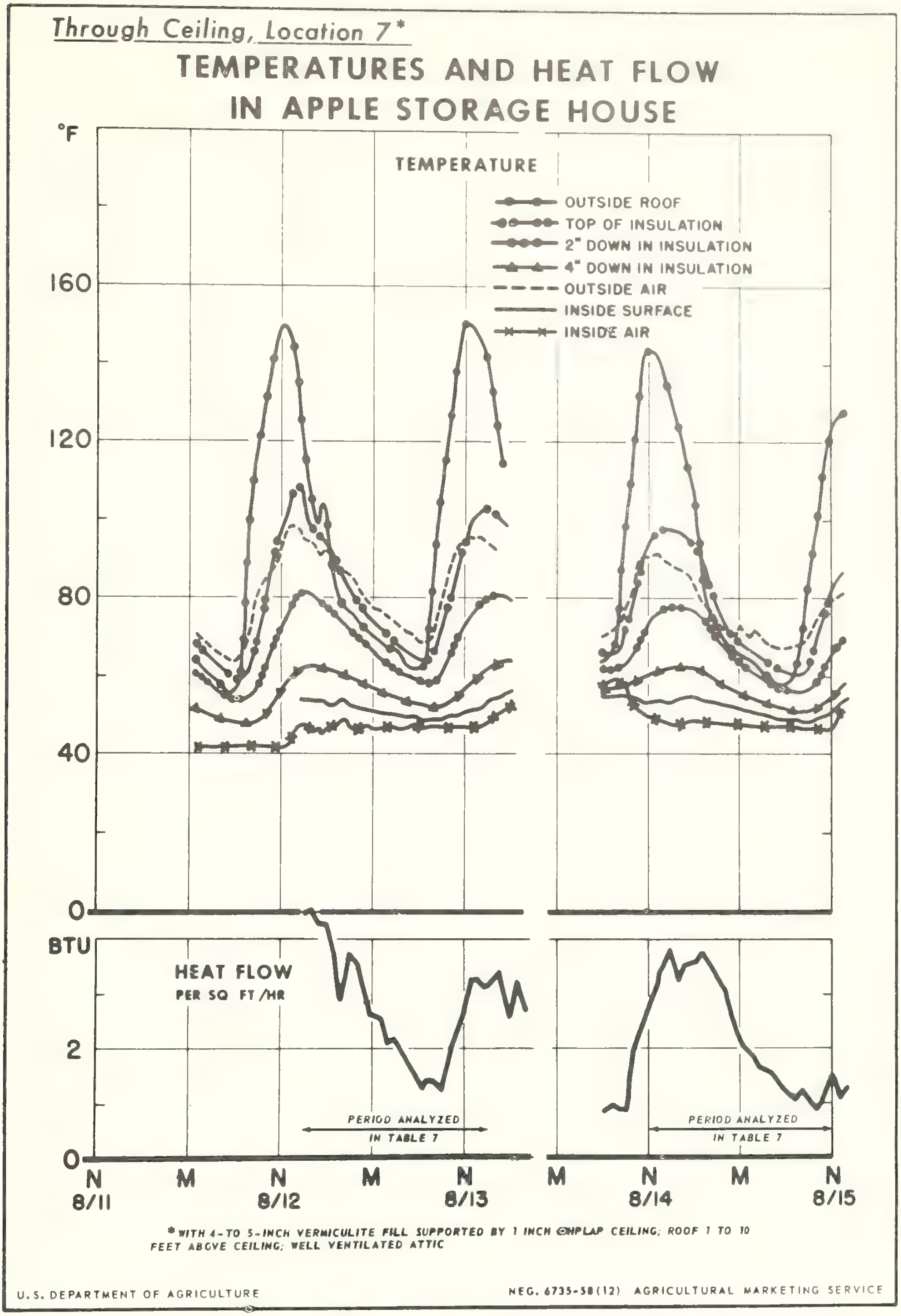

FIGURE 26

The question of moisture absorption by insulation in an exposed fill of this type always arises. To obtain some data on this subject, samples of insulation were collected and moisture determinations made as previously described [*14*]. Samples were collected from a top and bottom location that was well removed from any possible leakage from the roof ventilators, and also a sample was taken from an area directly under one ventilator. In August the sam-

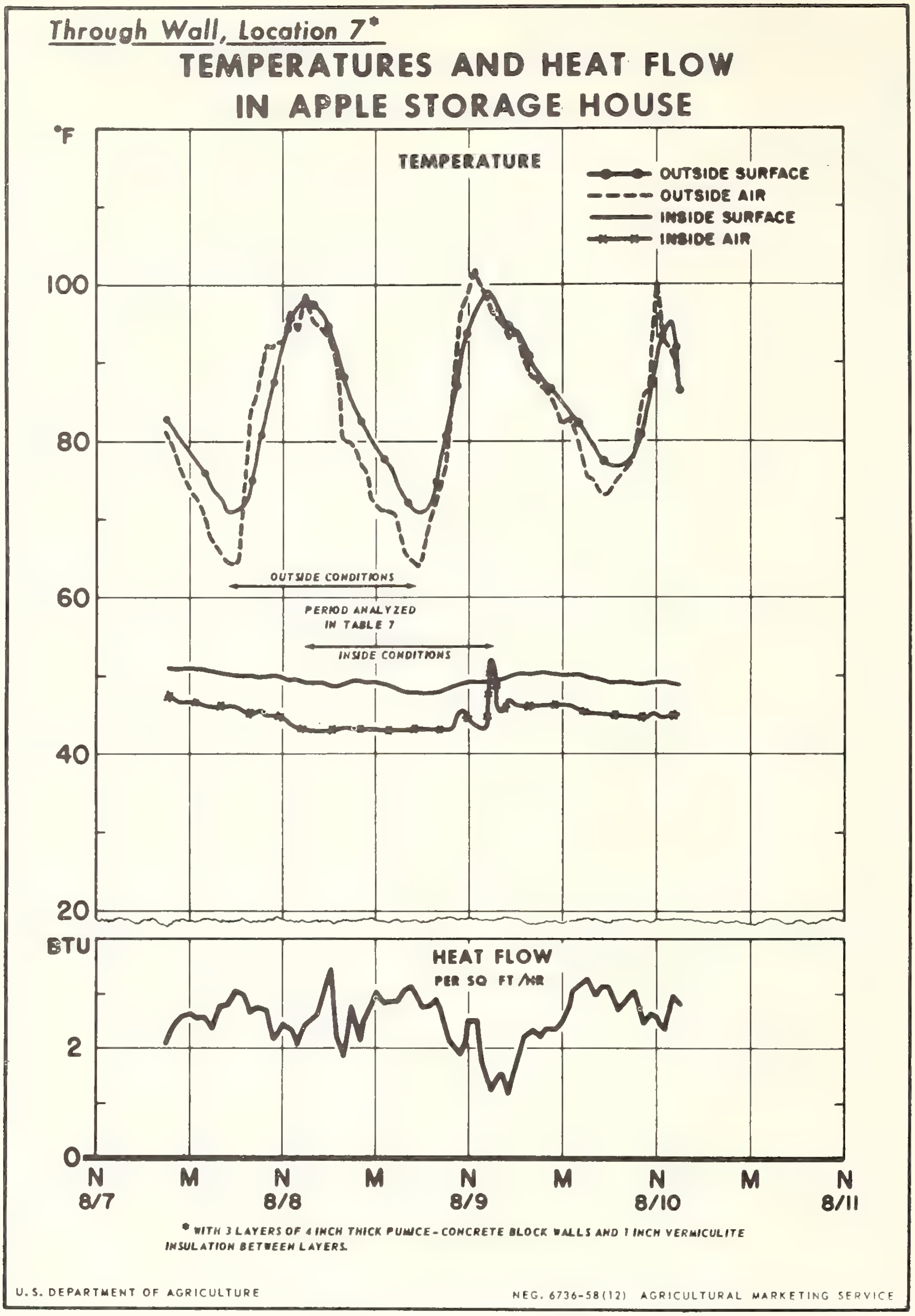

FIGURE 27

ple was taken at the bottom of the insulation at this location, as it was felt that the greatest residual moisture from any leakage would be at the bottom. For the November and January tests, samples were taken at the top of the insulation at this location.

Figure 28 presents the data obtained. The change in moisture content in the protected location between August and January is not great, nor are there any remarkable differences

Table 14.—*Average temperatures, heat flow, and transmittance through wall and ceiling at location 7*

Factor observed (averages)	Unit	Wall		Ceiling				
		Aug. 7–10	Aug. 11–12	Aug. 12–13	Aug. 14–15	Aug. 16–17	Aug. 17–18	Average
Outside air temperature	°F.	82.6	78.3	83.2	77.3	68.8	73.0	......
Outside black ball temperature	°F.	88.6	85.6	87.4	82.3	75.0	80.0	......
Outside S. wall temperature	°F.	84.4	79.9					
Inside wall temperature	°F.	49.5	47.7	....	....	....	....	....
Outside roof deck temperature	°F.	....	....	93.1	89.9	83.6	90.3	
Inside roof deck temperature	°F.	....	....	87.1	83.3	78.4	82.0	
Attic air temperature	°F.	....	....	83.9	79.4	72.8	77.1	......
Top of insulation temperature	°F.	....	....	81.5	78.0	71.7	74.8	....
Temperature 1″ down in insulation	°F.	....	....	74.5	71.7	67.3	69.6	
Temperature 2″ down in insulation	°F.	....	....	68.6	66.8	63.6	65.3	
Temperature 3″ down in insulation	°F.	....	....	62.6	61.4	59.6	60.4	....
Temperature at bottom of insulation	°F.	....	....	57.0	56.5	56.2	56.1	....
Inside ceiling temperature	°F.	....	....	51.2	51.3	52.3	51.1	....
Temperature difference across insulation	°F.	34.9	32.2	30.3	26.7	19.4	23.7	....
Heat flow—Btu/hr/sq ft	Btu	2.29	1.74	2.56	2.20	1.63	1.98	....
Observed U′—Btu/hr/sq/ft/°F. Td.	Btu	.0655	.0572	.0845	.0825	.084	.0939	.0843
Calculated U′—Btu/hr/sq ft/°F. Td.	Btu	.104	.104	.0853	.0853	.0853	.0853	....

between top and bottom location; but the sample taken directly beneath the ventilator shows that between the November and January sampling a great deal of moisture had entered the insulation. In all probability this has been caused by snow coming in through the ventilator and then melting as the weather moderated. This occurrence has been noted in other storages and points up the fact that, for storages of this type, actual leakage of moisture through roofs or ventilators is a more serious factor than moisture migration through the insulation due to temperature differences. Undoubtedly, moisture had migrated through the insulation, but since there was no vapor seal at the inside surface of the fill, the moisture did not build up to any appreciable extent in those locations not subjected to roof or ventilator leakage. The problem of providing a good system of protecting the insulation under a ventilator from leakage still remains, and deserves consideration from anyone constructing a storage where a ventilated attic is used.

DISCUSSION

Effect of Diurnal Variation on Total Refrigeration Load

From the foregoing data, it is obvious that there can be a considerable difference in the diurnal variation in heat flow rates, depending on the insulation and exposure of the insulated surface to solar radiation. The importance of this variable heat gain is governed by the following factors: (1) The relation between transmission heat gain and the total refrigeration load on the particular room; (2) the relation between the average temperature difference between inside and outside and the difference between average and maximum outside sol-air temperature, which in many cases are approximately indicated by outside surface temperatures; (3) the tendency of room contents and cold surfaces to absorb some of the peak load, and decrease the maximum instantaneous transmission heat gain; and (4) climatic conditions at the storage location, particularly those governing diurnal temperature and solar radiation variation.

The first factor is more or less inherent in the type of storage. For instance, with the average apple or pear storage, heat gain from transmission is normally 20 to 25 percent of the design load. If the transmission heat flow is double the average at midday, the overall load increase due to this factor during the receiving season is probably not more than 10 percent.

The opposite of this situation occurs in the storage designed to handle products already cooled or frozen, such as a meat cooler or a frozen food storage room. Here transmission heat gains are a large part of the load, possibly 50 to 75 percent, and doubling the heat flow rate at midday might increase the overall load 25 to 35 percent.

The effect of the second factor is best illustrated by figure 29. The ratio of maximum to average calculated heat flow rates is plotted against different λ_e/λ_s ratios through the range of 0.1 to 1.0 for different combinations of average outside design conditions and inside temperatures. Details of this calculation are given

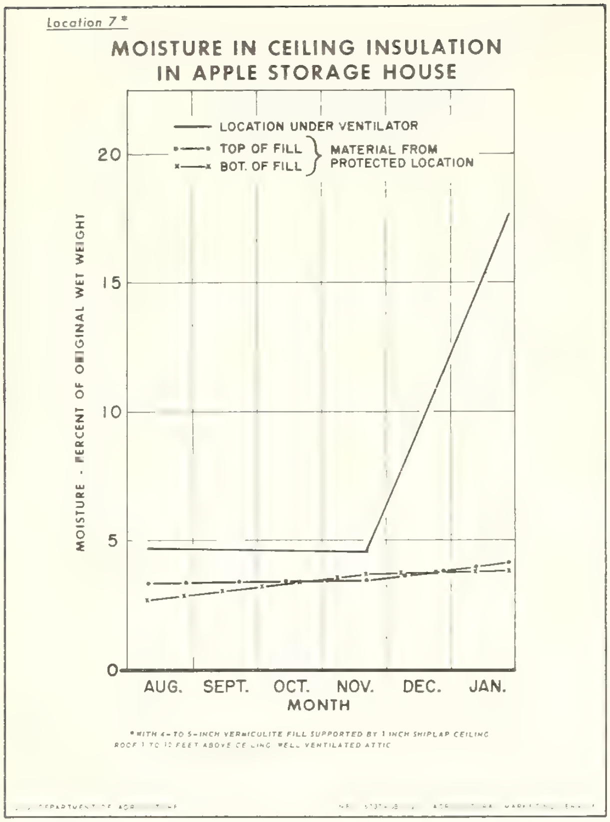

FIGURE 28

in appendix B, but it may be stated briefly that the design conditions given on the figure determine the average temperature difference at which the various storages operate. The amplitude of variation between maximum and average sol-air temperature has been taken from the ASHAE Guide for the 85° outside design condition and has been arbitrarily decreased somewhat for the other outside design conditions. It can be seen that with freezer storage application, the average temperature difference is a greater factor than the sol-air temperature amplitude and that the ratio of maximum to average heat flow for a given λ_e/λ_s ratio is less than is experienced with a cooler operating at the same outside design condition. Coolers that do not operate in the warmest part of the year or that are located in mild climates show a considerably higher ratio of maximum to average flow rate, because in these instances the average design temperature difference is about as great as the amplitude of sol-air temperature. The steep slope of the lines for the 55° outside temperature design indicates that a storage that has been designed on an optimistic expectation of low outside temperatures may find the maximum heat flow rate at midday a very serious factor.

The third factor affecting the importance of diurnal variations in heat flow is discussed in some detail in the ASHAE Guide as it pertains to air-conditioning applications, under the subject, "Instantaneous Heat Gains vs. Instantaneous Cooling Loads." It has been pointed out that when heat flows from the interior room surface, it does not all immediately manifest itself as a load on the cooling equipment. The heat removed from the interior surface by convection is soon imposed as a cooling load, but the portion that is transferred by radiation may be absorbed by cold surfaces of the room or goods stored in the room and may not appear as a cooling load until these surfaces have been raised to a temperature slightly above the room air temperature. This action tends to spread out high instantaneous loads over longer periods and cut down the peak loads that actually have to be delivered by the cooling equipment.

If the room is empty or has only a small amount of stored product, it may approach the condition where the instantaneous heat gain and the cooling load are nearly equal. This is the situation that prevailed at location 1 during the test period. It often occurs when a room is first placed in operation, and, if the insulation is such as to allow a high ratio of maximum to average heat flow, more than normal variation in room temperature may result.

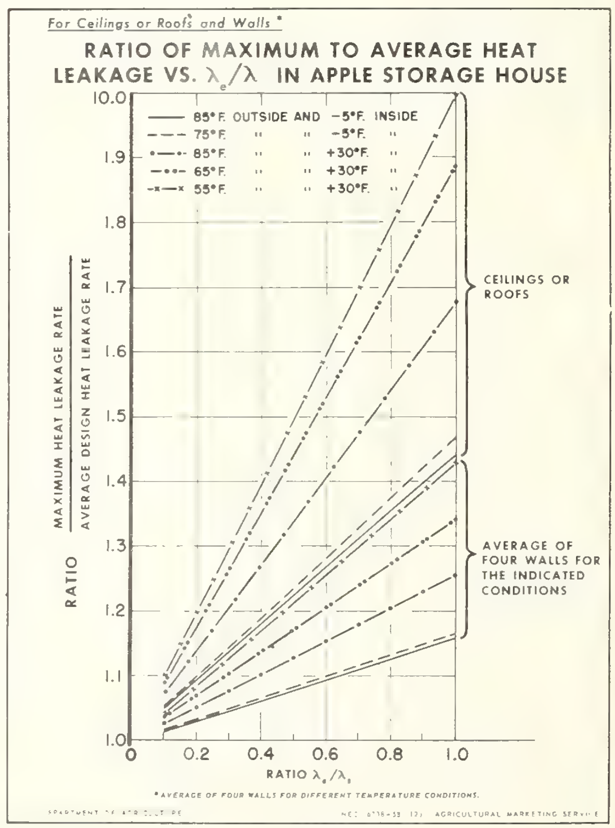

FIGURE 29

The variation of diurnal temperatures at the storage location will also affect the extent of the heat flow rate variation. Coastal locations often are subjected to an average daily temperature variation of approximately 12°. The 20° daily variation as given by the ASHAE Guide has been selected as being generally characteristic of the large midcontinent area of the United States. In desert or semi-arid regions, daily variations of 30° to 35° are general. Most of the test data presented herein show ranges of this latter order.

The first three factors tend to diminsh the overall effect of the diurnal variation in heat flow and to explain why most cold storage heat gains are satisfactorily calculated without extensive analysis of this factor. In the past, the use of slightly greater temperature differences for those surfaces exposed to solar radiation has served successfully in place of a detailed analysis of diurnal heat flow variation. Part of the success of this procedure has resulted from the use of fewer types of insulation and from the heat storage characteristics of those in use, which were favorable to providing a load-stabilizing effect.

In appendix B, the decrement factors and time lag for each of the walls and ceilings observed in this study have been calculated. Also in appendix B, a similar calculation has been made for other insulation arrangements which do not appear in this report but which are in common use in cold storages.

From a study of these values, it is apparent that insulators presently available exhibit a wide range in heat storage characteristics. Quite a number of materials now available have very little heat storage capacity and hence slight load-stabilizing effect. This applies to some of the newer types of board-form and bat-type insulation, as well as to reflective insulators.

When using a new type of insulating material, it is customary to use sufficient material to provide a thermal resistance comparable to that normally used with a material whose utility has been proved by experience, and then to take the necessary precautions to see that the material does not lose its thermal resistance from various causes such as moisture infiltration or physical damage. Little attention has been paid to comparing heat storage capacity of the new insulator with that of the known insulator. Some of the experiences reported here and calculations of the characteristics of some materials that are now finding acceptance as cold storage insulators indicate that consideration of this point is warranted.

Effect of Variation of Heat Flow Rate on Inside Temperatures

From a practical standpoint, the diurnal variation in heat flow rate becomes critical in a given storage when the temperature variation produced in the storage room by this variable flow becomes noticeable. In practice, it may be quite difficult to evaluate temperature variation from this source. In some cases, variations in other portions of the refrigeration load occur in step with the heat flow variation and increase temperature variations; in other cases, these variations may act to cancel out the heat transmission fluctuations. In some instances, the control system and capacity variation of the refrigeration system are sufficiently flexible to compensate for the heat flow variations, and modulate to meet the varying load with little temperature variation.

A rough evaluation of the average systematic variation in room temperature that may be attributed to diurnal variation in heat flow has been made for the various experimental locations. These figures are given in table 2 for each location. It must be emphasized that these are estimates based on examination of the test records obtained from the various storages, and allowance has been made for fluctuations due to defrosting or shutdown periods of adjustment; therefore, the figures do not represent precise measurements.

At location 1, the room temperature fluctuations were 8° to 9°. This was observed in the period before receiving fruit and also during a period of several days after loading with warm fruit had started. In this case, reserve capacity was not available to cope with the maximum load, and the full effect of maximum loads was entirely visible. Had more capacity been available, part of this temperature fluctuation would have been eliminated by capacity modulation.

At locations 6 and 7, a systematic variation in air temperature of 2.0° to 2.5° was noted. The tests at both locations were conducted during extremely warm weather and it is possible, particularly in the case of location 6, that this variation represents a normal and tolerable variation under extreme outside conditions.

At location 3, a fluctuation of 1.0° to 1.5° in room air temperature was noted. A similar variation was noted from other records obtained during the receiving season. None of these tests was performed during as warm weather as was experienced at locations 6 and 7. Also, this storage has available abundant refrigeration capacity, so it is possible that the variation that has been observed is that which is necessary to place additional capacity in operation.

At location 4, a diurnal variation in room temperature of approximately 1° was noted. No observations were made at this location during the receiving season, but the observations were made during the more critical periods of the late storage season.

At location 2 during the late storage season in June, a systematic variation of about 0.5° was attributed to variation in transmission heat flow. During the receiving season, a variation of about 2° was noted, but probably this was due to the amount of warm fruit entering the storage in the afternoon, imposing a greater cooling demand than the refrigeration system could produce without some slip in temperature. The record during June included supply air temperatures from the cooling system, and this record shows that during the daytime the supply temperature was quite steady, but during the night there was considerable cycling. In this instance, the control system was able to follow the load and produce a very uniform room temperature.

At location 5, as might be expected, there was no systematic variation in room temperature that could be related to diurnal temperature variation.

These observations illustrate the difficulty of isolating from practical observation that portion of room temperature variation that is due to variation in heat flow through walls and ceiling, and also show how surplus refrigeration capacity and reasonably sensitive control may often mask the variation. On the other hand, the case of the storage without surplus capacity and a large variation in heat flow rate produced an intolerable variation in room temperature. From these experiences, location 3 may be considered as something of a standard of comparison, inasmuch as 4-inch sheet cork insulation has been generally accepted as a standard insulation for this type of service. Since 1.0° to 1.5° of room temperature variation was noted in this installation, this may be used as a standard for evaluating the locations with reflective insulation to see whether or not the room temperature variations observed therein were excessive.

On this basis, the performances at location 2 and location 4 appeared adequate, whereas that at location 1 was not. The performance at location 7 was somewhat questionable as to fluctuation in room temperature; and examination of the data in table 7 shows maximum heat flow rates for the ceiling that are higher than for most of the other installations. At location 6, the air temperature variation is somewhat greater than at location 3, but this is probably because the test was conducted under extreme conditions. The comparison does serve to point out that the heat storage capacity of the insulation at location 6 is not much difference than that at location 3. This is confirmed by comparison of the calculated and observed lag time for the two roofs. Nevertheless, this result is revealing because, on first thought, one might easily assume that there would be a big difference in the heat storage and lag time for 12 inches of insulation as against 4 inches of insulation. This illustrates that the density and specific heat of the material, as well as the conductivity and thickness used, must be considered to arrive at a proper conclusion regarding maximum loads that may be encountered with a given material.

Suggested Design Procedure Using Insulation With Small Heat Storage Capacity

Again considering location 3 as a reasonable standard, it appears that under the conditions to be expected with apple storages starting operation in mid-September, a maximum heat flow rate of 3 Btu/hr/sq ft is a reasonable peak value to use as a design figure. Therefore, it is suggested that, for storages of this type, insulated with material having less heat storage capacity than 4 inches of corkboard, the thermal resistance should be increased so that the maximum transmission rate at mid-day design conditions does not exceed 3 Btu/hr/sq ft. If the refrigeration machinery is selected on the basis of average daily load, then the average heat gain from transmission should be calculated as ⅔ of this maximum. Such an arrangement will provide approximately the same balance of equipment capacity and maximum load as if 4-inch corkboard insulation had been used.

When prefabricated reflective insulation is used, the procedure recommended is probably the most economical way of overcoming high heat flow rates at mid-day insofar as roofs are concerned. In the case of walls, the combination of some mass or some semi-insulator such as cinder block to form a composite wall may produce a desirable amount of heat storage effect and the most economical answer to the problem. Where certain low-density board or bat-type insulators have insufficient heat storage capacity to keep the maximum flow rate to desirable levels, it may be more economical to alter the design and combine additional mass with the insulation rather than add to the insulation thickness.

The recommendation made is specifically for apple storages, but it could be extended to other types of storages. When use of new insulator "N" is desired, one should consider the standard accepted insulation, designated as insulation "S," for the application, and calculate the average heat gain per unit of the area with insulation "S" for the temperature difference involved. From the tables in the appendix, obtain the λ_e/λ_s ratio for insulation "S," or calculate the ratio by the methods illustrated. From figure 29 and the appropriate design condition curve, find the ratio of maximum to average heat flow. Apply this ratio to the average transmission rate to determine the maximum, and use this maximum rate to determine the thickness of insulation "N" that is to be used.

CONCLUSIONS

Maximum heat flow rates for insulated surfaces exposed to solar radiation may be predicted by formulas presented in this report when the average daily temperature difference through the insulation, maximum surface temperature or maximum sol-air temperature, overall thermal transmittance, and decrement factors for the construction are known. Experimental observations of maximum and average heat flow for a number of different types of insulated walls and ceilings have been compared with calculations and a reasonable agreement has been found in most cases.

The maximum heat flow rates are of greatest importance in those structures having little heat storage capacity, because in such instances the maximum heat flow is proportional to the maximum observed temperature difference between outside and inside surface. Maximum heat flow rates are of greater importance for mild-temperature coolers than for freezers, and are of particular importance for coolers designed for operation during autumn and spring where outside design temperatures of 55° to 65° are used. In these cases, the amplitude of surface temperature variation is often greater than the average temperature difference, whereas in the case of freezers and mild-temperature storages designed for operation during the warmest season of the year, the amplitude of surface temperature variation is usually less than the average temperature difference.

Maximum heat flow rates are of more importance in structures where transmission heat gains comprise a large part of the total refrigeration loads, and are of particular importance in those instances where, for reasons of economy, the equipment capacity has been selected with little safety factor.

Calculations of decrement factors and time lag for various insulated walls and ceilings that are currently used in cold storages are presented. Comparison of these factors for new types of insulation with types that have had long acceptance will indicate those instances where investigation should be made of the maximum heat flow rate. This will usually be necessary with reflective insulation installed in frame structures.

For such insulation in apple storages, it is recommended that the insulation be selected with such a transmission value as will limit the maximum heat flow rate to 3 Btu/hr/sq ft and that the average daily load calculation should be based on two-thirds of this value.

In certain cases, it may be more economical to combine mass with the insulator to improve its heat storage or load-stabilizing characteristics, rather than adding extra insulation.

A comparison of aluminum paint on a builtup roof, as against black paint on the same roof, indicated that the average amount of heat transmitted per day was decreased about 5 percent with the aluminum-painted roof.

Some data gathered regarding the effect of wooden studs and joists in reflective and fill-type insulation indicate that when the spaces between layers of reflective surfaces are small, there is little tendency of a wood member bounding the side of the space to radiate or receive heat from the various surfaces, and the heat flow at the inside face of the stud or joist is very much the same as if the walls were constructed of wood having the depth of the member. Much the same thing occurs with a wooden member in fill insulation; the amount of side leakage to the fill is not excessive. When layers of reflective material are separated by 6 or 7 inches in a 2-foot-wide space, radiation and absorption of heat by the wood member becomes a factor to the extent that the heat flow from the inside surface is practically uniform and is not any higher at the joist location than elsewhere. The overall transmittance is adversely affected, but the heat storage capacity and maximum heat flow characteristics are benefited by this action.

LITERATURE CITED

(1) American Society of Heating and Air Conditioning Engineers.
1956. ASHAE GUIDE. New York, N.Y.

(2) Eckert, E. R. G.
1950. INTRODUCTION TO THE TRANSFER OF HEAT AND MASS. New York, N.Y.

(3) Housing and Home Finance Agency.
1954. THE THERMAL INSULATING VALUE OF AIR SPACES. Off. Adminr., Div. Housing Res. Housing Res. Paper No. 32. Washington.

(4) Hukill, W. V., and Wooten, L. B.
1947. COORDINATED MANAGEMENT OF HARVESTING, STORING, AND MARKETING NORTHWEST APPLES. U.S. Dept. Agr. Cir. 759.

(5) Ingersoll, L. R., Zobell, O. J., and Ingersoll, A. C.
1954. HEAT CONDUCTION WITH ENGINEERING, GEOLOGICAL AND OTHER APPLICATIONS Ch. 5. Univ. Wis. Madison.

(6) Jakob, Max, and Hawkins, G. A.
1950. ELEMENTS OF HEAT TRANSFER

AND INSULATION. New York, N.Y.
(7) JOHNSON, H. A.
1948. PERIODIC HEAT TRANSFER AT THE INNER SURFACE OF A HOMOGENEOUS WALL. Amer. Soc. Heating and Ventilating Engin. Trans. 54: 143.
(8) KERSTEN, M. S.
1949. THERMAL PROPERTIES OF SOILS. Univ. Minn. Engin. Expt. Sta. Bul. 28.
(9) MACKEY, C. O.
1945. SUMMER WEATHER DATA AND SOL-AIR TEMPERATURE — STUDY OF DATA FOR LINCOLN, NEBR. Amer. Soc. Heating and Ventilating Engin. Trans. 51: 93.
(10) ———— and WRIGHT, L. T., JR.
1943. SUMMER COMFORT FACTORS AS INFLUENCED BY THERMAL PROPERTIES OF BUILDING MATERIALS. Amer. Soc. Heating and Ventilating Engin. Trans. 49: 148.
(11) ———— and WRIGHT, L. T., JR.
1944. PERIODIC HEAT FLOW—HOMOGENEOUS WALLS OR ROOFS. Amer. Soc. Heating and Ventilating Engin. Trans. 50: 293.
(12) ———— and WRIGHT, L. T., JR.
1946. PERIODIC HEAT FLOW—COMPOSITE WALLS OR ROOFS. Amer. Soc. Heating and Ventilating Engin. Trans. 52: 283.
(13) SAINSBURY, G. F.
1950. GROUND HEAT IN COLD STORAGES. Refrig. Engin. 58(11): 1066.
(14) ————
1953. ROOF INSULATING METHODS. Refrig. Engin. 61(3): 286.
(15) ————
1953. REFLECTIVE INSULATION — ITS PERFORMANCE IN FRUIT STORAGE WAREHOUSES. Refrig. Engin. 61(4): 383.
(16) SCHMIDT, E.
1924. BEITRAGE ZUR TECHISCHEN MECHANIK UND TECHNISCHEN PHYSIK. Berlin.
(17) STEWART, J. P.
1948. SOLAR HEAT GAINS THROUGH WALLS AND ROOFS FOR COOLING LOAD CALCULATIONS. Amer. Soc. Heating and Ventilating Engin. Trans. 54: 361.
(18) WARD, W. H., and SEWELL, E. C.
1950. PROTECTION OF THE GROUND FROM THERMAL EFFECTS OF INDUSTRIAL PLANT. Geotechnique 2(1): 64–81.

APPENDIX A

Heat flow rates from the floor at location 2 have been calculated using temperature differences taken from a diagram of the temperature profiles in the ground beneath the center of the storage. The details of construction of this diagram are as follows:

From the heat flow and temperature observations it was determined that the conductivity of the soil beneath the floor was 13.5, and from the heat released during the interval measured it appeared that soil having the following characteristics would satisfy the observed conditions:

Dry density	130 lb./cf.
Moisture content	1¾ %
Diffusivity	0.039 sq. ft./hr.

Construction of the diagram will be simplified in this instance by considering the concrete floor to have characteristics similar to the soil. Conductivity of concrete ranges from 12 to 16. The diffusivity ranges from 0.045 to 0.06. During the first day or two, the assumption that the concrete has the same characteristics as the soil involves some inaccuracy, but after the slab has been cooled to the point where the temperature profile through it is nearly a straight line, there is little distortion in the construction from this assumption.

The initial temperature is 65° F. and this temperature is assumed to prevail to a depth of 4 feet into the ground. At 4 feet, the ground temperature begins to decline and at a depth of 40 feet the temperature approaches the average annual temperature of 52° F. with an annual fluctuation of only ± ½°, or a temperature range of 1°.

Temperature fluctuation at various depths has been determined by the following formula obtained from Ingersoll, Zobel, and Ingersoll [*5*].

$$T_r = 2T_o\, e^{-x\sqrt{\pi/aP}} \qquad (1\text{–A})$$

where: T_r is temperature range at depth X
T_o is amplitude of seasonal temperature variation at surface
x is depth in feet
a is diffusivity in square feet per hour
P is the period of the cycle (in this case 1 year, or 8,760 hours)

For convenience, the temperature range at several depths was calculated and the results plotted on semilogarithmic paper. The points were then connected by a straight line and the relation of temperature range vs. depth could be read for any desired point.

The shape of the curve of annual temperature variation at the surface is assumed to be sinusoidal. At increasing depths, the curve of annual temperature variation is similarly shaped but lags behind the surface. The lag may be determined by calculating the wave velocity through the ground and dividing the depth by this velocity.

$$\text{Wave velocity} = 2\sqrt{\pi a/P} \qquad (2\text{–A})$$

The lag was determined for several depths and plotted on rectangular coordinates so that temperature lag for all points could be read as desired.

Since the number of days in the year is so close to 360, the above determined lag can be treated as lag angle in degrees. The starting date, October 1, was assumed to be 60 days after the maximum temperature point and therefore can be treated as a lead angle. The actual temperature of the ground at any depth, x, has been calculated as follows:

$$T_x = 52 + T_{r_x} \cos\,(60 - \text{lag angle for depth x}) \qquad (3\text{–A})$$

The temperature profile in the ground at the time refrigeration was started is calculated on this basis.

Start the construction at the top of figure 30, plotting temperature to a scale of 1″ = 10° and depth beneath the floor to the scale 1″ = 10″. If we take 6-inch distance intervals in making the plot of profiles, the time interval will be:

$$\text{Time interval} = \frac{(\text{distance-interval})^2}{2 \times \text{diffusivity}} = \frac{0.5 \times 0.5}{2 \times 0.039} = 3.2 \text{ hr.} \qquad (4\text{–A})$$

The air temperature is plotted to the left of the boundary of the floor at a distance that equals

$$\frac{\text{conductivity of ground}}{\text{surface to air film coefficient}} = \frac{13.5}{1.65} = 8.2 \text{ inches} \qquad (5\text{–A})$$

The upper plot on figure 30 is marked off with 6-inch depth divisions starting with A–A, B–B, C–C, etc. These are located so that the floor surface, O, is midway between A–A and B–B.

It is assumed that when the refrigeration is

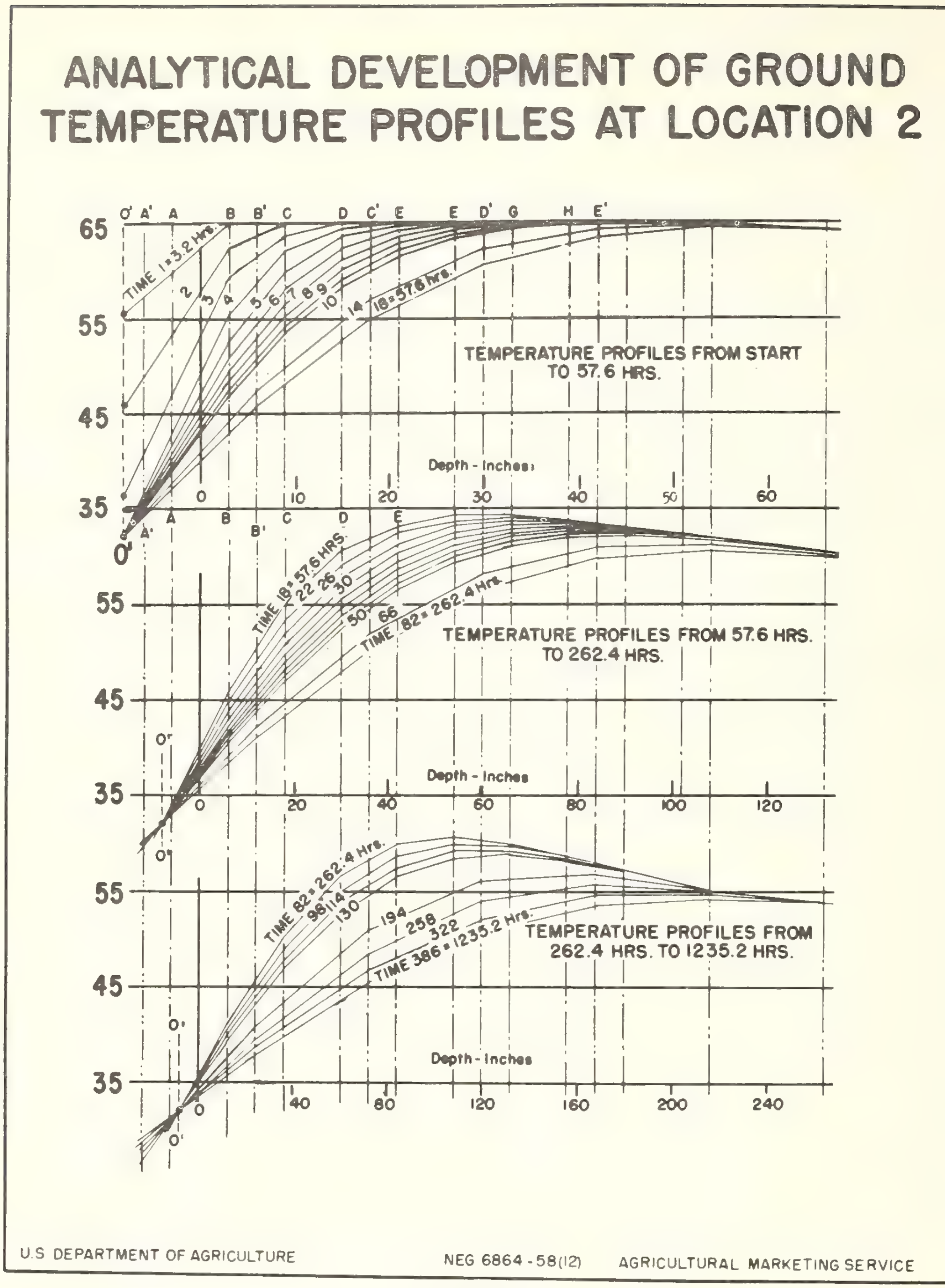

FIGURE 30

started, the air temperature drops at the rate of 3° per hour. At time 1 (3.2 hours) the air temperature is 55.6° and this point is located on the air temperature line and time 1 profile is drawn from this point to the intersection of B–B and the initial temperature line (65°). From the intersection of the time 1 profile and A–A, a line is drawn to the intersection of initial temperature (65° F.) and C–C and the point where this line meets B–B is the intersection of time 2 profile and B–B. The time 2 profile is completed by connecting this point to C–C and 65 and also to the air temperature (45.8° F. at time 2) on the air temperature line.

The point where time 3 profile intersects B–B is determined by the straight line connecting

A–A to C–C on the time 2 profile. The point where time 3 profile intersects C–C is determined by the straight line connecting B–B to D–D on the time 2 profile. The profile is completed by connecting the point B–B to the air temperature determined for time 3 and by connecting the point on C–C to D–D at 65.

In this manner, the various profiles may be constructed. By time 4, the air temperature has reached 32° F. and here it is held constant.

Upon reaching time 10, the temperature changes per unit of time in each unit of depth are becoming so small there is difficulty in constructing an accurate figure. At this point the distance intervals are doubled, which means that each profile is then 4 time units apart. New depth division lines A′–A′, B′–B′, C′–C′, etc., are drawn, located so that the floor surface is midway between A′–A′ and B′–B′.

To present figure 30 in this report a change has been made in the depth scale at time 18 and again at time 82. This is merely for convenience in presentation.

At time 50 and at time 130 the depth intervals are again doubled to increase the ease of plotting and each doubling of depth interval is accompanied by a fourfold increase in the number of time units between profiles.

When the various profiles have been produced, heat flow rates are calculated by reading from the chart the various temperatures at the indicated time intervals as shown in table 15. Difference between surface and air temperature multiplied by inside film coefficient, 1.65, determines heat flow from the surface. Temperature difference between surface and the 1-foot depth multiplied by conductivity per foot of soil gives the heat conducted through the first foot of soil. Note that as the profile through this section becomes straighter, this calculated value approaches the calculated heat flow rate from the surface. This also holds true for the heat conducted through the second foot of soil. In other words, when the temperature profile between two points is a straight line, conduction accounts for all of the heat leaving the section.

The heat flow rates at the various times as determined in table 15 are plotted on figure 7 and may be compared with the heat flow rates determined from experiment.

TABLE 15.—*Calculation of heat flow rates from temperature profiles shown in figure 30*

Time interval	Time from start		Air temperature	Surface temperature	Temperature difference air to surface	Heat flow rate	Temperature 1 foot down	Temperature difference in first foot	Heat flow rate	Temperature 2 feet down	Temperature difference in second foot	Heat flow
	Hours	Days										
No.			°*F.*	°*F.*	°*F.*	*Btu/hr/sq ft*	°*F.*	°*F.*	*Btu/hr/sq ft*	°*F.*	°*F.*	*Btu/hr/sq ft*
2	6.4	....	45.8	58.0	12.2	20.1	....	....	....	....	....	....
4	12.8	½	32.0	49.2	17.2	28.4	63.1	13.9	15.6	....	....	....
8	25.6	1+	32.0	43.8	11.8	19.5	57.6	13.8	15.5	....	....	....
14	45.0	2−	32.0	40.8	8.8	14.5	52.2	11.4	12.8	....	....	....
22	70.5	3−	32.0	39.4	7.4	12.2	49.0	9.6	10.8	....	....	....
30	96.0	4	32.0	38.2	6.2	10.2	46.8	8.6	9.7	....	....	....
42	134.0	5.5	32.0	37.2	5.2	8.6	44.6	7.4	8.3	....	....	....
50	160.0	6.67	32.0	36.8	4.8	7.9	43.7	6.9	7.8	....	....	....
66	211.0	8.8	32.0	36.2	4.2	6.9	42.2	6.0	6.8	....	....	....
82	262.0	11.0	32.0	35.7	3.7	6.2	41.0	5.3	6.0	....	....	....
98	314.0	13.1	32.0	35.4	3.4	5.6	40.3	4.9	5.5	....	....	....
114	365.0	15.2	32.0	35.1	3.1	5.1	39.7	4.6	5.4	....	....	....
130	416.0	17.3	32.0	34.9	2.9	4.8	39.1	4.2	4.7	43.0	3.9	4.4
194	621.0	25.9	32.0	34.2	2.2	3.6	37.4	3.2	3.6	40.6	3.2	3.6
258	826.0	34.4	32.0	....	....	....	36.6	....	....	39.4	2.8	3.2
322	1030.0	43.0	32.0	....	....	....	36.0	....	....	38.5	2.5	2.8
386	1235.2	51.5	32.0	....	....	....	35.5	....	....	37.7	2.2	2.5

APPENDIX B

Basic Relations and Equations

The symbols used in the appendixes and elsewhere in the report have the following meanings and dimensions:

t_a = outdoor dry bulb temperature (degrees F.).

t_e = sol-air temperature (degrees F.).

t_{em} = maximum sol-air temperature (degrees F.).

t_{ea} = average daily sol-air temperature (degrees F.).

t_s = outside surface temperature (degrees F.).

t_{sm} = maximum outside surface temperature (degrees F.).

t_{sa} = average daily outside surface temperature (degrees F.).

t_o = inside surface temperature (degrees F.).

t_{oa} = average daily inside surface temperature (degrees F.).

t_i = average daily inside air temperature (degrees F.).

q = heat flow rate (Btu/hr/sq ft).

q_{max} = maximum rate of heat flow actually encountered (Btu/hr/sq ft).

L = thickness of material (ft).

K = thermal conductivity (Btu/ft thickness/sq ft/hr/°F. Td. in Part II of report. In Part I conductivity is given per inch of thickness).

ρ = density of material (lb/cu ft).

C = specific heat of material (Btu/lb/°F.).

h_o = inside air film heat transfer coefficient (value of 1.65 Btu/hr/sq ft/°F. Td. used in these calculations).

h_L = outside air film heat transfer coefficient (value of 4 Btu/hr/sq ft/°F. Td. used in these calculations).

U = overall thermal transmittance including film factors (Btu/hr/sq ft/°F. Td.).

U' = overall thermal transmittance excluding film factors (Btu/hr/sq ft/°F. Td.).

a = Thermal diffusivity (sq ft/hr).

A = area of surface (sq ft).

I = the intensity of solar radiation incident upon the outside surface (Btu/hr/sq ft).

b = the absorptivity of the outside surface for solar radiation (dimensionless).

θ = time (measured in hours after noon).

n = the harmonic coefficient ($n = 1$ for first harmonic or fundamental, $n = 2$ for second harmonic, etc.).

t_n = the harmonic temperature coefficient (t_1 for first harmonic, t_2 for second harmonic, etc.).

a_n = the harmonic phase angle degrees (a_1 for first harmonic, a_2 for second harmonic, etc.).

ϕ_n = the harmonic lag angle, degrees (ϕ_1 for first harmonic, ϕ_2 for second harmonic, etc.).

λ_n = the harmonic decrement factor.

λ_1 = the fundamental decrement factor for first harmonic.

λ_2 = the second harmonic decrement factor.

λ_e = the equivalent decrement factor that closely approximates λ_n.

λ_s = the decrement factor for steady flow; i.e., without storage of heat.

The following summarizes the basic formulas regarding period heat flow as set forth in the reports by Mackey and Wright [*10, 11,* and *12*] and by Stewart [*17*].

The sol-air temperature is defined as the temperature of outdoor air which, in contact with a shaded building surface, would give the same rate of heat transfer and the same temperature distribution through the material as exists with the actual dry-bulb temperature of the outdoor air and the actual intensity of solar radiation incident upon the surface. This relation is expressed as follows:

$$t_e = t_a + \frac{bI}{h_L} = t_a + \frac{bI}{4.} \qquad (1\text{–B})$$

The equation which describes the periodic sol-air temperature as a function of time is:

$$t_e = t_{ea} + \sum_{n=1}^{\infty} t_n \cos (15n\theta - a_n) \qquad (2\text{–B})$$

The equation for the temperature of the inside surface of the building material at any time, where the incident solar radiation and outside air temperature are periodic and the temperature of the inside air is constant, h_L equals 4, and h_o equals 1.65, is as follows:

$$t_o = t_i + \frac{0.606\,(t_{ea} - t_i)}{0.856 + \frac{L}{K}} + \sum_{n=1}^{\infty} \lambda_n t_n \cos (15n\theta - a_n - \phi_n) \qquad (3\text{–B})$$

The instantaneous rate of heat transfer from the inside surface to the inside air is:

$$q = 1.65\ (t_o - t_i) \qquad (4\text{–B})$$

An approximate solution has been presented for the temperature of the inside surface of the material which is much simpler than equation 3–B and which gives acceptable results.

Let the steady-flow mean daily temperature of the inside surface be represented by t_{oa}, and

$$t_{oa} = t_i + \frac{0.606\ (t_{ea} - t_i)}{0.856 + \frac{L}{K}} \qquad (5\text{–B})$$

or

$$t_{oa} = t_i + \frac{U}{1.65}\ [t_{ea} - t_i] \qquad (6\text{–B})$$

The inside surface temperature of the material may be approximated in terms of sol-air temperature at a time which is earlier by the fundamental time lag, in hours ($\phi_1/15$).

The temperature of the inside surface of material at a time ($\theta + \frac{\phi_1}{15}$) hours after noon is related to the sol-air temperature at a time θ hours after noon as follows:

$$(t_o)_{\theta + \frac{\phi_1}{15}} = t_{oa} + \lambda_e[(t_e)_\theta - t_{ea}] \qquad (7\text{–B})$$

Also

$$(t_o)_{\theta + \frac{\phi_1}{15}} = t_i + \frac{U}{1.65}(t_{ea} - t_i) + \lambda_e\ [(t_e)_\theta - t_{ea}] \qquad (8\text{–B})$$

Equation 8–B may be used to determine rate of heat flow if t_i is subtracted from both sides and both sides are multiplied by 1.65 (h_o).

This operation reduces to the following form:

$$(q)_{\theta + \frac{\phi_1}{15}} = \left[(t_o)_{\theta + \frac{\phi_1}{15}} - t_i\right] 1.65 = U\ (t_{ea} - t_i) + 1.65\lambda_e\ [(t_e)_\theta - t_{ea}] \qquad (9\text{–B})$$

$$(q)_{\theta + \frac{\phi_1}{15}} = U\left[t_{ea} - t_i + \frac{1.65\lambda_e}{U}[(t_e)_\theta - t_{ea}]\right] \qquad (10\text{–B})$$

The maximum heat flow from the inside surface occurs approximately at $\phi_1/15$ hours (the fundamental time lag) after the maximum sol-air temperature occurs; therefore:

$$q_{max} = U\left[t_{ea} - t_i + \frac{1.65\lambda_e}{U}(t_{em} - t_{ea})\right] \qquad (11\text{–B})$$

The equations for the decrement factor λ and the lag angle ϕ are extremely complex and are given in the original references. Mackey and Wright presented graphic solutions that are very useful; figure 31 presents the graph from which the decrement factor may be read and figure 32 gives value for the lag angle.

Up to this point, the discussion has considered the use of a single homogeneous material through which the heat is flowing. Very few such structures will actually be encountered. To use the foregoing charts, it is necessary to determine the equivalent homogeneous structure. This has been defined as the simple homogeneous wall or roof which will have the same variation in inside surface temperature with time as does the actual composite wall or roof under identical ambient conditions.

The references contain several methods for determining the equivalent homogeneous con-

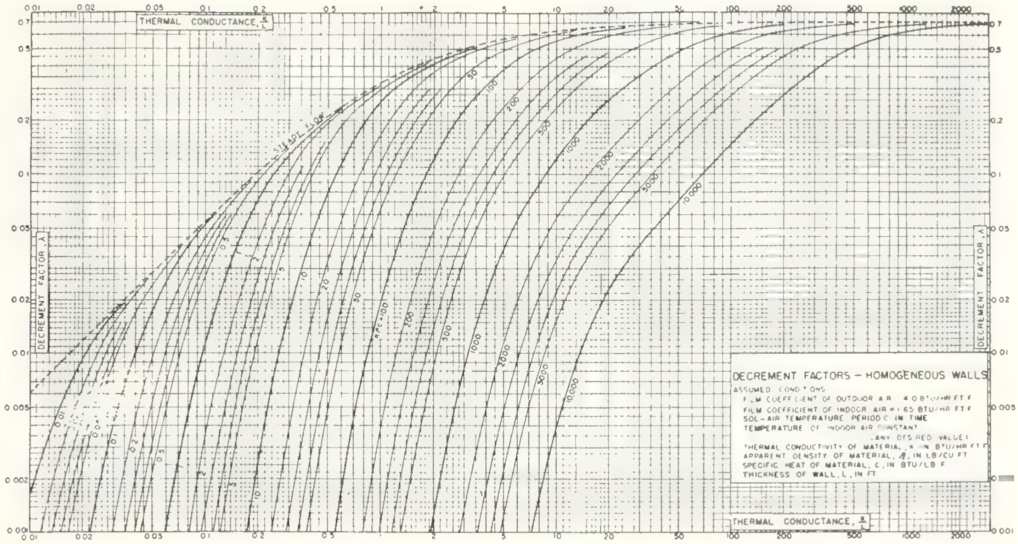

FIGURE 31.—*Chart for determining decrement factors.*

Reprinted by permission from Report No. 1299, "Periodic Heat Flow—Composite Walls or Roofs," by C. O. Mackey and L. T. Wright, Jr.. Transactions of A.S.H.V.E., vol. 52, 1946, p. 283.

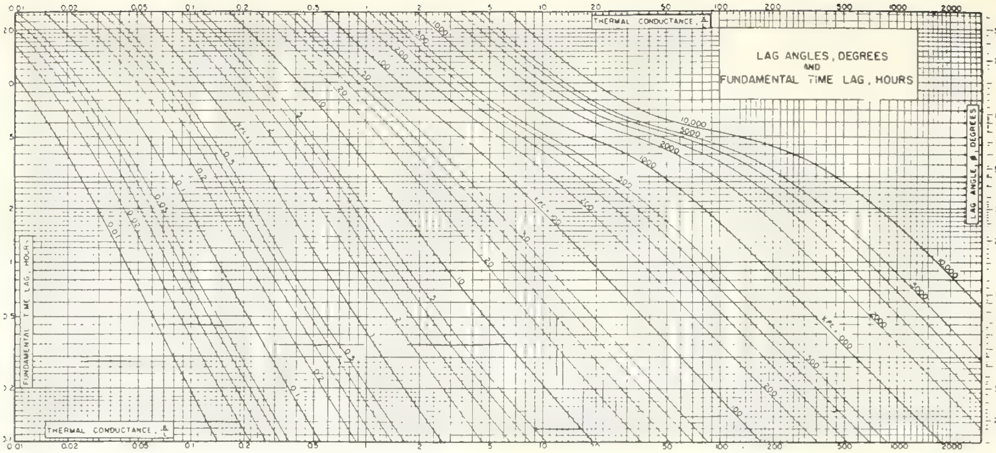

FIGURE 32.—*Chart for determining lag time and lag angles (assumed conditions the same as in figure 31).*

Reprinted by permission from Report No. 1299, "Periodic Heat Flow—Composite Walls or Roofs," by C. O. Mackey and L. T. Wright, Jr., Transactions of A.S.H.V.E., vol. 52, 1946, p. 283.

struction. The one used in this report is that detailed in Stewart's report [*17*] and is as follows:

The fundamental time lag (hours) is first determined for each layer separately by calculating the thermal conductance (K/L) and $K\rho C$, and by using figure 32. The sum of the time lags of the several layers is then equal to the time lag of the combined wall. The thermal conductance of the combined wall equals the reciprocal of the sum of the thermal resistance of the several layers, and this equals the thermal conductivity of the equivalent homogeneous material $(K/L)_e$.

Using the equivalent thermal conductance $(K/L)_e$ of the structure and the combined time lag, the equivalent $(K\rho C)_e$ of the structure is read from figure 32. Using $(K/L)_e$ and $(K\rho C)_e$, the fundamental (first harmonic) decrement factor λ_1 is obtained from figure 31. The second harmonic decrement factor, λ_2, is then obtained from figure 31 by using the same $(K/L)_e$ but 2 times $(K\rho C)_e$. The equivalent decrement factor λ_e is determined from the following schedule, as suggested by Mackey, for variously oriented surfaces:

Horizontal roof .... $\lambda_e = 0.7\lambda_1 + 0.3\lambda_2$
North wall .... $\lambda_e = 0.7\lambda_1 + 0.3\lambda_2$
East wall .... $\lambda_e = 0.2\lambda_1 + 0.8\lambda_2$
South wall .... $\lambda_e = 0.6\lambda_1 + 0.4\lambda_2$
West wall .... $\lambda_e = 0.4\lambda_1 + 0.6\lambda_2$

The equivalent decrement factor λ_e approximates λ_n as determined from the fundamental, second harmonic, and higher harmonic decrement factors.

Calculation of the λ_e, λ_s and Fundamental Time Lag for the Various Walls and Ceilings Studied

The calculations for the equivalent decrement factor, λ_e, the decrement factor without storage, λ_s, and fundamental time lag, ϕ, are made in the manner described above and with the use of figures 31 and 32.

Table 16 shows the calculations for the walls and ceilings at the various test locations. In certain cases, the thermal resistance determined by test has been used in the calculations.

When a material appears for the first time in the table, the ρ, C, and $K\rho C$ values are given. Upon successive appearances in the table, these quantities for a given material are not given.

Table 17 shows similar calculations for typical wall and roof constructions commonly used in storage practice, but not tested in the experimental work reported herein.

Relation of Outside Surface Temperature and Sol-Air Temperature for Average Daily Conditions and Maximum Conditions

Earlier in appendix B, sol-air temperature has been expressed by equation 1–B, as follows:

$$t_e = t_a + \frac{bI}{h_L} \qquad (12\text{–B})$$

It has been defined as the temperature which, in contact with a shaded building surface, would give the same rate of heat transfer as exists with the actual dry bulb temperature of the outdoor air and the actual intensity of solar radiation incident upon the surface. Thus we may write the instantaneous rate of heat flow into the outside surface as follows:

$$q = h_L\ (t_e - t_s) \qquad (13\text{–B})$$

If the average entry of heat into the outside surface over a 24-hour cycle is calculated for the case where all periodic temperatures and solar intensities return to their starting values, and where cooling equipment is operated within the structure, then the average heat flow into the surface will be:

$$q_a = h_L\ (t_{ea} - t_{sa}) \qquad (14\text{–B})$$

Furthermore, if outside conditions are cyclic with a 24-hour period and inside conditions are constant, the average daily rate of heat entering the outside surface will equal that leaving the inside surface, although at almost every instant during the period the two quantities may be different. Since average heat flow from the inside surface and average surface temperature have been measured in the experimental work, the average daily sol-air temperature may be calculated using the customary value of 4 for h_L. In most of the cases given in table 7, the average daily sol-air temperature so determined would be from 0.2° to 0.7° F. higher than the average surface temperature given in that table.

When the relation between sol-air and surface temperature at a particular instant is considered, the problem becomes more complex. Whenever the surface is receiving and absorbing solar radiation, the surface temperature is raised above the surrounding air temperature and a large part of the heat absorbed is discharged to the surrounding air, while another part is conducted away from the surface and into the material beneath the surface. The rate at which this may occur depends on the characteristics of the material. A portion of the heat conducted into the material may be absorbed in raising the temperature of the material at a given point if the temperature difference across a given unit of material at that point is not sufficient to conduct the heat away as fast as it enters.

The experimental records show that during the morning hours when solar radiation is first being received, the change in surface temperature can be very rapid, and under such a condition a large part of the heat entering the surface is being absorbed by raising the temperature of the materials directly beneath the outside surface.

At location 3 the presence of thermocouples within the insulating material on the roof enables us to draw temperature profiles through the material at different times of the day and these in turn can be used to estimate the rate of heat entry to the outside surface at maximum conditions. These data can then be used to approximate the relation between maximum surface temperature and maximum sol-air temperature.

In making this analysis, some relations set forth by Jakob and Hawkins [*6*] are useful. In that reference, it is shown that, with a given temperature distribution through a plate, the rate of heat flow at any point X is

$$q_x = -KA\frac{\partial t}{\partial x} \qquad (15\text{–B})$$

The slope of the temperature distribution curve is $\frac{\partial t}{\partial x}$. If this is plotted as the first derived curve, the temperature gradient curve is obtained. If the ordinates of the temperature gradient curve are multiplied by a constant —KA, the heat flow at any point in the plate is indicated by the curve.

The change in the quantity of heat stored in a unit section of the plate $= KA\frac{\partial^2 t}{\partial x^2}dx$ (16–B).

The second derived curve may be obtained by plotting the slope of the temperature gradient curve at various points through the plate, and the rate of heat stored in each element is a constant KAdx times the second derived curve.

The rate of heat storage also is equal to

$$A\,dx\,\rho C\frac{\partial t}{\partial \theta} \qquad (17\text{–B})$$

Therefore:

$$A\,dx\,\rho C\frac{\partial t}{\partial \theta} = \frac{K\,A\partial^2 t\,dx}{\partial x^2} \qquad (18\text{–B})$$

$$\frac{\partial t}{\partial \theta} = \frac{K}{\rho C}\frac{\partial^2 t}{\partial x^2} = a\frac{\partial^2 t}{\partial x^2} \qquad (19\text{–B})$$

If a temperature distribution curve is selected at such a time that heat is neither being stored nor released in the section at the outer surface, then all the heat entering the material must be passing on into the material because of conduction, and an estimate of this flow can be made by plotting a temperature gradient curve at this time. Fortunately, such a situation occurs at the time of maximum outside surface temperature. As the maximum is approached, the temperature of the surface material is increasing and therefore heat is being stored in the material, and after passing through the maximum the temperature of the surface is decreasing and the material is releasing heat; but at the maximum point the change of temperature of the surface material with respect to time is zero, and heat is neither being stored nor released by the layer of material at the surface. Therefore, all the heat entering the material is being carried away by conduction.

Two diagrams are presented showing temperature distribution curves and the derived curves for temperature gradient through the insulation at location 3 (figs. 33 and 34). One is for a day when the roof had a coat of aluminum paint and the other is for a day when the roof was painted black.

In the first case, the rate of heat flow in from the outside surface at the time of maximum surface temperature is 5.6 Btu/hr/sq ft and in the second case is 6.35 Btu/hr/sq ft. Using h_L equal to 4, equation 13–B then indicates that at this condition the difference between sol-air temperature and surface temperature is in the order of 1.5° for this kind of roof structure.

One point deserves further comment. The temperature distribution curves were determined from temperatures recorded at finite distances apart (2 inches) in the insulation and

TABLE 16.—*Calculation of the λ_e, λ_s and fundamental time lag for the various walls and ceilings studied*

Location and description of construction	Thermal conductivity K	Thickness L	Thermal resistance L/K	Thermal conductance K/L	Time lag ϕ	ρ	C	KρC	λ_1	λ_2	λ_e	λ_s	λ_e/λ_s
		Feet			*Hours*	*Lb/cu ft*	*Btu/lb./°F.*						
Location 1:													
Roof:													
5 reflective spaces			[1] 10.0		0	0		0					
1/4" Masonite	0.062	0.021	.34	3.0	.13	36	0.65	1.45	0.055	0.055	0.055	0.055	1.0
Combined roof			10.34	.0968	.13			.008					
East wall:													
8" pumice block	.135	.67	5.0	.20	6.0	45	.16	.97					
2 reflective spaces			6.		0	0							
2 pr accordion-type reflective spaces			10.4		0	0							
1/4" Masonite	.062	.021	.34		.13			.075	.015	.0070	.0086	.024	.358
Combined wall			21.74	.046	6.13								
Location 2:													
Ceiling under attic:													
5 reflective spaces			[1] 40	.025	0	0		0	.0145	.0145	.0145	.0145	1.0
Sloping roof sections:													
Aluminum roofing on 1 x 6's spaced 12" on center and 5 reflective spaces			[1] 23.5	.0425	0	→0		0	.0245	.0245	.0245	.0245	1.0
South wall:													
5/8" lumber	.062	.052	[1] 0.84	1.19	.45	36	.65	1.45					
2 reflective spaces, 2 pr accordion spaces, and 1 space between corrugated siding			[1] 27.75			0		.0035	.020	.020	.020	.020	1.0
Combined wall			28.59	.035	.45								
Location 3:													
Roof:													
Roofing	.11	.0312	0.28		.1			1.2					
4" cork board	.0225	.33	14.66	.0682	2.6	7	.43	.068					
1 5/8" wood	.062	.135	2.18	.458	2.0	36	.65	1.45					
Combined roof			17.12	.0584	4.7			.1	.024	.015	.0213	.033	.645
North wall:													
6" concrete	1.	.5	.5	2	3.1	142	.156	22.2					
2 reflective spaces			6.1		0	0	0						
4 pr accordion-type reflective spaces			21.0		0	0	0						
3/8" plywood	.062	.0312	.5	2	.22	36	.65	1.45					
Combined wall			28.1	.0355	3.32			.025	.017	.013	.0158	.024	.659

(Continued)

Location 4:													
Roof:													
Roofing	.11	.0312	.28		.1								
5/8″ lumber	.062	.052	.84		.45								
3 reflective spaces and 4 pr accordion-type spaces			[1] 21.85		0								
3/8″ plywood	.062	.0312	.5		.22								
Combined roof			23.47	.0426	.77			.008	.024	.023	.0237	.024	.987
South wall:													
8″ concrete block	.78	.67	1.11	.9	3.2	65	.156	7.9					
2 reflective spaces and 2 pr accordion-type spaces			16.4		0								
3/8″ plywood	.062	.0312	.5		.22								
Combined wall			18.01	.0555	3.42			.07	.025	.017	.0218	.032	.681
Location 5:													
Ceiling:													
24″ shavings	.0342	2.	58.5	.017	30	8.8	.65	.196	[2]	[2]	[2]		[3]
5/8″ lumber	.062	.052	.84		.45								
Combined ceiling			59.34	.0168	30.45			.19	[2]	[2]	[2]	.01	[3]
Location 6:													
Roof:													
Roofing	.11	.0312	0.28		0.10								
5/8″ lumber	.062	.052	.84		.45								
11 5/8″ mineral wool	.0225	.97	43.00	.0232	4.5	3.5	.201	.0158					
1/4″ plywood	.062	.021	.34	3.	.13	36	.65	1.45					
Combined roof			44.46	.0224	5.18			.018	.009	.005	.0078	.0132	.591
West wall:													
6″ concrete	1.	.5	.5		3.1								
2 reflective spaces			7.6		0								
4 1/2″ Fiberglas bats	.0225	.375	16.66	.06	1.1	4.5	.21	.0213					
Combined wall			24.76	.0404	4.2			.043	.019	.012	.0148	.024	.616
Location 7:													
Ceiling:													
5″ Zonolite	.0383	.417	10.88	.092	1.8	8.2	.25	.0785					
5/8″ lumber	.062	.052	.84		.45								
Combined ceiling			11.72	.0853	2.25			.08	.046	.037	.043	.048	.896
South wall:													
4″ pumice block	[1] .083	.33	4.0	.25	3.3	67.5	.16	.89					
1″ Zonolite fill	.0383	.083	2.18	.46	.1	8.2	.25	.0785					
4″ pumice block	.083	.33	4.0		3.3								
1″ Zonolite fill	.0383	.083	2.18		.1								
4″ pumice block	.083	.33	4.0		3.3								
Combined wall			16.36	.0611	10.1			.3	.011	.004	.0082	.035	.234

[1] Thermal resistance determined by tests used in the calculations.

[2] Values are off the chart but λ_1 estimated at 0.0001.

[3] Less than 0.01.

TABLE 17.—*Calculation of λ_e, λ_s and fundamental time lag for various typical cold storage walls and ceiling*

Description of construction	Thermal conductivity K.	Thickness	Thermal resistance L/K	Thermal conductance K/L	Time lag of element	ρ	C	KρC	λ_1	λ_2	λ_e	λ_s	λ_e/λ_s
		Feet			*Hours*	*Lb/cu ft*	*Btu/lb/°F.*						
Ceiling A:													
Roofing	0.11	0.0312	0.28		0.1			1.2					
2″ Styrofoam	.0208	.167	8.00	0.125	.11	1.8	0.25	.00936					
½″ cement plaster	1.	.0416	.04		.1			22.2					
2″ Styrofoam	.0208	.167	8.00	.125	.11								
Combined ceiling			16.32	.0616	.42			.009	0.035	0.035	0.035	0.035	1.0
Ceiling B:													
Roofing	.11	.0312	0.28		0.1								
½″ cement plaster	1.0	.0416	.04		.1								
3″ Styrofoam	.0208	.25	12.00		.25								
3″ gypsum cement	.1385	.25	1.80	.555	1.8	51.2	.259	1.84					
1″ Pyroform	.02	.083	4.16	.24	.3	15.2	.259	.079					
Combined ceiling			18.28	.0545	2.55			.046	.028	.022	.0262	.031	.845
Ceiling C:													
Roofing	.11	.0312	0.28		0.10								
4″ Foamglass	.03165	.33	10.45		1.30	9	.2	.057					
⅝″ wood	.062	.052	.84		.45								
Combined ceiling			11.57	.0864	1.85			.07	.047	.040	.045	.048	.94
Ceiling D:													
Roofing	.11	.0312	0.28		0.1								
6″ Styrofoam	.0208	.5	24.05		.9								
⅝″ wood	.062	.052	.84		.45								
Combined ceiling			25.17	.0398	1.45			.013	.022	.021	.0217	.0225	.954
Ceiling E:													
Roofing	.11	.0312	0.28		0.1								
6″ corkboard	.0225	.5	22.2		5.	7	.43	.068					
⅝″ wood	.062	.052	.84		.45								
Combined ceiling			23.32	.0429	5.55			.07	.016	.0085	.0137	.025	.548
Wall A:													
6″ concrete	1.	.5	0.5		3.1	142	.156	22.2					
4″ sheet corkboard	.0225	.33	14.66		2.6	7	.43	.068					
Combined wall			15.16	.0659	5.7			.16	.023	.013	.0190	.038	.50
Wall B:													
8″ concrete block	.78	.67	1.11		3.2	65	.156	7.9					
4″ Fiberglas bats	.0225	.33	14.66		.85	4.5	.21	.0213					
¼″ Masonite	.062	.021	.34		.13								
Combined wall			16.11	.0611	4.18			.09	.028	.018	.0240	.035	.686

(Continued)

Wall C:													
6″ concrete	1.	.5	0.5		3.1								
3″ Styrofoam	.0208	.025	12.00		.25	1.8	.25	.00936					
Combined wall			12.5	.08	3.35			.12	.038	.028	.340	.045	.756
Wall D:													
½″ cement plaster	1.	.0416	0.04		0.1								
2″ Foamglass block	.03165	.167	5.25	.19	.35	9	.2	.57					
¼″ cement plaster	1.	.021	.02		.0								
2″ Foamglass block	.03165	.167	5.25		.35								
Combined wall			10.56	.0946	.8			.04	.053	.052	.0526	.053	.993
Wall E:													
6″ concrete	1.	.5	0.5		3.1			35.					
12″ shavings	.0342	1.	30.12		15.0	8.8	.65	.196					
⅝ wood	.062	.052	.84		.45								
Combined wall			31.46	.0318	18.55			.23	.001	.00035	.00074	.0185	.04
Wall F:													
6″ concrete	1.	.5	0.5		3.1								
6″ redwood bark	.0217	.5	23.00		1.8	4	.23	.02					
⅝″ wood	.062	.052	.84		.45								
Combined wall			24.34	.0411	5.35			.06	.016	.009	.0132	.024	.55
Wall G:													
1¼″ wood	.062	.104	1.68		1.3	36	.65	1.45					
12″ shavings	.0342	1.	30.12		15.0								
⅝″ wood	.062	.052	.84		.45								
Combined wall			32.64	.0306	16.75			.19	.0015	.00045	.00108	.018	.060
Wall H:													
6″ concrete	1.	.5	0.5		3.1	7	.43	.068					
6″ cork	.0225	.5	22.2		5.0								
½″ plaster	1.	.0416	.05		.1								
Combined wall			22.75	.044	8.2			.12	.01	.005	.007	.025	.28
Wall J:													
6″ concrete	1.	.5	0.5		3.1			35					
6″ Styrofoam	.0208	.5	24.05	.0416	.9	1.8	.25	.00936					
½″ plaster	1.	.0416	.05		.1								
Combined wall			24.6	.0406	4.1			.045	.018	.012	.0156	.024	.65
Wall K:													
1¼″ wood	.062	.104	1.68		1.3								
9″ shredded redwood bark	.0217	.75	34.5	.0290	3.7	4	.23	.02					
⅝″ wood	.062	.052	.84		.45								
Combined wall			37.02	.027	5.45			.027	.0105	.0058	.0086	.016	.537

(Continued)

TABLE 17.—*Calculation of λ_e, λ_s and fundamental time lag for various typical cold storage walls and ceiling*—Continued

Description of construction	Thermal c onductivity K.	Thickness	Thermal resistance L K	Thermal conductance K L	Time lag of element	ρ	C	$K\rho C$	λ_1	λ_2	λ_e	λ_s	λ_e/λ_s
		Feet			*Hours*	*Lb/cu ft*	*Btu/lb/°F.*						
Wall L:													
½″ cement plaster	1.	.0416	0.04		0.1								
4″ Foamglass block	.03165	.33	10.45	.0957	1.3	9	.2	.057					
¼″ cement plaster	1.	.021	.02		.0								
4″ Foamglass block	.03165	.33	10.45		1.3								
½″ cement plaster	1	.0416	.04		.1								
Combined wall			21.00	.0476	2.8			.038	.024	.018	.0216	.027	.8
Wall M:													
6″ concrete	1.	.5	0.5		3.1								
8″ Fiberglas P.F	.0225	.667	29.65	.0337	3.8	6	.21	.028					
⅛″ hardboard	.062	.01	.17	5.9				1.45					
Combined wall			30.32	.033	6.9			.055	.01	.0045	.0078	.02	.39

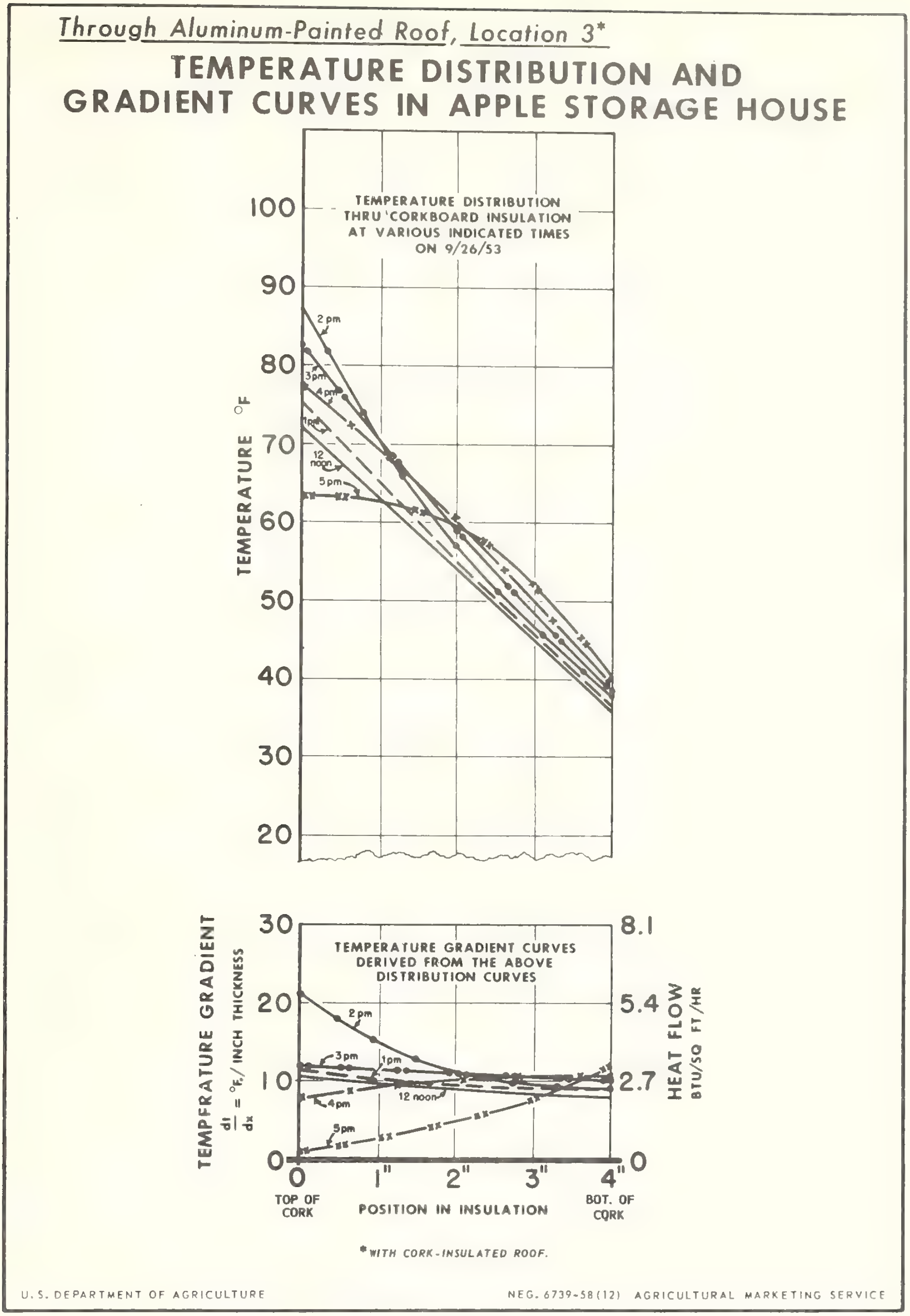

FIGURE 33

therefore probably do not exactly show the distribution in the outer layer of insulation, because if they were exact, the temperature gradient curve would have a short portion at zero slope at the surface. For the data presented for the roof with black paint, this condition is approximated. However, in both cases, the slope for the temperature gradient line approximates zero 1 hour after the maximum surface temperature has been reached.

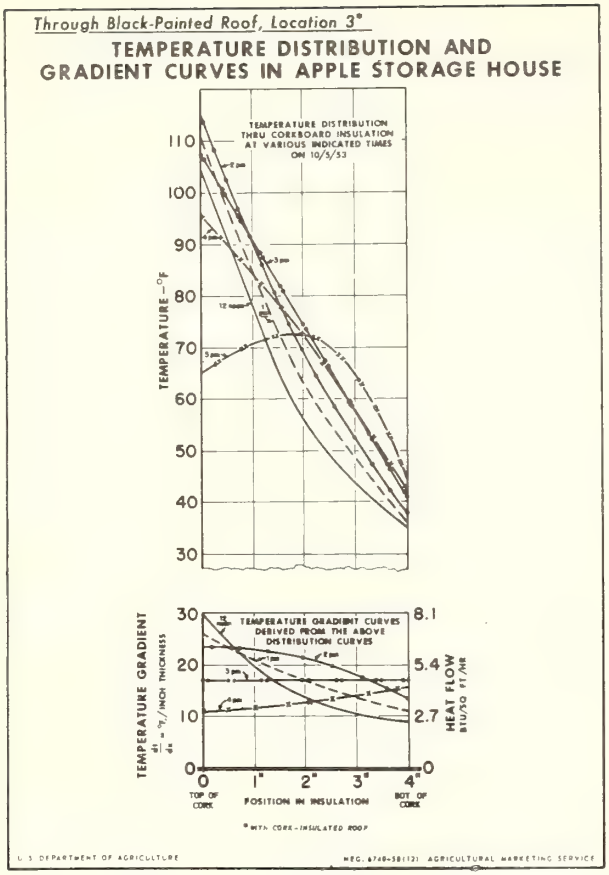

FIGURE 34

If heat flow values were taken from this latter curve, the difference between sol-air temperatures and surface temperatures would be somewhat less than at the time of maximum surface temperature. However, it appears that the differences derived for time of maximum surface temperature are the correct differences to use.

When the amplitude of surface temperature variation that has been encountered in the tests is considered, then the error introduced by using average and maximum surface temperatures in place of sol-air temperatures is not great. The foregoing analysis was made for the case where the surface consists essentially of an insulating material with a high thermal resistance and the heat can enter the material at a restricted rate. If the material is a good conductor of heat, then there is a substantial error introduced by using surface temperature as an approximate sol-air temperature. There were not sufficient data available from any of these tests to correctly evaluate this error; however, some analysis of the data from the west-facing wall at location 6 indicated that the error at the time of maximum surface temperature would be greater than 5° and might run as high as 10° to 15°. It is probable that the estimate of maximum heat leakage rate for the wall at locations 3, 4, and 6 would be in error, because the outer wall surface is composed of a good conductor and the wall surface temperature would be substantially lower than sol-air temperature at the time of maximum outside condition. The other walls tested have exterior surfaces that are portions of the insulation, and here the sol-air and surface temperature should be fairly close together.

Calculation of Ratio of Maximum to Average Heat Flow Rates for Various Design Conditions

Consider the case of a cooler operated through the summer months and designed on the basis of average temperatures as follows:

Walls—outside temperature ...... 85° F.
Ceiling—outside temperature ...... 95° F.
Inside room temperature ...... 30° F.

From the ASHAE Guide, use a maximum sol-air design temperature for north, east, south, and west walls that averages 14° above the mean sol-air temperature and for horizontal surfaces use a maximum sol-air temperature that is 44° above the average. The average amplitude of sol-air temperature variation for the walls has been calculated from the 1 p.m. values, because this is the time when the roof sol-air temperature is maximum. The average assumes that all four walls have the same area.

The ratio of maximum to average heat flow for the walls will be as follows:

$$\frac{q_{max}}{q_a} = \frac{U\left([85 - 30] + \frac{\lambda_e}{\lambda_s} 14\right)}{U\,(85 - 30)} = \frac{55 + \frac{\lambda_e}{\lambda_s} 14}{55}$$

With this formula, the ratio of maximum to average heat flow may be calculated for the selected values of λ_e/λ_s and the values plotted on figure 29.

A similar calculation has been made for the ceiling, using 95° as the average outside temperature and 44° as the amplitude of sol-air temperature variation.

Calculations were made for freezer storages using these same outside conditions and a minus 5° inside temperature.

For mild-temperature storages that operate only in the cooler portions of the year, two sets of calculations were made. One was based on 65° average outside temperature and the other on 55°.

For the 65° condition, the average roof surface temperature was assumed to be 75° and the amplitude of sol-air temperature variation for this surface was taken as 40°. The amplitude of sol-air temperature variation for the walls was assumed to be 12°.

For the 55° condition, the average roof surface temperature was assumed to be 65°. The amplitude of sol-air temperature variation for the roof was 35° and that for the walls was 11°.

The amplitudes of sol-air temperature variation that have been used for the 65° and 55° design conditions have been selected by arbitrarily reducing the values used for the 85° condition. However, a study of some of the surface temperatures shown in table 7 indicates that the values used are reasonable and have been encountered in actual experience.

The ratio of maximum to average heat flow for the walls is much less than for a ceiling operating under the same design condition because solar load is maximum on the different walls at different times. Actually, the east, south, and west walls each experience a time during the day when the ratio of maximum to average flow is comparable to that experienced by the ceiling.

The values shown in figure 31 were calculated from the data in the ASHAE Guide, which gives information regarding design sol-air temperatures to be expected in an industrial atmosphere.

Using the data reported by Mackey [*9*] for Lincoln, Nebr., which were considered as typical data for a clear atmosphere, an investigation was made of the difference in amplitude of sol-air temperature variation for roofs and walls of a structure located in a clear-atmosphere region. For summer design conditions, the amplitude of sol-air temperature variation for the roof would be raised from 44° to 53°. For the walls, little change would occur.

☆ U. S. GOVERNMENT PRINTING OFFICE: 1959—500492